UNIVERSITY OF MINNESOTA

DEVELOPMENT AND APPLICATION OF ON-LINE, INTEGRATED CONTROL STRATEGIES FOR OPTIMAL METERING, INCIDENT MANAGEMENT AND DRIVER GUIDANCE IN FREEWAY NETWORKS

PHASE I

FINAL REPORT

Department of Civil and Mineral Engineering

Institute of Technology

DEVELOPMENT AND APPLICATION OF ON-LINE, INTEGRATED CONTROL STRATEGIES FOR OPTIMAL METERING, INCIDENT MANAGEMENT AND DRIVER GUIDANCE IN FREEWAY NETWORKS

PHASE I

FINAL REPORT

ENHANCEMENTS AND FIELD TESTING OF ENHANCED RATE-SELECTION, CONTROL-SIMULATION METHOD

Principal Investigators: Yorgos J. Stephanedes and Eil Kwon
Graduate Research Assistants: Kaikuo Chang and Nikos Vairamidis

Department of Civil and Mineral Engineering
University of Minnesota
Minneapolis, Minnesota

April 1993

TABLE OF CONTENTS

I. INTRODUCTION

I.1 Problem Statement

Managing freeway congestion requires an integrated approach involving demand-responsive ramp metering, incident management and driver guidance. While a freeway network acts as a system, i.e., conditions on any part affect other parts in the network, the state of the art in real-time freeway management has not reached the point where comprehensive, network-wide optimal control schemes are automatically generated and implemented through on-line optimization and coordination of various control actions. A major difficulty lies in the lack of efficient computational algorithms implementable for on-line optimization, and the lack of accurate on-line predictors, that can predict traffic demand and diversion in freeway networks.

As a result of the above limitations, most traffic responsive metering systems, such as the Twin Cities freeway control system, employ automatic rate-selection procedures. These procedures select the most appropriate metering rates for a ramp from a pre-determined library using the information received from loop detectors on the main freeway, upstream and downstream from the ramp. Although this method provides a degree of self-adjustment to prevailing traffic conditions, the lack of an efficient analysis tool to evaluate and update the key components of the control, i.e., thresholds and rate-libraries, significantly restricts the effectiveness of control.

For example, Figures 1-1 and 1-2 show the volume-occupancy measurements for 3 consecutive days at a mainline detector, located at the north-bound I-35W freeway (station #61N), where most ramps are centrally controlled with automatic rate-selection strategies. As indicated in Figure 1-1, at this location traffic volume reaches its maximum at a 23% critical occupancy. Since this maximum volume cannot be reached again once occupancy exceeds the critical value, unless congestion dissipates completely, it is crucial to maintain the occupancy level below or at the critical value to prevent congestion. However, as Figure 1-2 shows, the occupancy at this location exceeded its critical value 3 days in a row during almost the same time interval; and this indicates that the effectiveness of the current automatic rate-selection control substantially depends on adjusting the thresholds and rate-libraries, so that they can achieve optimal traffic performance.

To address the above problems, a computer-based control-emulation method that can evaluate various automatic rate-selection strategies has been developed by this research team. Further, software was developed that operationalizes this method for field applications. While a prototype version has been completed and tested off-line, the software still requires substantial

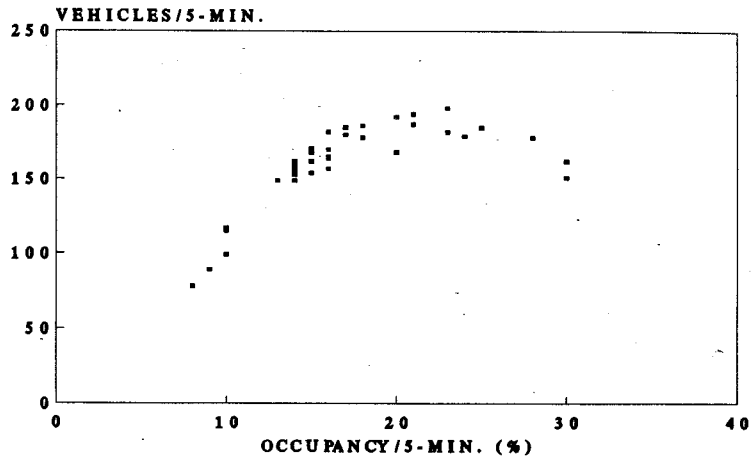

(a)

Nov. 13, 1990

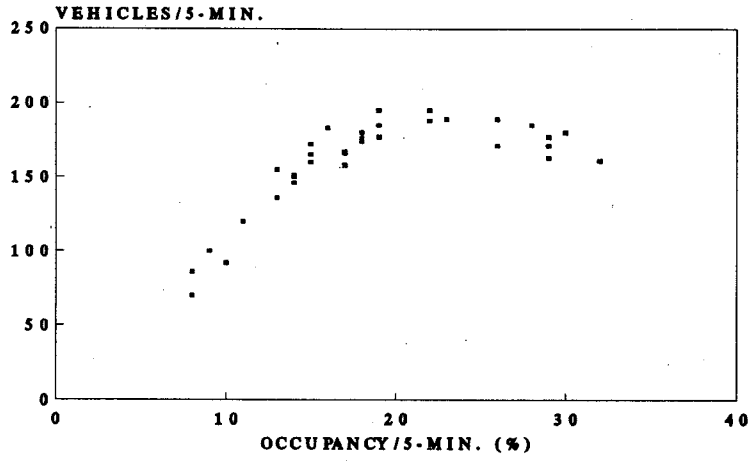

(b)

Nov. 14, 1990

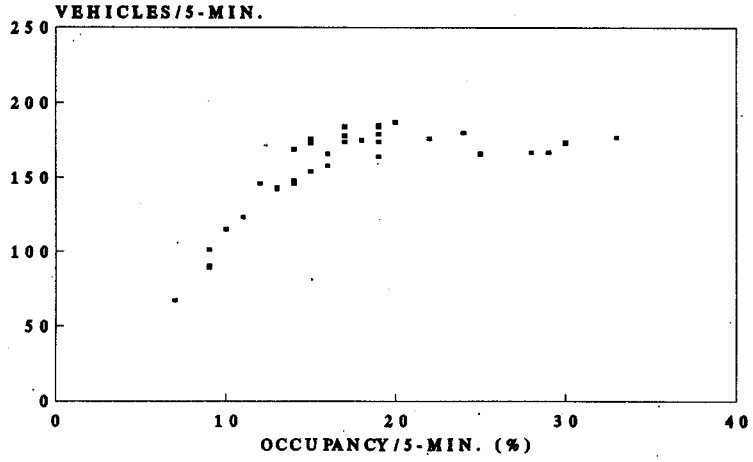

(c)

Nov. 15, 1990

Figure 1-1 Volume-occupancy measurements at station 61N1, Detector 298, 6:00-9:00 a.m.

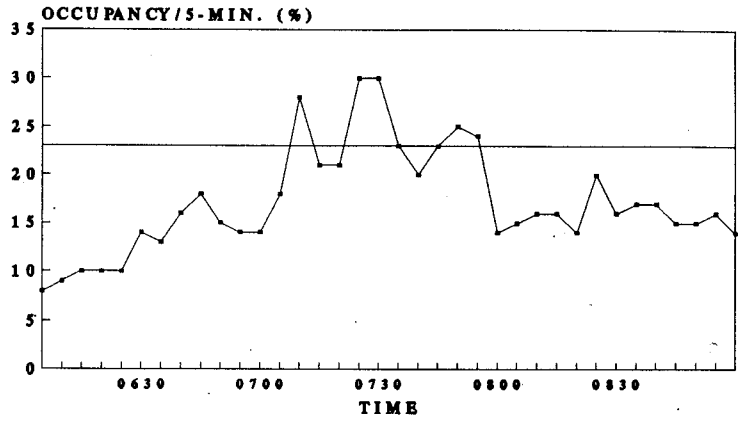

(a)

Nov. 13, 1990

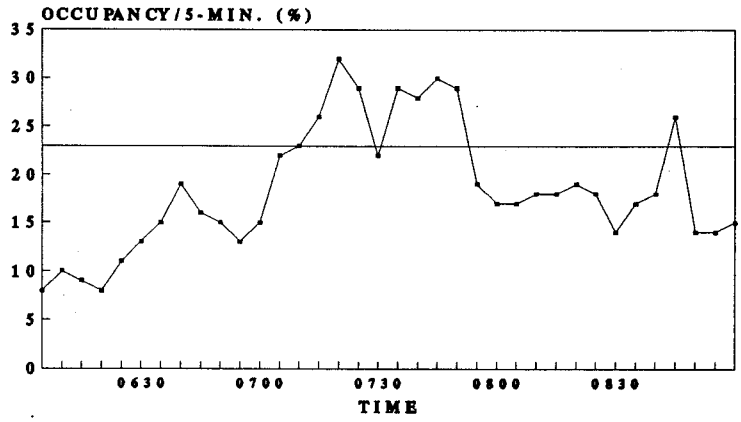

(b)

Nov. 14, 1990

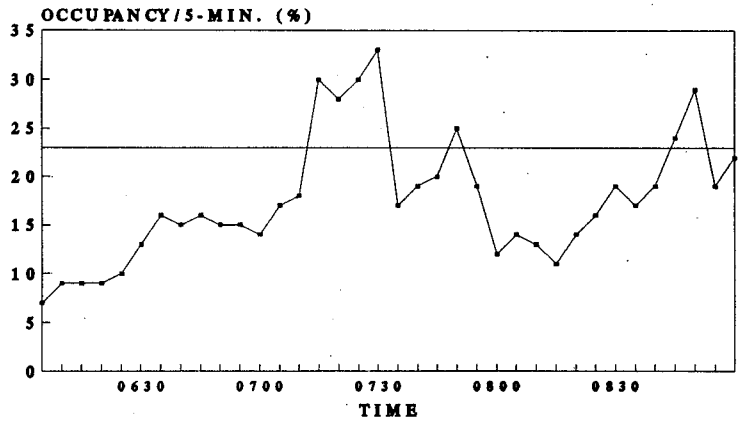

(c)

Nov. 15, 1990

Figure 1-2 Occupancy variation through time at station 61N1, Detector 298, 6:00-9:00 a.m.

enhancements before it becomes fully operational for traffic management. Such enhancements include, software field validation with new automatic rate-selection strategies in the real freeway environment, and development of efficient input/output modules. In addition, advanced real-time control strategies need to be developed, as well as on-line prediction/optimization, traveler information and incident management system modules.

I.2 Research Objectives

The main objective of this research is the enhancement and field testing of a control-emulation method and software that can be used for ramp rate selection in a real freeway environment. The new software will provide traffic engineers with a practical tool for updating and adjusting current automatic rate-selection strategies for efficient traffic-responsive freeway management. Further, a methodology will be developed to determine the best rate-selection strategy using the control-emulation method. Finally, a preliminary study to develop on-line predictors, advanced traveler information systems and incident management systems will be performed. The accomplishments of this research would include:

- Development of interactive input-output modules for the control-emulation software.
- Development of an efficient methodology that can determine optimal, zone-based metering thresholds and rate-libraries for a given section of a freeway using the control-emulation software.
- Field experimentation of new optimal metering thresholds and rate-libraries in the test freeway section.
- Preliminary study for the development of on-line predictors, and advanced traveler information and incident management systems.

I.3 Report Organization

The second chapter of the report describes the enhanced control-emulation software with new input/output modules developed in this project. Chapter 3 develops two methods for determining a set of thresholds for a given freeway section. The first method determines a set of thresholds for a ramp using local traffic conditions. The second method employs the downhill simplex procedure and determines the best zone-thresholds for each ramp in a given freeway section. The thresholds determined with the first method can be used as initial values in the process that optimizes traffic zone thresholds. The field-application results of the new optimization method at a section of the I-494 freeway are included in Chapter 4. Chapter 5 summarizes the results from the preliminary study in the development of an on-line predictor for traffic demand exiting the freeway. Finally, Chapter 6 contains conclusions.

II. ENHANCEMENT OF THE PROTOTYPE CONTROL-EMULATION SOFTWARE: DEVELOPMENT OF INPUT-OUTPUT MODULE

II.1 Introduction

The control-emulation method developed in the previous phase of this research (Stephanedes et al, 1992b) required a separate text editor in preparing input files and accessing analysis results. This batch-file oriented approach for input-output process caused serious inconvenience and time-consuming manual effort even for the most experienced user in preparing input data and analyzing the results. To address this problem, an efficient user interface consisting of interactive input-output modules is developed in this research. The new interface enables the user to create and modify the input data on the monitor screen following on-line instructions. The input module generates the input data files automatically following user specifications. Similarly, the new output module can present the analysis results with tables and graphs on the screen according to the user's request. The detailed description of the new input-output procedures is attached in Appendix A. The following sections summarize the enhanced control-emulation method with new input-output procedures.

II.2 Overview of the control-emulation method

The control-emulation method emulates real-time rate-selection metering using simulated freeway traffic performance when the freeway demand pattern and geometrics are known. Figure 2-1 illustrates the key components of the method, i.e., ramp control and freeway performance emulation modules, interacting continuously through time. The ramp control module emulates the on-line automatic rate-selection process and determines metering rates using the traffic information provided by the freeway performance module. The key elements of the process include a set of volume/occupancy thresholds, a rate table and the locations of detector stations associated with each ramp. First, traffic volume/occupancy information at pre-defined detector locations are determined by the freeway performance module, which adopts a dynamic simulation methodology based on continuum modeling. Upstream volume information and the highest downstream occupancy among detector stations are then compared with the pre-determined volume/occupancy thresholds. Using the rate table, two rates are identified and the more restrictive rate is selected. Following a time delay, the freeway performance module uses that rate for determining the number of vehicles entering the freeway system. The method can facilitate freeway traffic management by aiding in the design of new traffic-responsive ramp strategies, and in the evaluation of existing control schemes such as volume/occupancy thresholds and rate-libraries.

Currently, the method can be run on an IBM-compatible personal computer with 1-M-byte

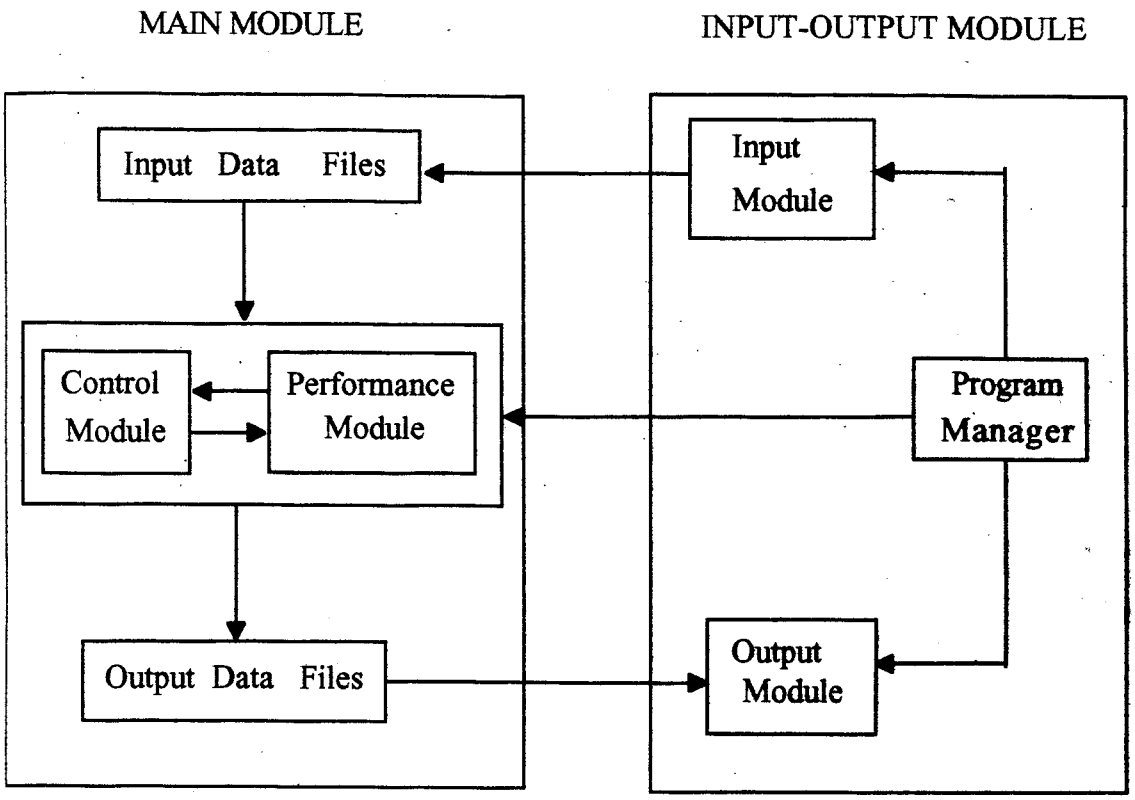

Figure 2-1 Structure of Control-Emulation Package

RAM and a hard disc. All the files included in the control-emulation package should be installed on a hard disc in one directory. The user may make another directory for data files. The hard disc needs 3-M-byte free space for running the package. Many graphic monitors and printing devices are supported by the package. It is not necessary to use a floating point processor. The output module supports a variety of monitor devices; nevertheless, best results are obtained with an 800x600 VGA monitor. The module also supports a wide range of printing devices including the HP plotter and Laser printers.

II.3 Input module and data requirements

The new input module enables the user to generate the input data files through an interactive screen editor. Three input data files are needed for running the main control-emulation module: 1) A general information and highway geometry file, 2) a traffic demand file, and 3) a ramp control policy file. The input module allows the user to create and edit two of the three files, the geometry file and the control policy file. Due to the relatively large and repetitive nature of the traffic demand file, it was decided that interactive editing of this file would not be included in the input module. As with both of the other files, the traffic demand file can be edited with a standard text editor.

After the user selects the "specifying input data" option from the main menu screen (see Fig. 2-2), the main menu of the input module prompts some options to the user (Figure 2-3). The user can select an option from the main input menu, and get into the sub-menu to specify a particular data set. Figure 2-3 also lists the input data sets requested from each sub-menu. The data are normally entered in table form according to input data requirements described in Appendix A. The input module provides interactive menus and tables for guiding the user to specify and modify the data. Detailed description of the functions of the input module is presented in Appendix A.

Input requirements for General Information and Highway Geometry

First, the user has to prepare five groups of data which are related to control-emulation parameters as well as the freeway and ramp geometry. The first group of the data named "introductory information" includes the parameters of the freeway system such as number of zones, entrance ramps, exit ramps, and detector stations, and time parameters such as total control-emulation time, a demand input period, and a period for printing outputs. The second group of the data specifies traffic speed and density relationships that will be used for estimating the freeway speed during the control-emulation process. The third and fourth group of the data called "freeway and ramp configuration" specify the characteristics of each freeway and ramp zone such as length and width of the zone, the speed-density relationship used in the zone,

maximum and minimum ramp metering rates, etc.. The fifth group of the data requires detector station specification such as the position of each detector station, and coefficients for converting density into occupancy. The detailed definition and format of these data are described in Section A.2.2.1 and summarized in Table A-1 and Figure A-1 in Appendix A.

Traffic Demand Data

The traffic demand data should be specified for the upstream of the freeway and entrance ramps, and exit ramps. This information is stored in the traffic demand data file including the downstream flow rate and occupancy of the freeway, if necessary. The data are arranged in four parts in the file: upstream demand, diverging flow, downstream flow, and downstream occupancy. Detailed data description and format are summarized in Table A-3 and Figure A-4 in Appendix A.

Ramp Control Policy

Finally, for each controlled ramp, occupancy/volume thresholds, red time interval for each metering rate, and detector stations associated with each ramp need to be specified and stored in the control policy file. Detailed data description and format are summarized in Table A-4 and Figure A-5 in Appendix A.

II.4 Output Module

The output module allows the user to graphically display the results obtained from the main module both on the screen and in hardcopy form. Figure 2-4 shows the menu structure of the output module. It includes the options the user can select, the display functions for the output, and the data type that can be viewed and printed from the output module. Nine output data files are generated by the main module. They are briefly discussed in the following paragraphs. Detailed description is presented in Section A.3.2 in Appendix A.

The input data description file contains most of the input information. It cannot be displayed on the screen interactively, but the file can be printed directly and be viewed with a text editor. The user can examine this file to check whether the package interprets the input data correctly. The last file with file extension .FST provides information to the output module for making tables and graphs.

Traffic flow data files include the files with file extension .VOL, .OSD, and .ODT. They store volume, speed, and density of each 100-foot section for every output period, respectively, and these data can be tabulated and graphed in many ways according to the user's request. For instance, Figures 2-5 to 2-7 illustrate a three dimensional graph, a two dimensional contour and slice of the freeway volume for hypothetical demand. The user can examine these graphs to find where and when the freeway congestion occurs as well as how far it extends and how long it lasts. The same kinds of graph are also used for displaying the data in the detector station data files,

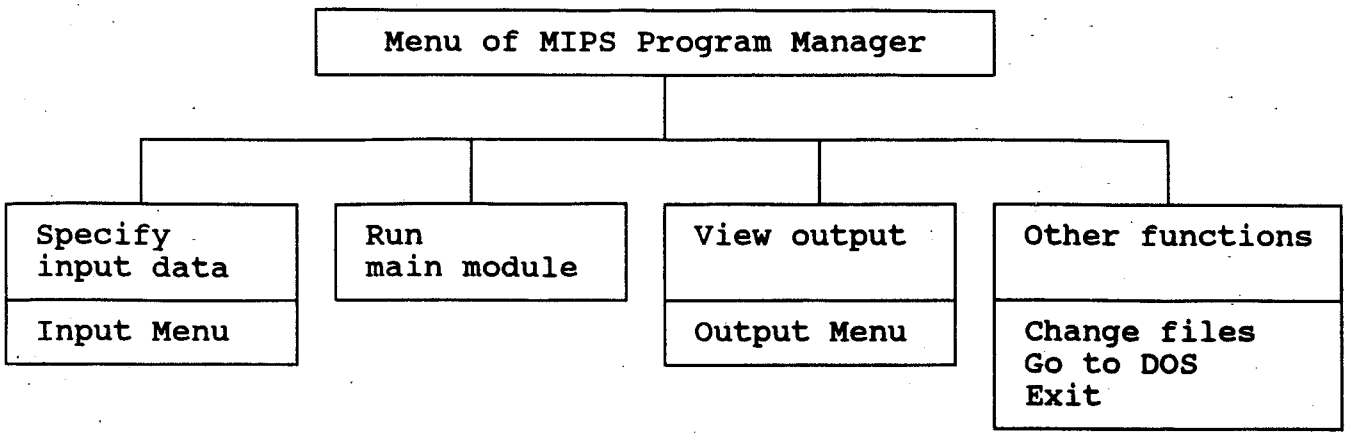

Figure 2-2 Menu Options of MIPS Program Manager

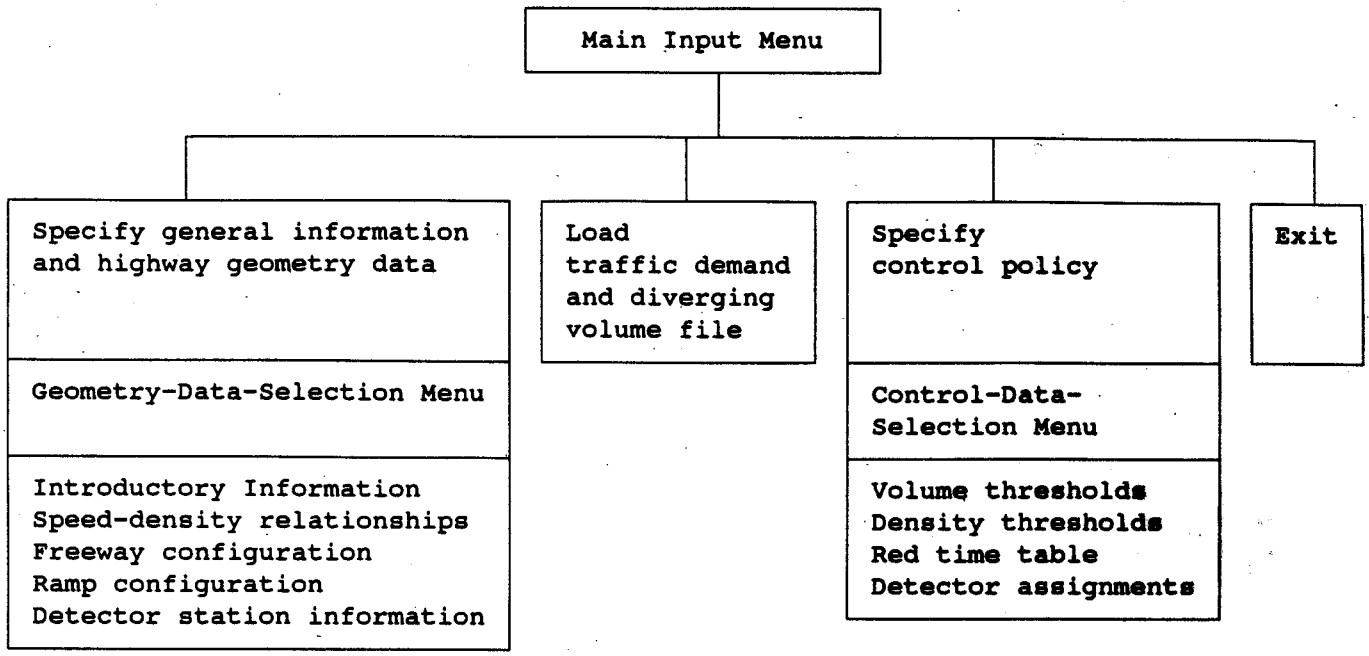

Figure 2-3 Menu Options of Input Module

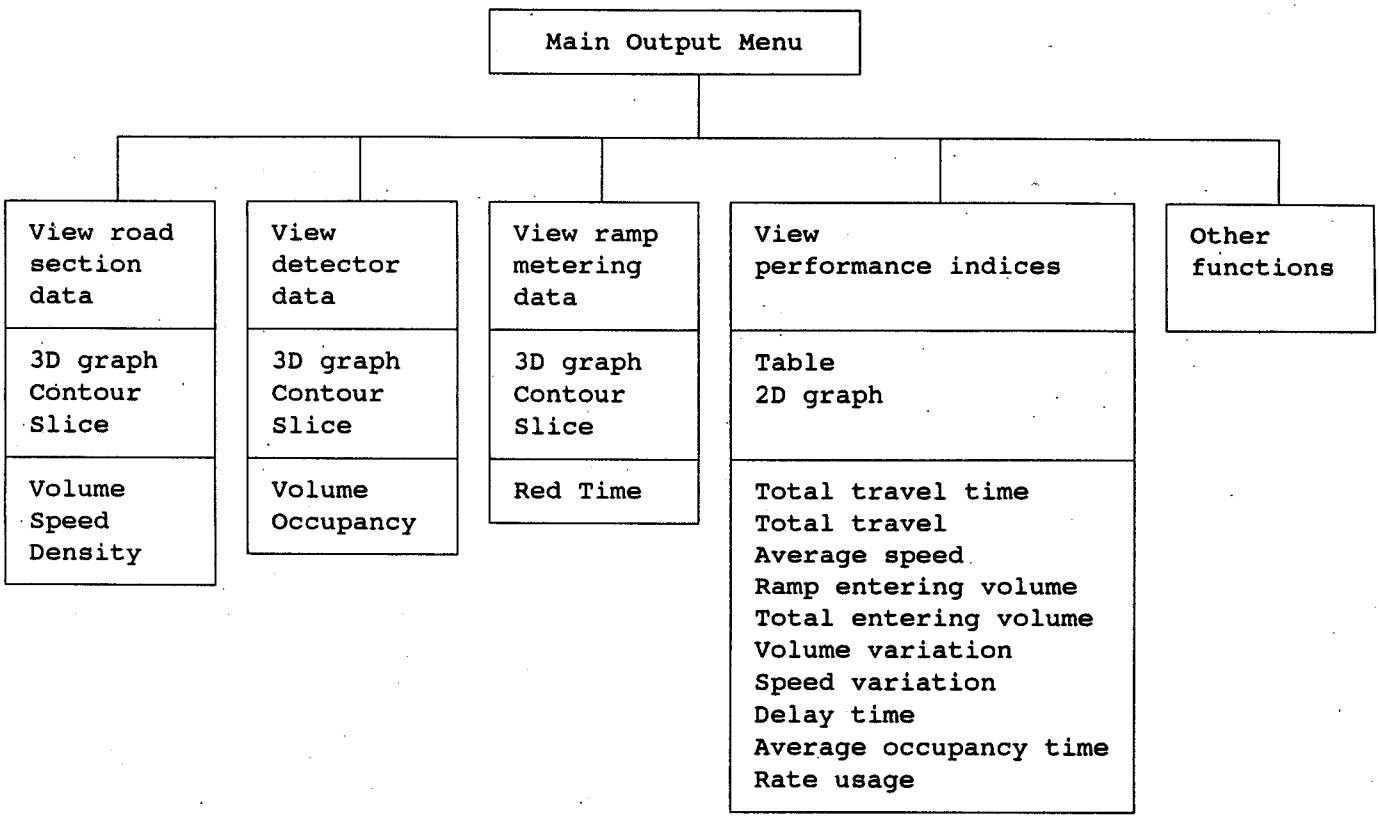

Figure 2-4 Menu Options of Output Module

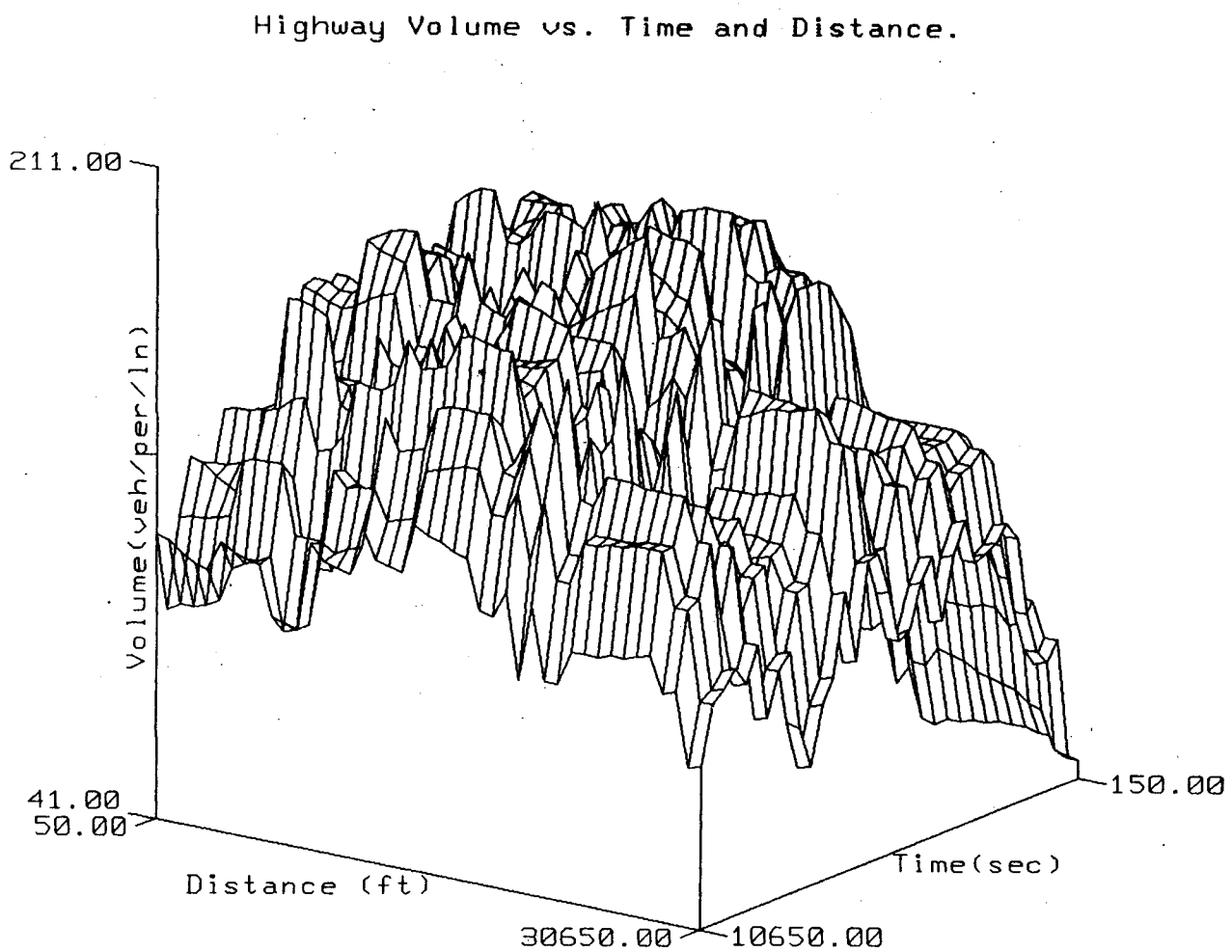

Figure 2-5 Three dimensional graph of volume for hypothetical demand

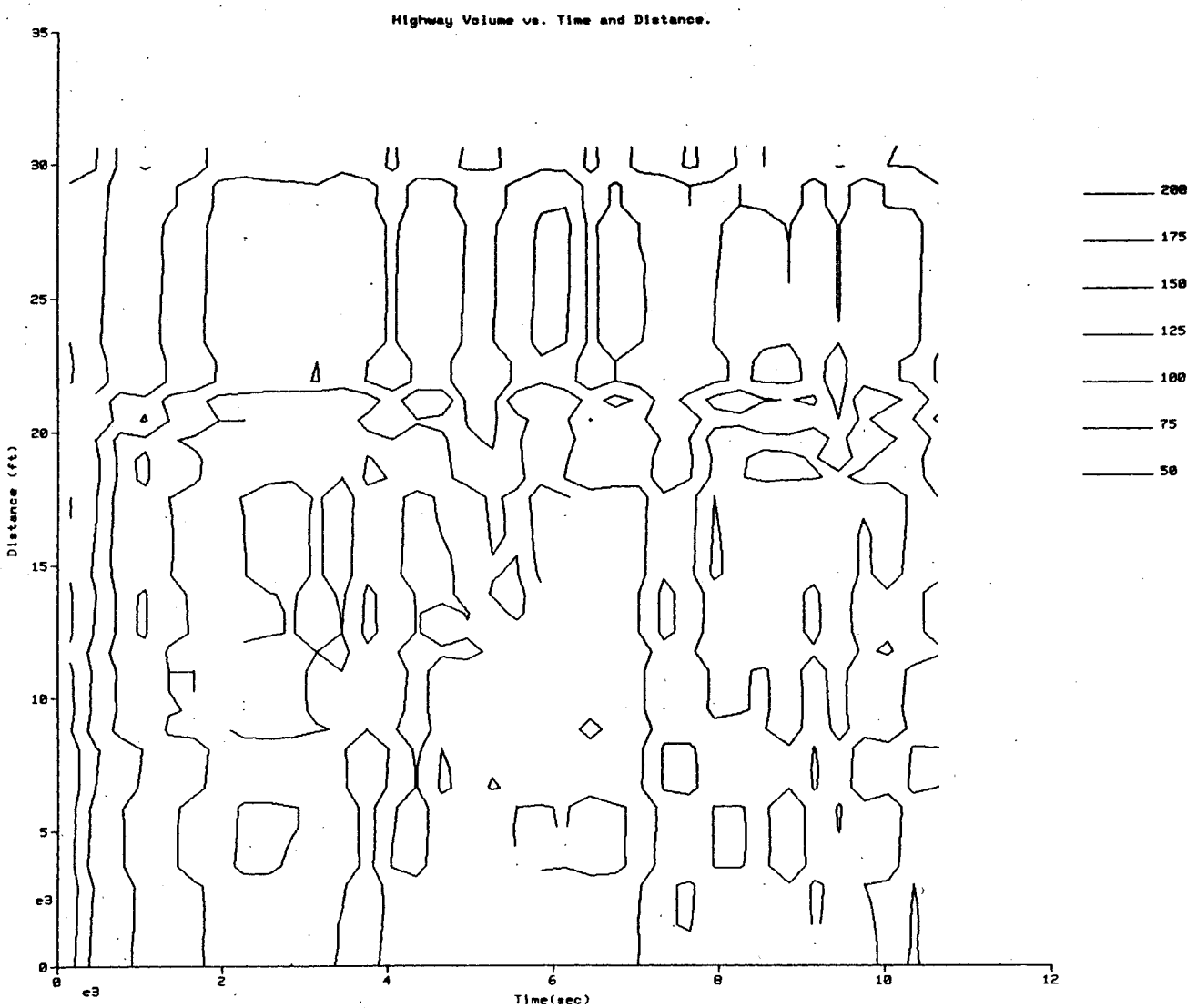

Figure 2-6 Two dimensional contour of volume for hypothetical demand

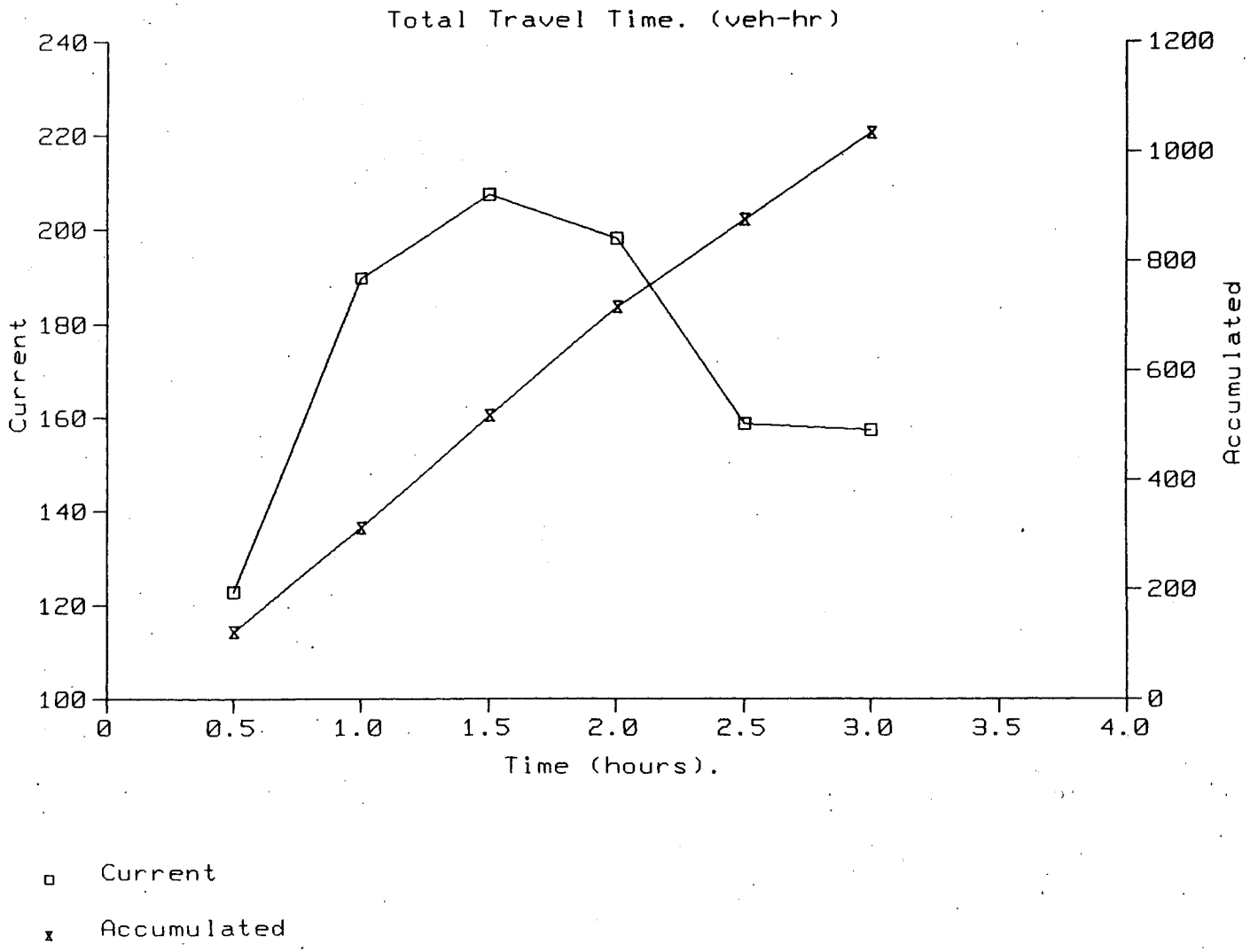

Figure 2-7 Two dimensional slice of volume for hypothetical demand

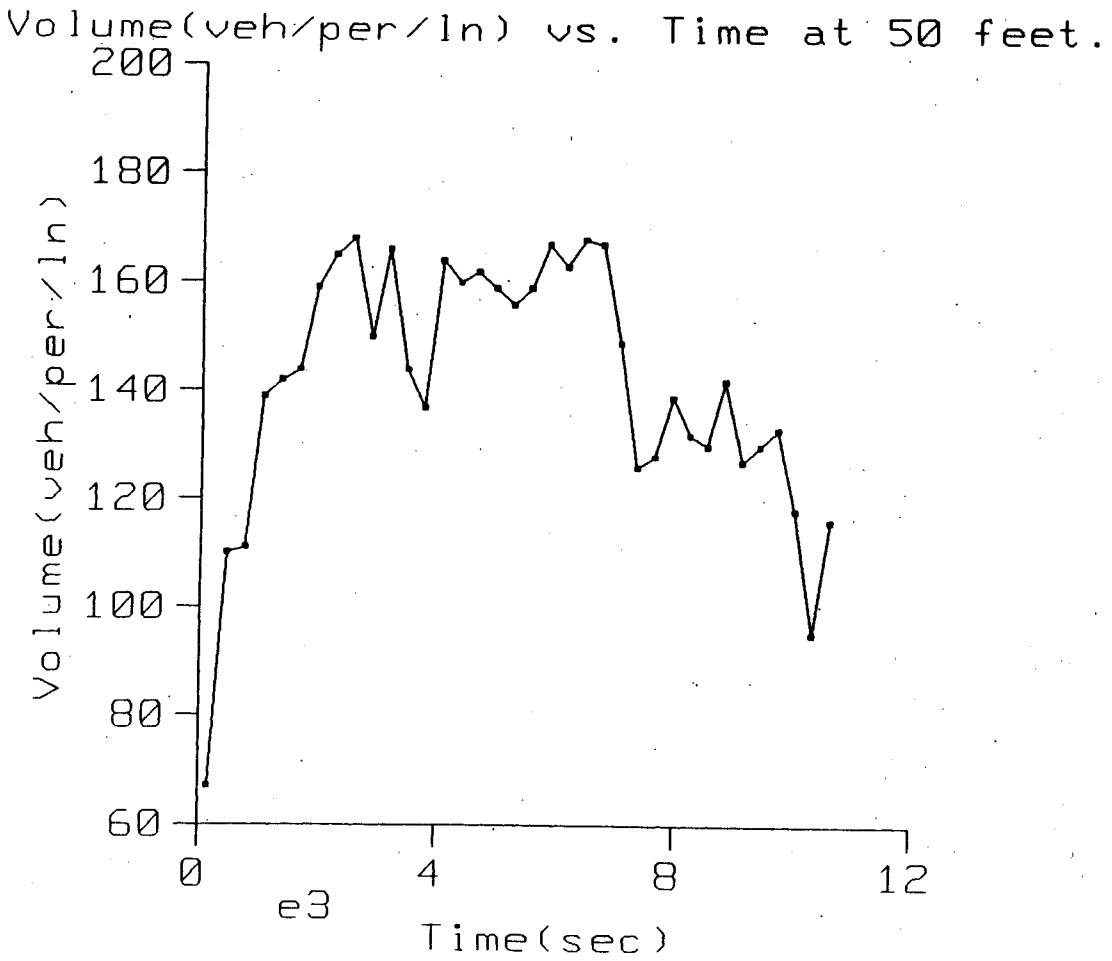

Figure 2-8 Two dimensional performance graph of total travel time for hypothetical demand

.DVL and .DOC, and red time data file, .MTR.

The detector station data file contains previous one-minute volume and occupancy data for each 30 seconds from each detector station, and *the red time data file* records the red time of each ramp meter for every 30 seconds.

The system performance index file, *.OPF, stores system performance indices for every half-hour period. The system performance indices include total travel time, total travel, average speed, entering volume, volume and speed variation, delay time, average occupancy time, and metering rate usage. Detailed description of these indices is presented in Section A.3.2.2 in Appendix A. Figure 2-8 illustrates a two dimensional performance graph of the total travel time from the output module. Other performance indices can also be displayed with similar graphs. From these indices and graphs the user can easily compare the effects of different control strategies on the controlled freeway system.

II.5 Limitations of the current version

The current version of the control-emulation software has the following limitations in terms of freeway section length and emulation time period. These limitations are mainly due to the computer memory restriction.

QUANTITY	MAXIMUM
Miles	14
Zones	100
Speed-Density Relationships	10
Speed-Density Pairs/Relationships	20
Detector Stations	40
Ramps (on)	20
Ramps (off)	20
Emulation Time	6 hours

Since the current version of the control-emulation software uses the zone number to identify the location of each zone, the freeway and ramp zone numbers must be sequential starting from one, from upstream to downstream, first for the freeway and then for the ramps. Further, the ramp control policy file requires specification of exactly six occupancy thresholds, six volume thresholds, six red time levels, and the detector stations associated with each ramp.

II.6 Conclusion

The original file-oriented input-output method of the control-emulation software is enhanced by introducing an interactive input-output module. The new input-output module

provides an interactive screen interface that allows the user to input data following screen prompts, tables, and graphs, as well as to summarize results with screen- and printed tables and graphs. Through this input-output module, the user can easily handle the control-emulation package.

In particular, the input module can be used for treating all highway geometry and ramp control policy data, with the exception of data describing traffic demand and diverging flow. The user can edit and modify the data from the screen following appropriate menus and prompts. Detailed definition of each input data item is described in Appendix A.

The new output module displays the emulation results on the screen with tables and graphs. System performance indices are summarized in tables and two-dimensional graphs. Traffic flow data, detector measurements, and ramp control data are plotted in three types of graph, the three-dimensional graph, two-dimensional contour, and two-dimensional slice. The user can easily analyze the effect of a control policy with these tables and graphs. With the new enhanced input-output modules, the control-emulation method provides traffic engineers a convenient tool for comparing and evaluating real-time metering control policies prior to implementation.

III. DEVELOPMENT OF METHODOLOGIES TO DETERMINE METERING THRESHOLDS AND RATE-TABLES USING CONTROL-EMULATION

III.1 Introduction

The automatic rate-selection metering control selects metering rates for a ramp from a pre-determined rate-library using the volume/occupancy information received from loop detectors on the main freeway. For instance, in Minneapolis metering rates at a ramp within a zone, which is defined by upstream and downstream bottleneck boundaries, are determined based on volume data from one mainline station upstream within the zone, and occupancy data from up to 9 mainline stations downstream of that ramp (Fig. 3-1). For each ramp, Minnesota Department of Transportation (Mn/DOT) traffic engineers have used historical data to derive a set of volume/occupancy thresholds and a rate-table consisting of 6 metering rates. Further, rate selection, every 30 seconds, is based on two measurements, i.e., the 1-minute upstream volume and the highest 1-minute occupancy selected from up to 9 downstream detector stations associated with each ramp. Therefore, the performance of the rate-selection control largely depends on how effectively the key components of the control, i.e., thresholds and rate-libraries, can be determined, so that they can achieve optimal traffic performance. Figures 3-2a and 3-2b illustrate an example set of metering thresholds and a typical set of volume/occupancy measurements at the I-35W freeway in Minneapolis.

In this research, a two-step methodology was developed to determine the metering thresholds and rate-tables for a given section of freeway using the control-emulation method. The first step determines the initial metering thresholds/rate-tables for each ramp using local traffic conditions. This step is required for initializing the second step (optimization) and can be skipped if such initial values are available from other sources, such as expert traffic engineers. The method uses factorial design procedure to systematically enumerate different sets of metering thresholds/rate-tables. The performance of each threshold set is then estimated using the control-emulation method and the set with the best performance is selected. The method could also be applicable in determining initial thresholds for a new section of freeway where no automatic rate-selection metering control has been implemented and no prior expertise from traffic engineers is available.

The 2nd step of the methodology is initiated with the values determined in the first step, and determines the best set of thresholds and rate-libraries for the current Mn/DOT zone metering control using the control-emulation method and the downhill simplex optimization procedure (Nedler and Mead, 1965). The method determines the optimal set of metering thresholds and rates for each ramp in a given section zone of freeway for the given traffic demand. Figure 3-3 illustrates the overall process to determine metering thresholds and rate-tables using the two-step

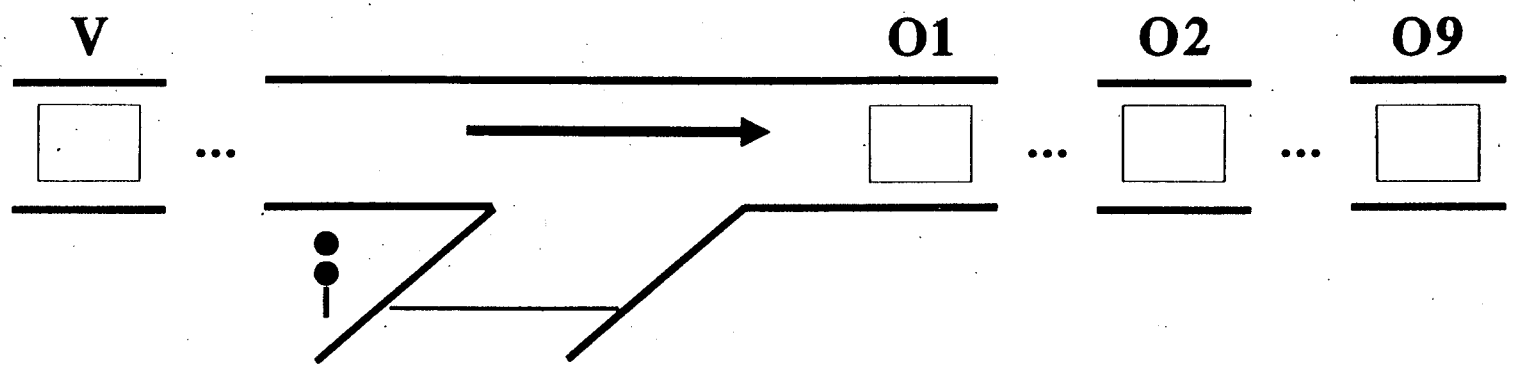

TMC Control

Upstream Volume = V

Downstream Occupancy = max{O1, O2, ..., O9}

Figure 3-1 Mainline freeway station configuration for current TMC control

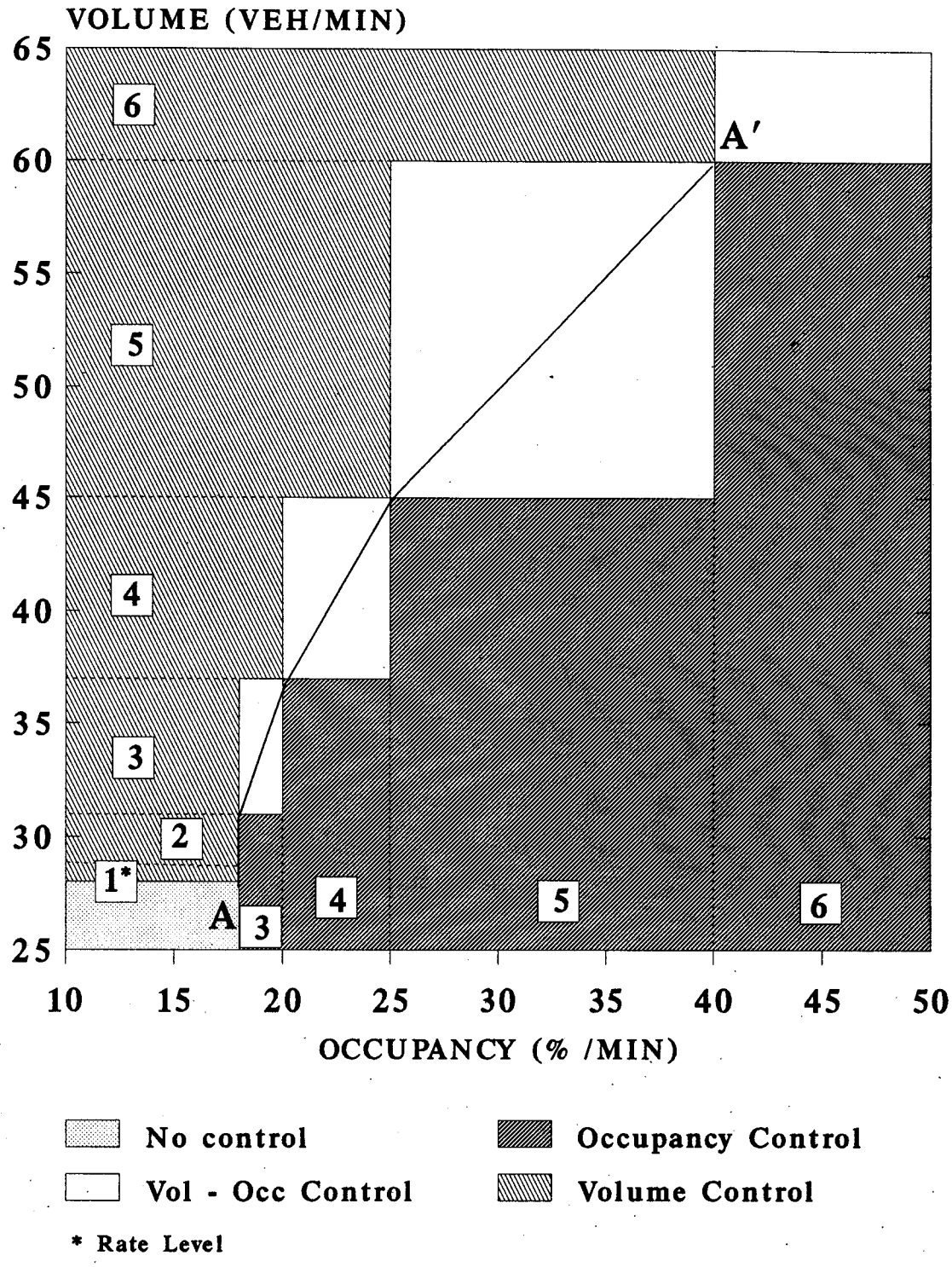

Figure 3.2a Example TMC metering thresholds (I-35W)

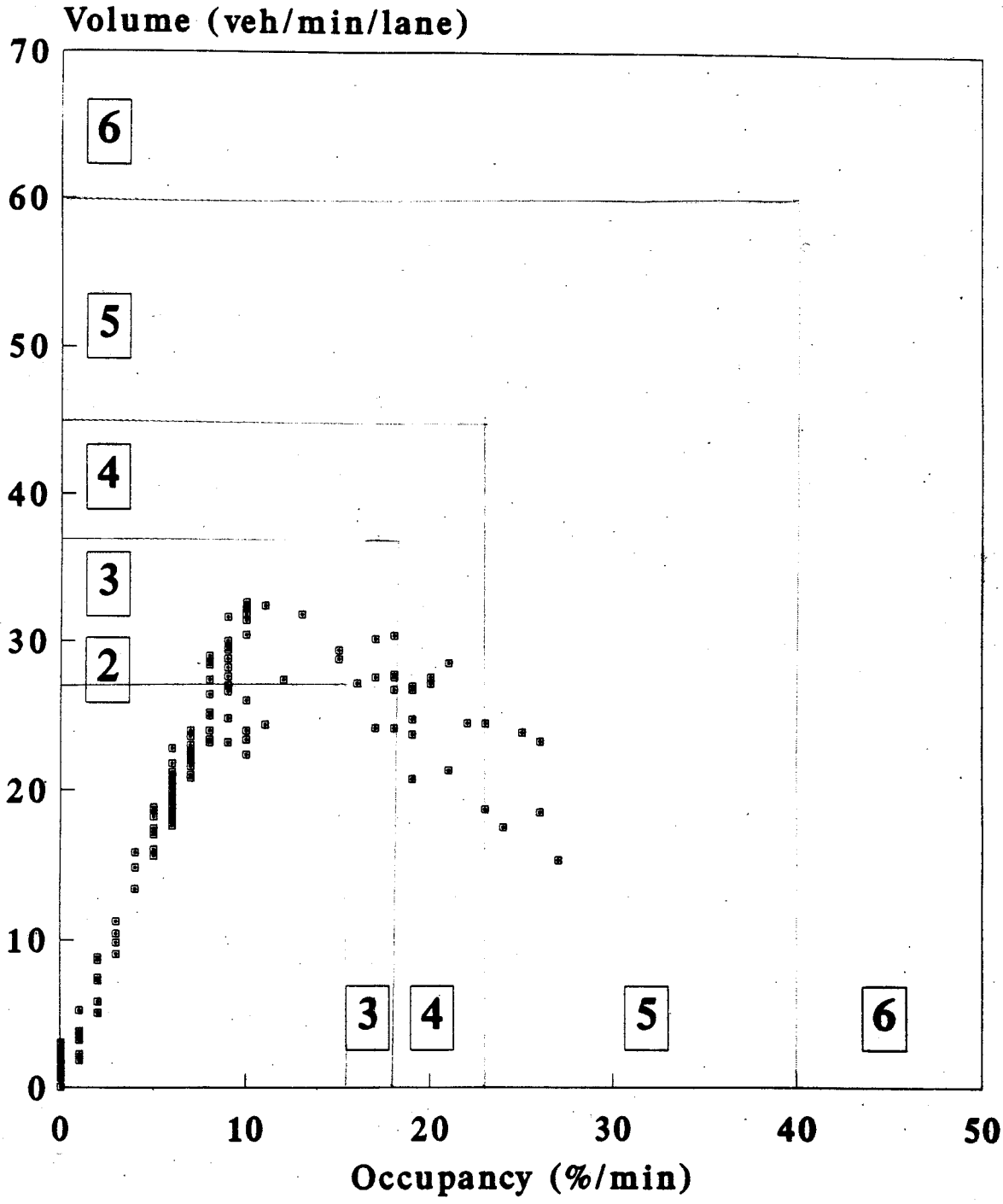

Figure 3.2b Metering thresholds and measured data (I-35W)

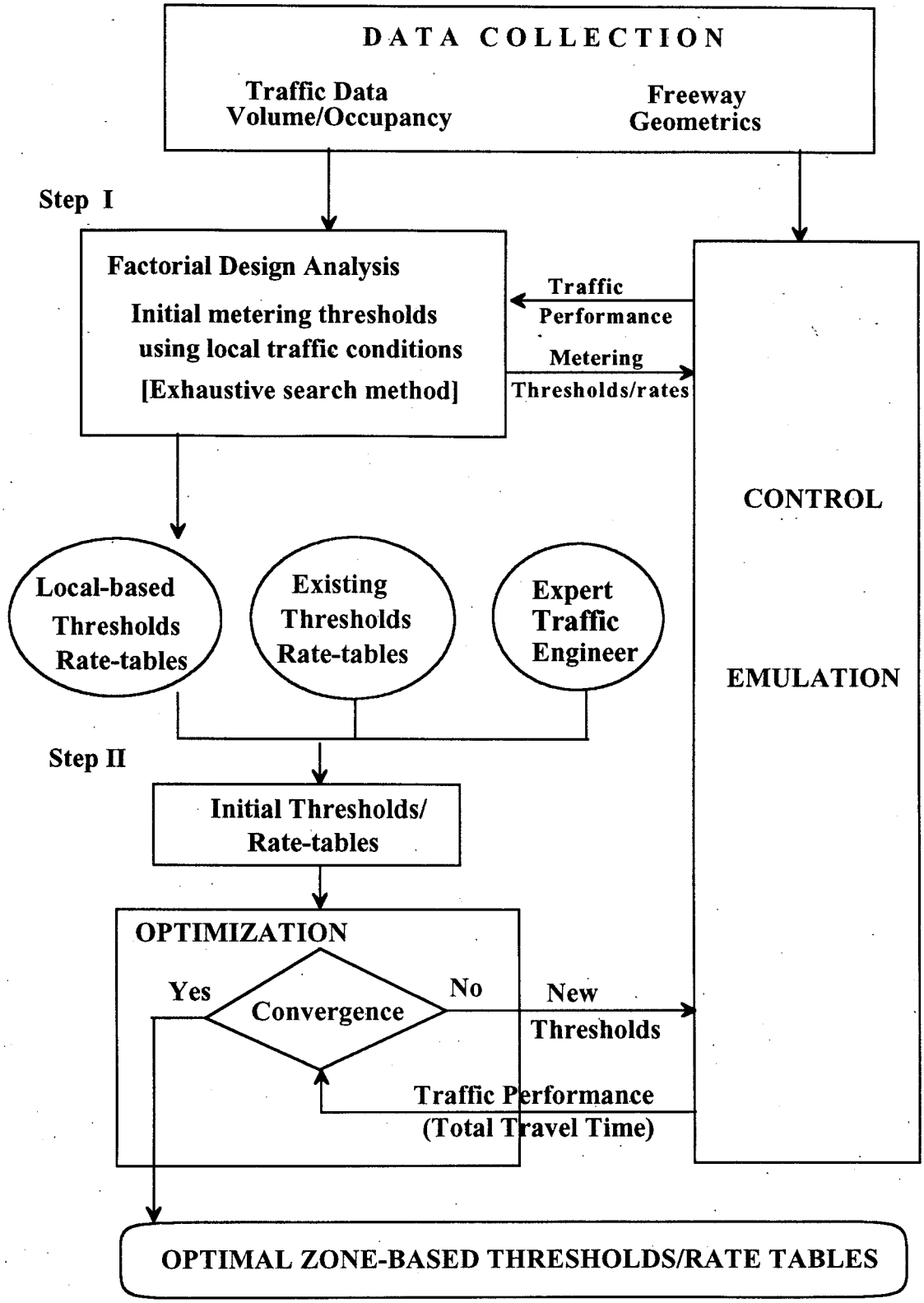

Figure 3.3 Overall process to determine thresholds using control-emulation

method developed in this chapter. As indicated in this figure, the metering thresholds determined with the 1st step can be used as initial thresholds in the optimization process. Based on these initial thresholds, the optimization module finds a new set of thresholds using the downhill simplex procedure. The performance of these new thresholds is then determined by the control-emulation module. The interaction between the optimization and the control-emulation modules continues through a number of interations until the optimization method converges to a certain pre-specified value, i.e., until no additional improvement can be obtained from any further iterations. The following sections summarize the two methods developed in this chapter.

III.2 Step I: Determination of initial metering thresholds using local traffic conditions

III.2.1 Design of method

Figure 3.4 shows the typical configuration of an entrance-ramp area. For initializing the control optimization process in the second step of the methodology, the first step of the method, developed in this section, determines the initial thresholds of the entrance-ramp by considering only local traffic conditions, i.e., the upstream volume and downstream occupancy. If initial values are available from other sources, this step can be skipped. Figure 3.5 illustrates the structure of the method that combines feedforward and feedback control. The upstream volume V_u and the downstream occupancy O_d are used as the input to the regulator, which determines the metering rates, V_r, that can keep the O_d close to $\hat{o}$, i.e., the critical occupancy.

By applying the conservation principle to the section between location 1 and 2 in Figure 3.4, the following equation can be obtained:

$$\dot{k}(t) = \left[V_u(t) + V_r(t) - V_d(t)\right]/L \qquad (3.1)$$

where the traffic density, k in veh/mile, is defined as the number of cars stored in the freeway section divided by the length L at time t. Since the traffic density is not directly measurable, it is convenient to replace k(t) in Equation 3.1 by the corresponding occupancy $O_d(t)$ using the approximate relationship as follows;

$$k = \alpha \cdot O_d$$

where $\alpha = \mu/(100 \cdot \lambda)$, μ is the number of lanes of the freeway and λ is the mean effective vehicle length (in miles). By replacing freeway density with occupancy, Equation 3.1 gives

$$\dot{O}_d(t) = \left[V_u(t) + V_r(t) - V_d(t)\right]/(L \cdot \alpha) \qquad (3.2)$$

Since the control input Vr is updated every T time units, we proceed to a time discretization of Equation 3.2 with sample time interval T which gives

$$O_d(t+T) = \beta \cdot O_d(t) + (1-\beta) \cdot \left[V_u(t) + V_r(t) - V_d(t)\right]/(L \cdot \alpha) \qquad (3.3)$$

the values for Vu, Vr, and Vd are assumed to be constant during the time interval T. The constant parameter β is dictated from the discretization procedure. Equation 3.3 assumes that

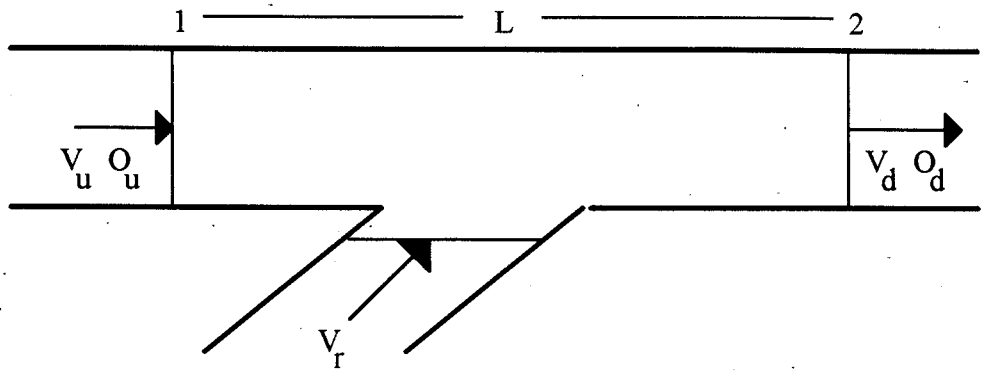

Figure 3.4 A typical entrance ramp area

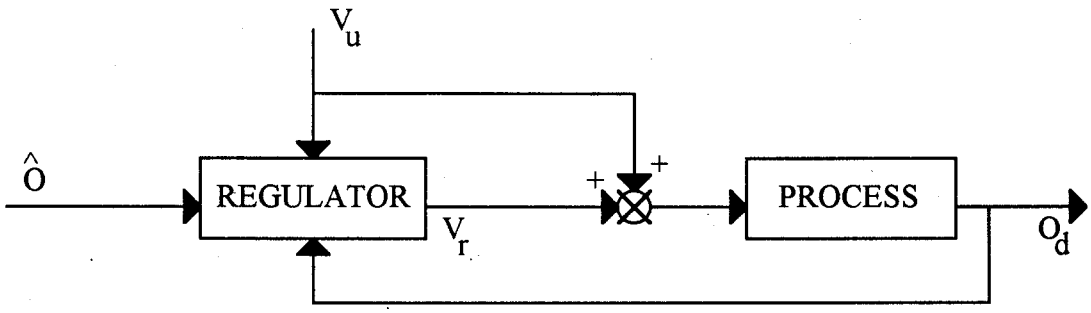

Figure 3.5 Feed forward/Feedback control logic

the occupancy variation at the downstream, i.e., location 2 in Figure 3.4, is a function of the net volume difference in the section between location 1 and 2. In general, because of geometric and traffic behavioral characteristics, a non-linear function, Q, can be assumed to estimate the downstream occupancy at time t+T as follows:

$$O_d(t+T) = \beta \cdot O_d(t) + (1-\beta) \cdot Q(V_u(t) + V_r(t)) \qquad (3.4)$$

By including the function Q (see Ch.4 for detailed expression of Q) in Equation 3.4, we incorporate the specific traffic characteristics of each freeway section. Use of Q makes necessary the calibration of Equation 3.4 with historical data.

Regulator Design

The regulator is designed so that the resulting metering rates can keep the downstream occupancy Od close to ô, the critical occupancy. Therefore by setting Od(t+T) = ô, the corresponding metering rates $V_r(t)$ for any values of $O_d(t)$ and $V_u(t)$ can be calculated from eqn. (3.4). Further, the resulting metering rates can be converted to red times, R(t), by assuming that in each cycle only one car is permitted to enter the freeway.

$$R(t) = \frac{3600}{V_r(t)} - 2 \qquad (3.5)$$

where R(t) is calculated in seconds.

For demonstration purposes, if we use a range for occupancy O_d from 0 % to 50 %, and for volume V_u 0 veh/min to 60 veh/min, then the calculated red times will take values as shown on Figure 3.6. The data shown in Figures 3.6 and 3.7 do not correspond to a real ramp metering application; they were calculated using an arbitrarily selected volume - occupancy curve (fundamental diagram). To be sure, by calculating the red times for all combinations of volume and occupancy we include values that are not realistic. For example, if occupancy and volume take a very small value, i.e., occ = 1 % and vol = 1 veh/min, there is no need to apply any metering and the calculation of the corresponding metering rate gives a negative value. On Figure 3.6 this corresponds to the area that is defined as "no control". Figure 3.7 shows the same information with the Figure 3.6 but in a 3D view. Figure 3.6 or Figure 3.7 can be used as a regulator in the control presented on Figure 3.5 to obtain specific values for the red times and the corresponding metering rates, given data for upstream volume and downstream occupancy.

III.2.2 Development of Factorial Design procedure

As described in the previous section, the resulting regulator from the proposed method is continuous and uses the upstream volume and the downstream occupancy as the input in determining the metering rates for a given ramp. To determine the control strategies for the automatic rate-selection system with this method, the following factors should be considered.

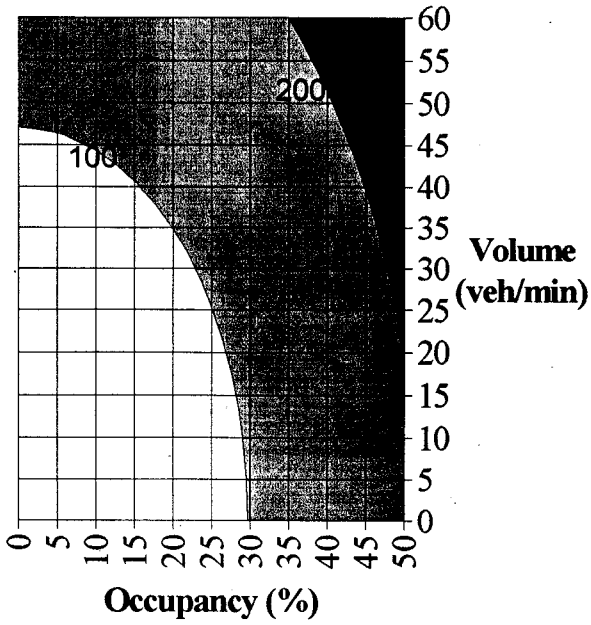

Figure 3.6 Contour plot of red times for the metering rate as a function of the freeway downstream occupancy and the freeway upstream volume

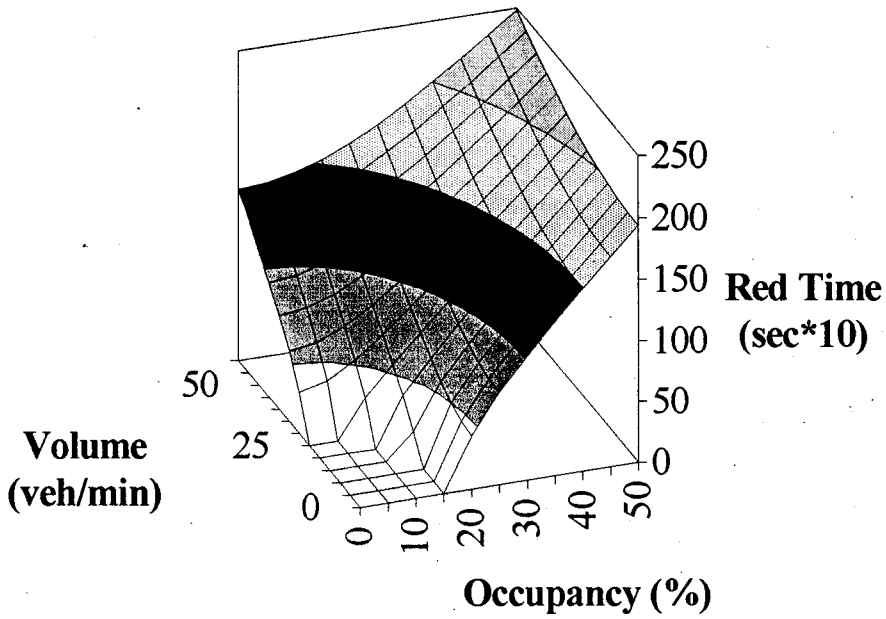

Figure 3.7 Red times as a function of the downstream occupancy and upstream volume

- Automatic rate selection systems are discrete (not continuous), i.e., use a predefined set of metering rates. For example, the Minneapolis and the Denver control systems use 6 metering rates for each entrance-ramp, the Chicago control system uses 5 rates, and the Los Angeles control system 15 metering rates.

- The selection of metering rates is based on the use of a number of control thresholds equal, to the number of metering rates. The selection of discrete metering rates using the contiuous formulation described in the previous section is performed by comparing each threshold with the traffic measurement. For example, if we have 5 metering rates R_1, R_2, ..., R_5 and 5 occupancy thresholds O_1, O_2, ..., O_5, the measured freeway occupancy O is compared with the occupancy thresholds. If $O < O_1$, no metering rate is applied, if $O_1 < O < O_2$, R_1 is applied; ...; and if $O_5 < O$, rate R_5 is applied.

The control resulting from the proposed method must be modified so that it provides a set of volume and occupancy thresholds given a number of predefined metering rates. By drawing the 2-dimensional image of Figure 3.7 we can sketch a contour graph of the function, similar to Fig.3.6, and draw the contours that correspond to the desired metering rates. For example, a contour plot of the red times is shown on Figure 3.8. On this graph we select the contour lines to be assigned to the desired metering rates. If there are 6 metering rates, the contour lines will result in a graph such as the one on Figure 3.8. All points on a contour line represent different freeway traffic conditions that result in the same metering rate. Any point, of this curve, can be used as the critical freeway traffic condition for which the control system must switch to a more restrictive metering rate. This results to an infinite number of possible threshold values for the same metering rate. Additionally, if we consider all the metering rates, an infinite number of combinations is available in selecting a threshold set. To reduce the complexity in deriving the threshold set we should consider the following:

- Any threshold point (O_i, V_i) that corresponds to a metering rate R_i must satisfy $O_{i-1} < O_i < O_{i+1}$ and $V_{i-1} < V_i < V_{i+1}$. This implies that the threshold point for rate i must correspond to a more congested traffic condition, in terms of occupancy and volume, than the threshold point for metering rate i-1.
- If we draw a curve that passes through all the threshold points, this curve has the following characteristics. The starting point of the curve, which is the threshold point for the first metering rate, determines how restrictive the control will be, as Figure 3.9a demonstrates. The slope of the curve determines the sensitivity of the control as volume and occupancy

change (Figure 3.9b).

If it is possible to derive the position of the threshold curve, the threshold point (O_i, V_i) is defined by the intersection of the threshold curve and the contour curve for the metering rate i. One way to define the position of the threshold set is to apply a factorial design analysis. This statistical method can provide information about the input data, such as presence of interaction between the input parameters, and perform test of significance for all the input parameters.

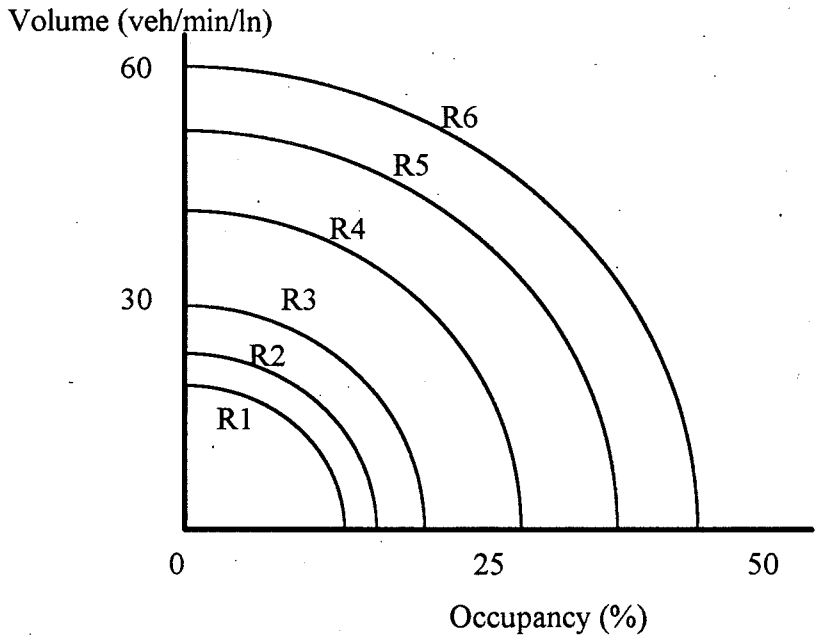

Figure 3.8 Contour plot of the 6 red times curves

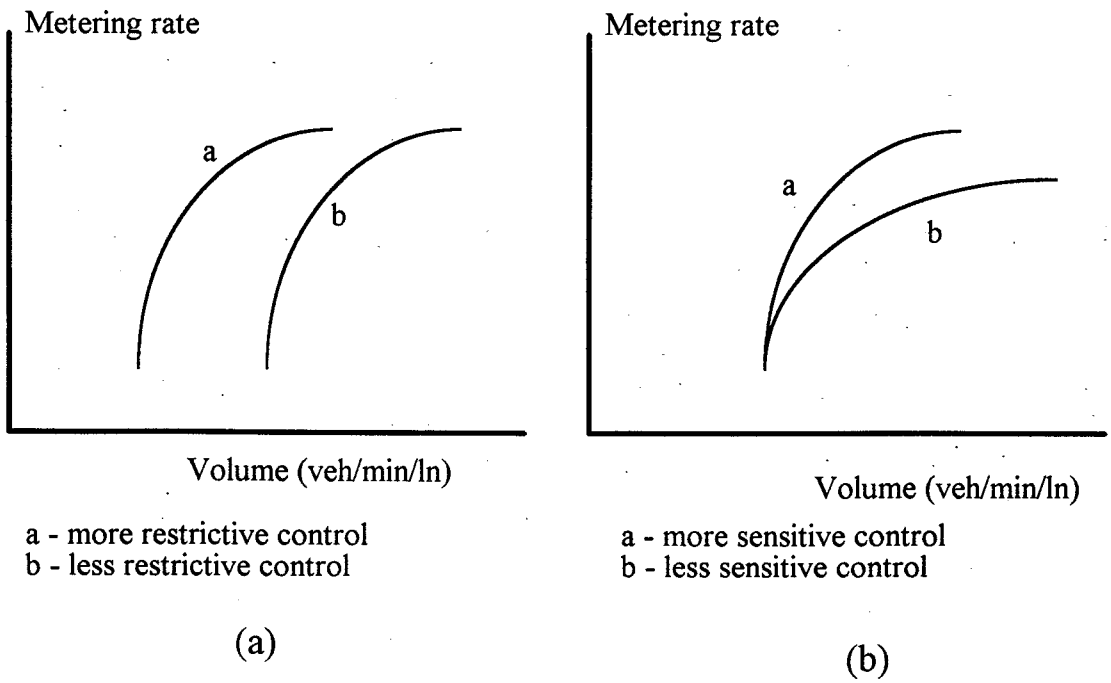

Figure 3.9 Different types of control curves

Additionally, because it does explicit search for all the possible inputs, the method can give information about the values of the input parameters which minimize or maximize the desirable output value. For example, we can find the threshold curve which minimizes the total travel time on the freeway. To be sure, if this (initial) threshold curve can be determined from other sources or engineering experience, this step can be skipped.

Factorial Design Analysis

Many experiments involve a study of the effects of two or more factors (Montgomery, 1992) In this application three factors are used to define the threshold curve: the starting point, the slope of the curve, and the shape of the curve. The factorial design investigates all possible combinations of the input factors. The effect of a factor is defined to be the change in response produced by a change in the value of the factor. This is frequently called main effect because it refers to the primary factors of interest in the experiment. The computational formulas for the factorial design analysis are summarized in Appendix D.

Application of Factorial Design Analysis

The factorial design analysis was performed for a typical entrance-ramp configuration (Figure 3.4). In addition, six metering rates were selected as the predefined metering rates of the entrance ramp, and a volume-occupancy curve (fundamental diagram) was assigned to describe the traffic flow behavior of the freeway section. Using this information the 6 metering curves were derived. Figure 3.10 shows the 6 metering curves and the different threshold curves used as input data for the factorial design. Three properties of the threshold curve were used as factors for the design, the position, the slope, and the shape of the curve. For each curve a threshold set was defined and it was used as input for a simulation program. This program was developed in the University of Minnesota to simulate different control policies [Stephanedes, et. al., 1992]. The program ran a three hour simulation for each case and gave the resulting freeway performance indexes, total travel time, total entering volume, ramp entering volume, speed variations and delay. For each property of the threshold curve 5 different inputs were selected and this resulted to 5^3 data inputs and to the same number of simulation outputs; these outputs were used in the factorial design analysis. Table 3.1 summarizes the results from the factorial design. As the results indicate the position of the threshold curve is the most important factor, the second important factor is the slope, and the least important factor is the shape of the curve. As mentioned in the beginning of this section the position of the threshold curve affects the behavior of the control, making it more or less restrictive, and the slope of the curve increases or decreases the sensitivity of the control. The explicit search that was performed for the factorial design analysis showed how each of the

threshold curve characteristics affect the control performance. This search also provided the data to perform a kind of optimization and find the curve which has the best performance. The curve with the best performance was the one that had as value for the first occupancy threshold the desired downstream occupancy, $O_1 = O_{cr}$. The possible shapes and the rotations of the curve are shown on Figure 3.10.

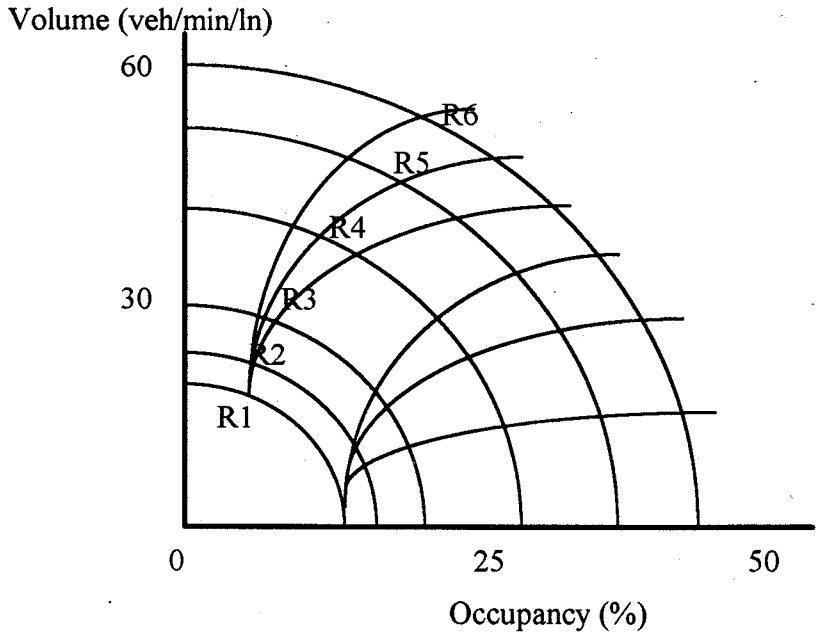

Figure 3.10 Contour plot of the 6 red times curves and 6 of the threshold curves used in the factorial design analysis

Table 3.1 **Results of the factorial design analysis (F values)**

	Position	Slope	Shape
Total Entering Volume (veh/hr)	91.446	11.234	3.882
Total Travel Time (veh.hrs)	21.388	4.550	2.247
Ramp Entering Volume (veh/hr)	90.991	11.160	3.882
Speed Variations (%)	12.422	2.796	1.926
Delay (Speed<45mph)	9.878	3.564	2.315

III.3 Step II: Determination of optimal zone-based metering thresholds and rate-tables

III.3.1 Method overview

The first step of the method, developed in the previous section, determines the initial metering thresholds for a ramp considering only local traffic conditions. Using the results from the first step as initial conditions, the second step of the method is developed in this section. Determining metering strategies that can optimize the performance of a freeway zone consisting of multiple ramps is the objective of the second step. The new method finds optimal metering thresholds of each ramp within a freeway zone, which is defined by upstream and downstream boundaries, so that the traffic performance of the entire zone can be optimized. Figure 3.11 illustrates an example freeway zone consisting of four entrance ramps. For each entrance ramp area, the method developed in the previous section can be applied and the initial, local-based metering thresholds for each ramp can be determined. These thresholds are then used to initialize the optimization process, combining the downhill simplex procedure and the control-emulation method, which finds the best set of thresholds and rate-tables that optimize the traffic performance of the entire zone. Appendix E briefly reviews existing optimization methods and summarizes the new optimization procedure.

III.3.2 Development of the optimization module with the downhill simplex method

In this research, the downhill simplex method was used to find the optimum values for the thresholds and the metering rates. The major advantage of the simplex method over other optimization methods is that it does not require any derivatives of the objective function. This is very important in this research, because the "function" that must be minimized is not an actual formula but the output of the control-emulation method. Further, the objective function to be

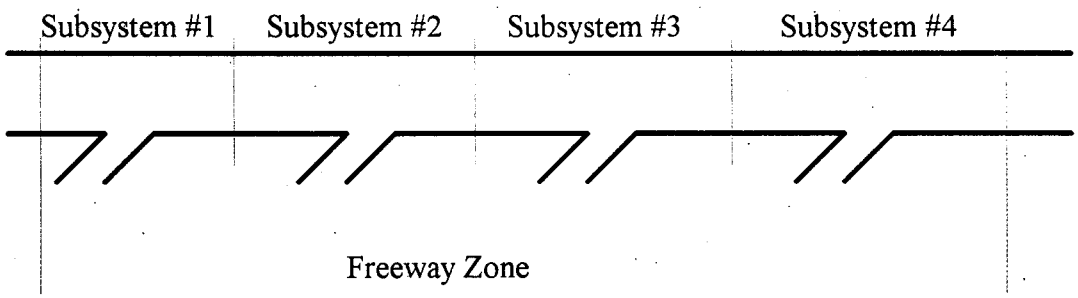

Figure 3.11 An example freeway zone including four entrance ramps

optimized can be a single performance index, such as Total Travel Time, or any combination of multiple indices. While the simplex procedure converges with most initial conditions, the value of initial points substantially affects the time needed to converge. Therefore, the initial thresholds determined with the first method, based on the local traffic conditions perform a critical function as initial thresholds in the optimization process.

III.4 Summary

This chapter developed two steps of a methodology that can determine metering thresholds and rate-tables for each ramp in a given section of freeway using the control-emulation method. The first step determines initial metering thresholds using the local traffic conditions. For each entrance ramp in a given freeway section, the method first identifies a statistical relationship among upstream volume, downstream occupancy and metering rates. Using this relationship, the metering rates that can make downstream occupancy close to the desired level can be determined for various values of upstream volume. Factorial design is then employed to systematically enumerate multiple alternative sets of metering thresholds and rate-tables for each ramp. The performance of each alternative set is calculated by the control-emulation method and the set with the best performance is selected.

The second step of this method developed in this chapter determines the optimal zone-based metering thresholds and rate-tables using the control-emulation method and the downhill simplex optimization procedure. This step is initialized with the metering thresholds determined in the first step of the method. The simplex optimization procedure does not require any derivatives of the objective function. Therefore, the output of the control-emulation method can be directly used as the optimization index. The performance of the traffic system based on the new thresholds is then determined by the control-emulation method. The interaction between the optimization and the control-emulation modules continues through a number of interations, until the optimization method converges to a certain pre-specified value, i.e., until no further improvements can be obtained from any further iterations. The method requires traffic data from the freeway section to calibrate the control-emulation module. The first step of the method also requires identification of statistical relationships among upstream volume, metering rates and downstream occupancy.

IV. FIELD-EVALUATION OF THE NEW OPTIMIZATION METHOD USING THE I-494 TEST SECTION

IV.1 Introduction

In this chapter, the new optimization method developed in the previous chapter was applied to a section of the I-494 freeway in Minneapolis. First, a set of metering thresholds was developed for each ramp using the initialization module. These thresholds, reflecting only local traffic conditions, were then used as initial thresholds in the optimization module, which determined the thresholds for each ramp by considering system-wide traffic conditions under the given management objective. The resulting optimal thresholds were then implemented at each ramp in the test section in December 1992. The traffic performance in the test section, before and after the new control, was then evaluated using the data collected from the loop detectors located in the test section. The rest of this chapter summarizes the evaluation results.

IV.2 Test freeway section and calibration of the control-emulation method

A section of the Westbound I-494 freeway from Portland Ave. to E. Bush Lake Road was selected as a test site in consultation with Mn/DOT Traffic Management Center (TMC). The selected 6.2-mile section of I-494 contains 19 entrance/exit ramps and a variety of highway geometrics including merging, diverging and weaving areas and, in particular, the junction with the I-35W freeway. The junction generates strong weaving effects and congestion that influence the performance of the control at all neighboring ramps. The test section is presented in Figure 4.1, which also includes the loop detector locations, including main freeway, entrance and exit ramps, where volume and occupancy measurements can be obtained every 5 minutes.

The method developed in the previous chapter requires traffic data, i.e., volume and occupancy, from the freeway section in question. The first data collection from the test section was conducted in May 1992. These data were used to test the control-emulation module and to develop the optimization procedure. Additional data collection was conducted for 6 weeks in November 1992 and February 1993. The data from the first three weeks represent the traffic performance with the previous Mn/DOT thresholds and were used to calibrate the control-emulation module and to initialize and develop zone-based thresholds for the test section. The data from the remaining three weeks were collected after the new optimized thresholds were implemented. For both periods, only the data collected on Tuesdays, Wednesdays, and Thursdays were used in this research, since these three weekdays are believed to represent normal weekday traffic patterns. Further, for the development of optimal zone-based thresholds traffic data from the days close to holidays were not used in this study.

First, the control-emulation method was tested and calibrated by simulating the current

TMC control policy at the test site. Figure 4.2 shows the simulated volume and real data for a weekday in May, 1992. Table 4-1a indicates that the absolute mean percentage error ranges between 0.46 and 9.89% for the a.m. rush hour and 0.09-22.3% for the p.m. rush hour. The relatively large error at detectors 187 and 189 can be attributed to the fact that the exact location of these two detectors was not available when the test was conducted.

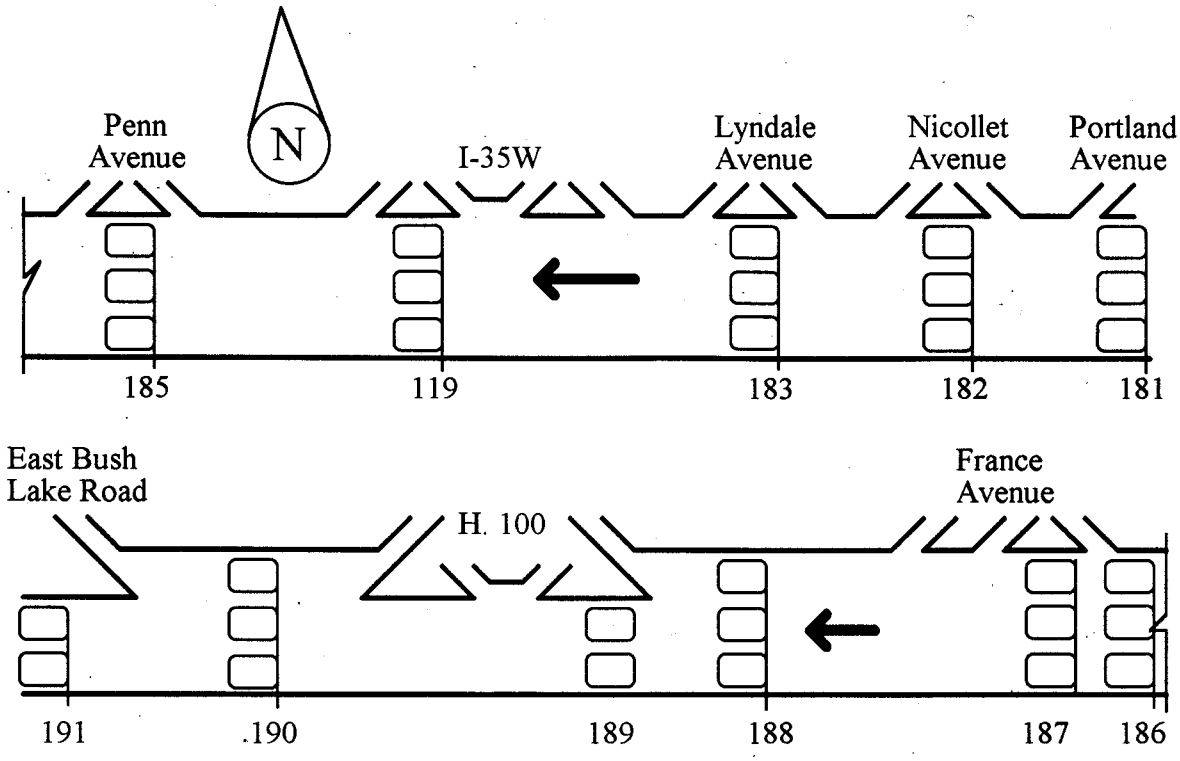

Figure 4.1 Location of test freeway section (I-494 Westbound)

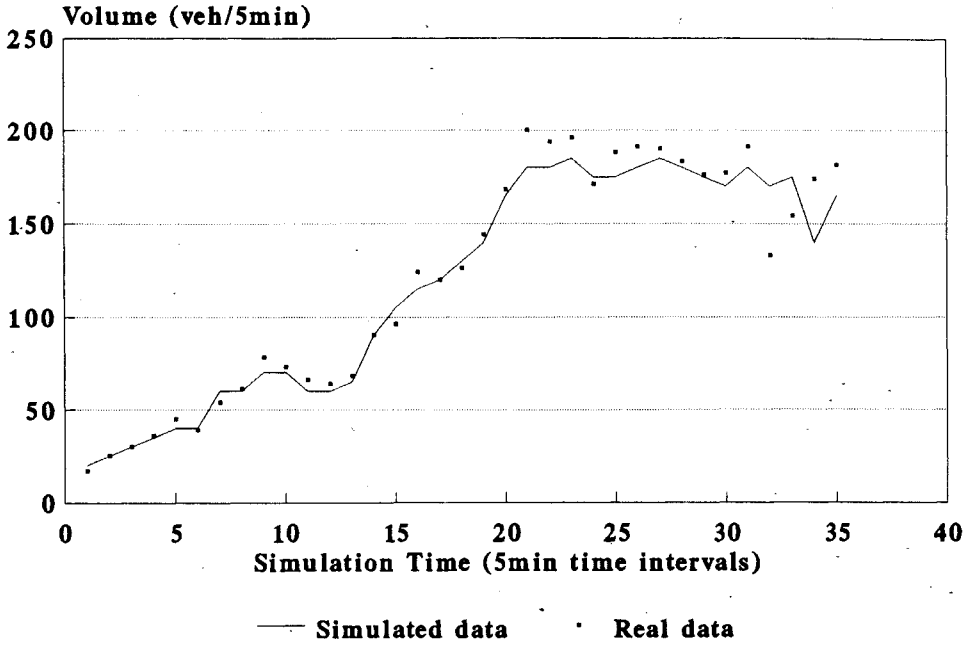

(6 a.m. - 9 a.m.)

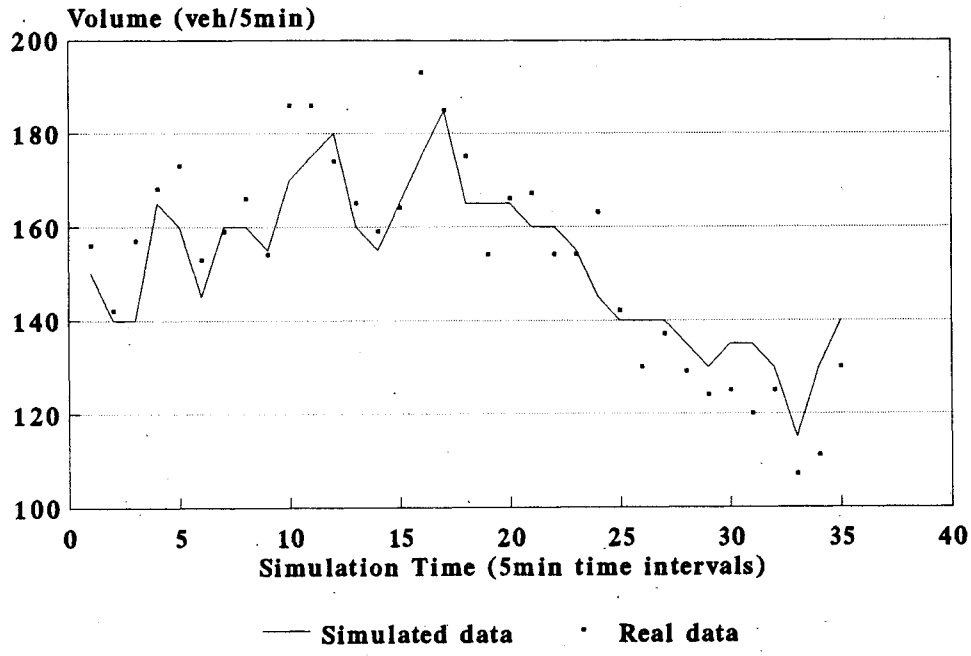

(4 p.m. - 7 p.m.)

Figure 4-2 Comparison between real and simulated volume values

(Weekday, May, 1992, Detector station 119)

Table 4-1a **Absolute mean percentage error**

Detector Station	A.M. Rush Hour (6 - 9 a.m.)	P.M. Rush Hour (4 - 7 p.m.)
181	0.486	0.089
182	3.471	0.412
183	1.231	0.734
119	1.492	0.189
185	2.451	1.909
186	0.462	1.892
187	3.320	13.420
188	-----[1]	5.954
189	9.892	22.252
190	4.429	13.510
191	-----[1]	1.288
Total	3.026[2]	5.604

[1] Comparison was not possible due to detector failure.

[2] Average over 9 detector stations.

IV.3 Determination of the initial metering thresholds using local traffic conditions

First, the local-condition based initial thresholds for each ramp in the test section were determined using the first step of the method developed in the previous chapter. The 5 minute volume and occupancy collected over a period of three weeks were used in this analysis. The threshold values produced from this step of the methodology were used as initial values for the optimization module. The procedure will be described in detail for one ramp, at Portland Avenue, since the same procedure was applied for all ramps.

Initially, the function Q (fundamental diagram) is calculated for each entrance ramp. The equation has the general form

$$Q(O) = a \cdot O + b \cdot O^2 + c \cdot O^3 \qquad (4.1)$$

The factors for Equation 4.1, summarize in Table 4.1, were calculated for each entrance ramp using traffic data. Figure 4.3 presents a graph of the data used for the Portland Avenue ramp. Each point represents a 5 minute measurement. The value of the volume on the graph is the result of the upstream volume of the zone plus the ramp entering volume minus the exit ramp volume. The value of the occupancy corresponds to the measurements from the first downstream detector. The solid line on the graph is the volume calculated by the least squares method, and the desired downstream occupancy is defined at the point where volume takes its highest value. In particular, for the Portland Avenue ramp the desired occupancy is approximately 18% as Figure 4.3 indicates. For every ramp Equation 3.4 was used to calculate the metering rates that correspond to given data on freeway traffic conditions. To eliminate the variable for the exit ramp demand this volume was expressed as a percentage, p, of the mainline volume. Table 4.2 summarizes the percentages used to express all exit demands determined by averaging all 3 weeks data (a.m. and p.m.). Additionally the constant β on Equation 3.4 was assumed to be $\beta = 1/2$. Equation 3.4 can be rewritten as

WHAT EXIT RAMP?

$$O_d(t+T) = \left(O_d(t) + Q\left((1-p)\cdot\left(V_u(t)+V_r(t)\right)\right)\right)/2 \qquad (4.2)$$

Equation 4.2 includes only three variables, the upstream volume V_u, the ramp entering volume V_r, and the downstream occupancy O_d. At this point, for each ramp, we replace the contiuous variable V_r (ramp volume) with the six metering rates V_{r1}, V_{r2}, ..., V_{r6} that are currently used by the TMC. Equation 4.2 becomes

$$O\left(O_d(t) + Q\left((1-p)\cdot\left(V_u(t)+V_{ri}(t)\right)\right)\right)/2 \qquad (4.3)$$
$$for \quad i = 1, 2, \ldots, 6$$

and this represents a family of six threshold curves corresponding to the six values for the metering rates. The six curves define 7 areas, six for the metering rates and one for "no control"

Table 4.1 **Factors of Equation 4.1 for each entrance ramp**

	a	b	c
Portland	42.779	-1.491	0.012
Nicollet	65.427	-4.123	0.070
Lyndale	50.506	-2.179	0.023
35W S-W	47.645	-1.418	0.004
Penn	61.137	-3.147	0.042
France N-W	44.596	-0.413	0.032
France S-W	58.780	-2.817	0.026
H100 N-W	52.733	-1.209	0.011
H100 S-W	35.115	-1.896	0.036

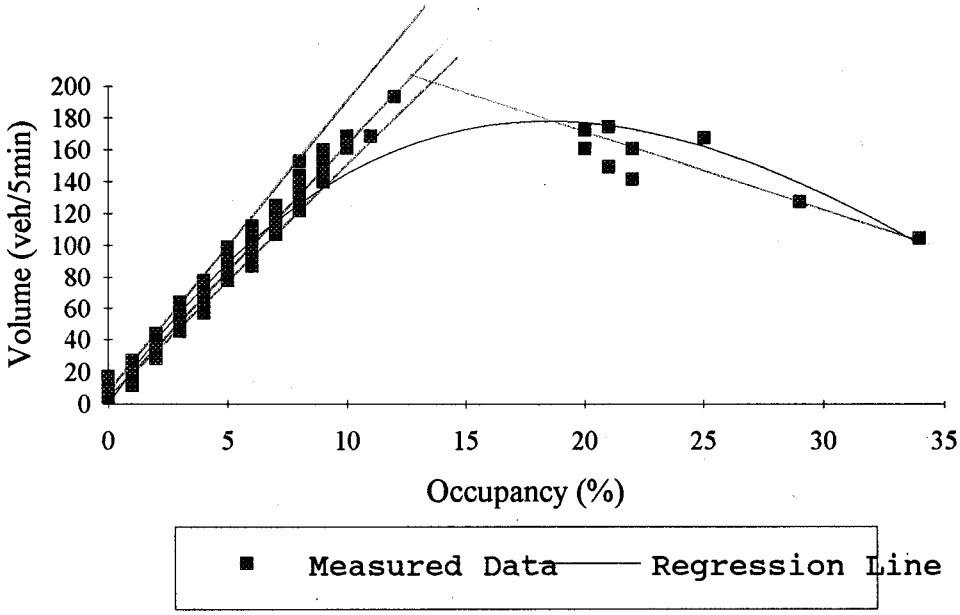

Figure 4.3 Sample traffic data (Portland Avenue)

Table 4.2 **Exit volume proportion (%) of mainline volume**

Exit Ramp Location (I-494 Westbound)	p (%)
Nicollet	7.6
Lyndale	8.0
35W N-W	18.8
35W S-W	14.4
Penn	16.3
France N-W	23.5
France S-W	6.8
H100 N-W	27.2
H100 S-W	22.8

These are entrance ramp names. Are they mislabeled? Why are there two labeled France?

ARE THESE INTENDED FOR AM TRAFFIC OR FOR PM TRAFFIC?

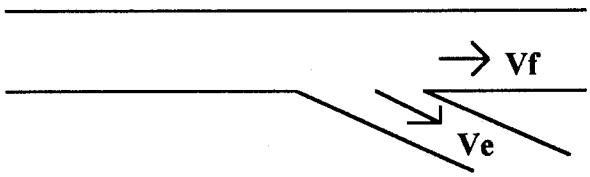

$$p = Ve / (Vf + Ve) * 100$$

Table 4.3 **Threshold values and metering rates for the test freeway section of I-494**

AM.	Red Times						Volume					
Portland	14	45	57	76	84	147	21	21	24	32	44	60
Nicollet	15	40	63	66	88	196	31	31	34	40	49	60
Lyndale	15	42	61	90	181	197	29	29	32	39	49	60
35W S-W	4	15	20	33	36	68	26	26	29	37	47	60
Penn	18	61	82	120	162	170	22	22	25	33	45	60
France N-W	13	42	55	57	94	194	28	28	31	38	49	62
France S-W	17	49	78	143	156	257	30	30	33	40	49	60
H100 N-W	6	17	26	46	71	84	30	30	33	40	49	59
H100 S-W	19	78	112	196	217	267	13	15	18	26	39	60

P.M.	Red Times						Volume					
Portland	8	24	43	47	75	100	19	19	23	31	44	60
Nicollet	13	34	47	74	89	168	30	30	33	40	49	60
Lyndale	10	27	34	39	48	71	28	28	31	38	48	60
35W S-W	8	24	28	46	48	95	26	26	29	37	47	60
Penn	11	33	61	72	75	135	20	20	24	32	44	60
France N-W	13	42	55	57	94	194	28	28	31	38	49	62
France S-W	16	46	70	120	126	179	30	30	33	40	49	60
H100 N-W	7	20	30	56	95	127	30	30	33	40	49	59
H100 S-W	18	36	46	60	86	130	13	13	16	24	28	60

For all ramps the occupancy thresholds are:

17 17 17 18 23 40

unit: 1/10 second.

We select a point on each curve, such that the coordinates of the six points are the six volume and occupancy thresholds. If the points are connected with a line, they form a curve, the threshold curve. To specify the position of the curve the results of the factorial design are used. After the threshold curve is defined, the threshold points are determined by the intersecting points of the curve with the 6 metering curves. Table 4.3 summarizes resulting threshold values and metering rates determined using the average week-day traffic demand pattern for the test section.

IV.4 Determination of the optimal thresholds using the downhill simplex method

IV.4.1 Determination of the optimization index

In this section, the volume/occupancy thresholds derived in the previous section, are used to initialize the zone optimization method. Because of hardware and software limitations in the current Mn/DOT control system in the test section, the following restrictions were applied in the optimization process:

- The values of the occupancy thresholds are fixed for the whole freeway system.
- The volume thresholds can be changed but they should be the same for all ramps in the control zone.
- The metering rates can be changed and they can be different across ramps. The red times must lie between the values of 0.8 sec and 25 sec.

The first restriction is necessary since the occupancy values are directly related to the sensitivity of the loop detectors.

TMC has two primary objectives: First, to reduce the delay on the freeway and keep the freeway traffic running smoothly (reduce the volume and speed variations), and, second, to achieve equal waiting times across entrance ramps. The use of the simplex algorithm in combination with the use of the total travel time including waiting time as the performance index satisfies both objectives. More specifically, at each step of the simplex algorithm the point with the highest value of total travel time including waiting time is replaced with another one. As a result the method first seeks to improve conditions at the ramps that have long delays and affect significantly the total travel time including waiting time of the system.

IV.4.2 Problem Reduction

The I-494 test section includes 9 ramps that are currently metered. For each ramp, the current control strategy uses a set of six metering rates. This makes a total of 9 x 6 = 54 variables. Additionally, a set of volume thresholds, i.e., 6 parameters, is used for the entire control zone. These values formulate an optimization problem with 54 + 6 = 60 dimensions. The minimization of a function with 60 dimensions would be very slow, i.e., lead to long computation time, and not very practical. A way to reduce the size of the problem is to replace any set of six thresholds t_1,

t_2, ..., t_6 by two parameters, p_1 and p_2, with the following procedure,

$$a_i = \frac{t_i - t_1}{t_6 - t_1}, \quad p_1 = t_1, p_2 = t_6 - t_1 \quad for \quad i = 1, 2, ..., 6 \tag{4.4}$$

Following this problem reduction, the set of a_1, a_2, ..., a_6 will be constant throughout the optimization procedure and only the values of p_1 and p_2 will change. The a_i values range from 0 to 1. For example, if the six thresholds t_i were: 26, 28, 30, 34, 40, and 60, the a_i's would be 0, 0.059, 0.118, 0.235, 0.412, and 1, and p_1 = 26, p_2 = 34. Using this procedure to reduce the problem size the optimization now has (9 x 2) + 2 = 20 dimensions.

IV.4.3 Determination of optimal thresholds

The downhill simplex method was used to determine the thresholds and metering rates that can minimize the total travel time of the main freeway and ramps in the test section. The total number of parameters used in the optimization process was 20. The first 18 parameters correspond to the metering rates of the 9 ramps, and the last two to the volume thresholds used for the entire control zone. An additional stopping rule for the optimization method was added to prevent the use of prohibited values for the parameters, i.e., negative values.

Table 4.4 shows the resulting optimal thresholds based on a typical weekday traffic demand pattern for the test freeway section. In general, the new thresholds are less restrictive than the existing TMC thresholds for the test section. Table 4.5 includes the traffic performance resulting from the new optimized thresholds along with that from the existing TMC thresholds computed for the same demand pattern. It can be noted that, while the new control allows more cars to enter the freeway, total travel time including waiting time can be substantially reduced since ramp waiting time is minimized.

IV.5 Implementation and evaluation of the optimized thresholds in the test section

The optimal thresholds determined in the previous section were implemented in the test section in January 1993 and the traffic data were collected over a 3-week period. To evaluate the performance of the optimized thresholds, the traffic conditions at the key bottleneck location in the test section, i.e., Detector station 189 located upstream of the Highway 100 interchange, were analyzed. Figure 4.4a-d illustrates the volume-occupancy measurements at this location collected in November-December 1992, before the new control was implemented. As indicated in these figures, this location was frequently congested or operated at capacity with the TMC thresholds. Figure 4.5a-c shows the volume-occupancy measurements at the same location after the new control was implemented in January 1993. It can be noted that, even though the new thresholds were less restrictive than the previous TMC thresholds, the traffic conditions at this

Table 4.4 **Optimized threshold values and metering rates for all ramps on the freeway section of I-494**

A.M	Red Times						Volume					
Portland	21	44	65	87	113	154	32	32	36	42	51	66
Nicollet	19	50	79	107	142	195	32	32	36	42	51	66
Lyndale	20	52	82	111	148	204	32	32	36	42	51	66
35W S-W	7	17	26	34	45	62	32	32	36	42	51	66
Penn	20	44	67	88	116	158	32	32	36	42	51	66
France N-W	18	45	71	96	128	176	32	32	36	42	51	66
France S-W	19	55	89	122	163	226	32	32	36	42	51	66
H100 N-W	9	21	32	43	57	78	32	32	36	42	51	66
H100 S-W	20	60	98	135	182	252	32	32	36	42	51	66

P.M	Red Times						Volume					
Portland	14	27	35	46	65	88	34	34	38	43	50	63
Nicollet	16	34	46	62	88	121	34	34	38	43	50	63
Lyndale	15	24	29	37	49	65	34	34	38	43	50	63
35W S-W	8	18	23	31	44	60	34	34	38	43	50	63
Penn	16	35	47	62	88	122	34	34	38	43	50	63
France N-W	17	43	60	82	120	167	34	34	38	43	50	63
France S-W	11	31	44	60	88	124	34	34	38	43	50	63
H100 N-W	7	22	31	42	62	88	34	34	38	43	50	63
H100 S-W	15	31	41	55	77	106	34	34	38	43	50	63

For all the ramps the occupancy thresholds are:

17 17 17 18 23 40

unit: 1/10 second

Table 4.5 Estimated traffic performance of the test section with the existing and new optimized control thresholds

Morning Peak Period

	Existing control	Optimized control
Total travel time (veh-hr)*	1809	1246
Total Travel (veh-mile)*	43045	44791
Average speed (mile/hr)*	56	56
Ramp entering volume (veh)	11128	11999
Freeway entering volume(veh)	10268	10268
Total entering volume (veh)	21396	22267
Volume variation (%)	7.91	6.91
Speed variation (%)	1.03	0.90

Afternoon Peak Period

Total travel time (veh-hr)*	11222	8815
Total Travel (veh-mile)*	59852	67155
Average speed (mile/hr)*	55	54
Ramp entering volume (veh)	16207	19663
Freeway entering volume(veh)	14657	14837
Total entering volume (veh)	30864	34500
Volume variation (%)	3.94	4.40
Speed variation (%)	0.86	1.77

*: Including both freeway and ramps.

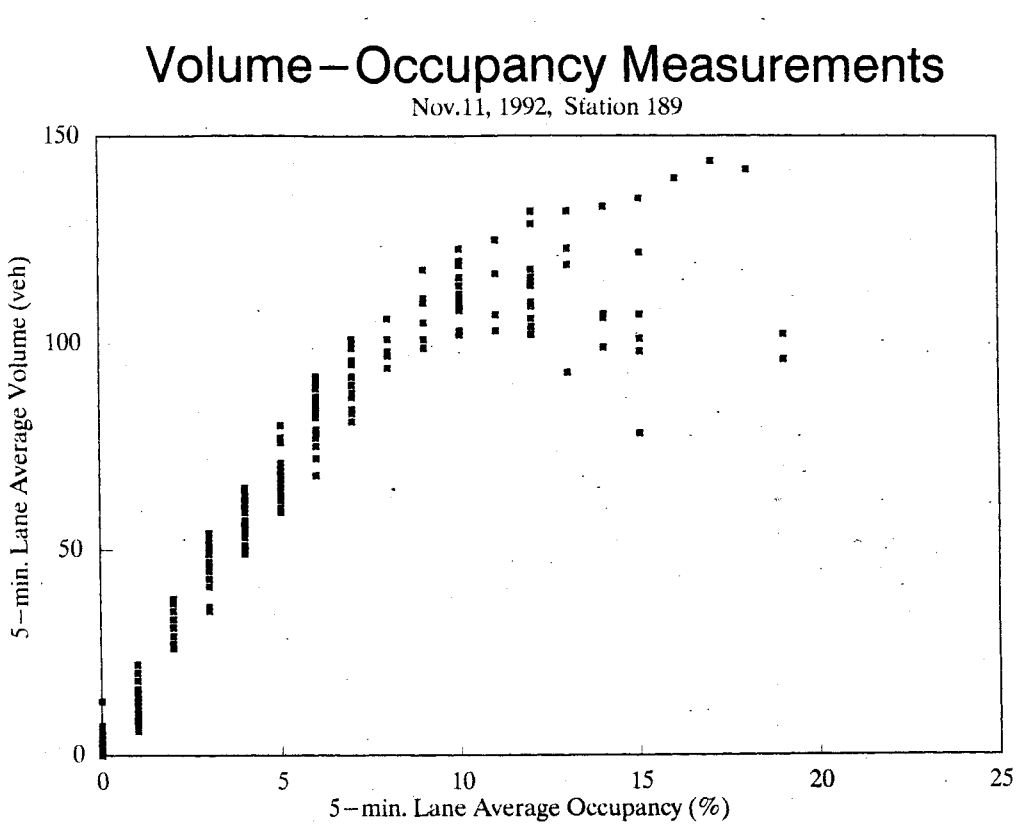

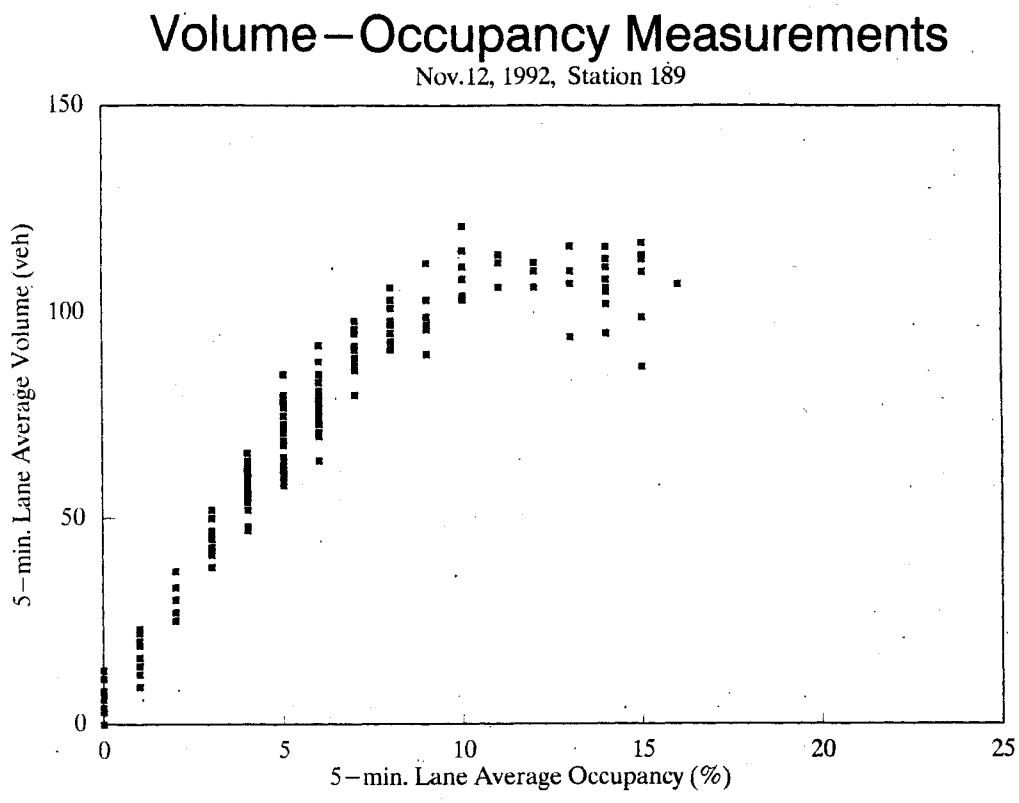

Figure 4.4a Volume-Occupancy measurements at detector station 189 (before new control)

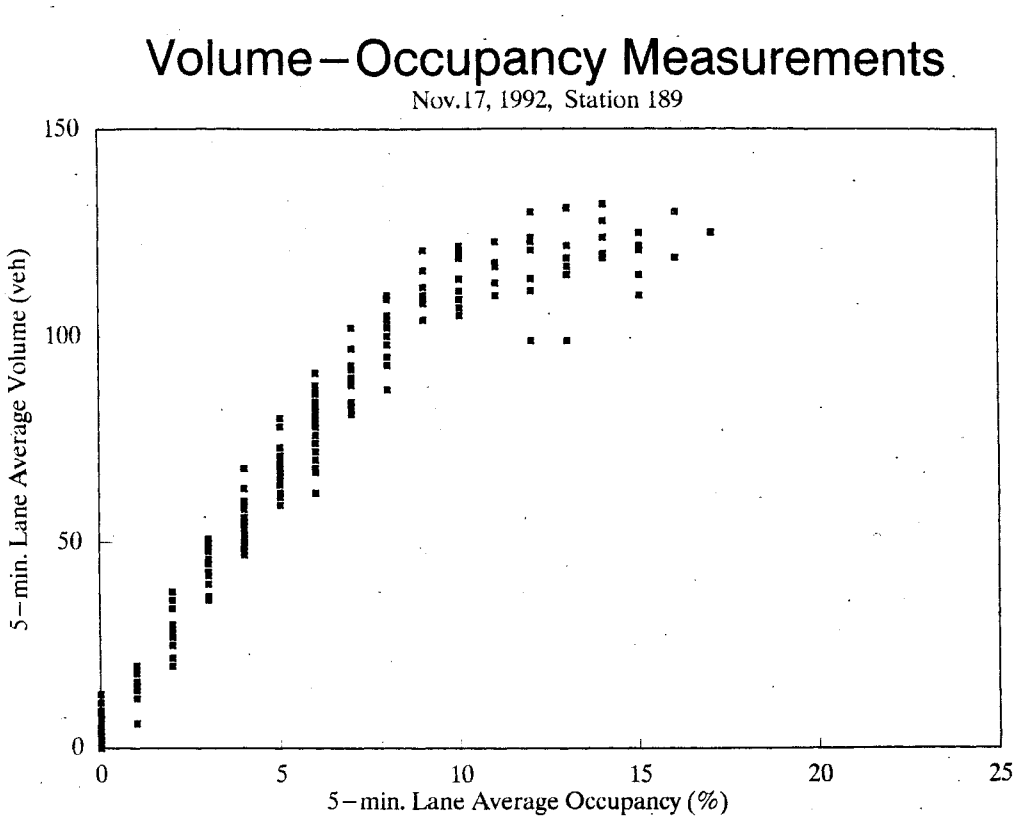

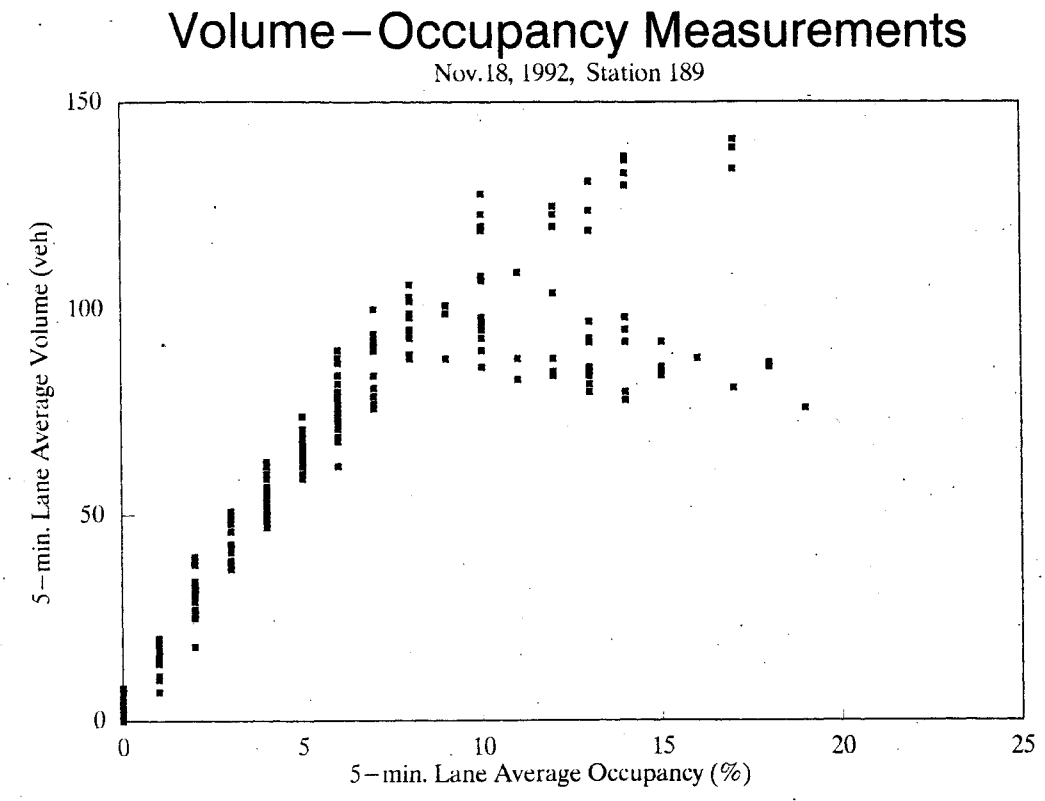

Figure 4.4b Volume-Occupancy measurements at detector station 189 (before new control)

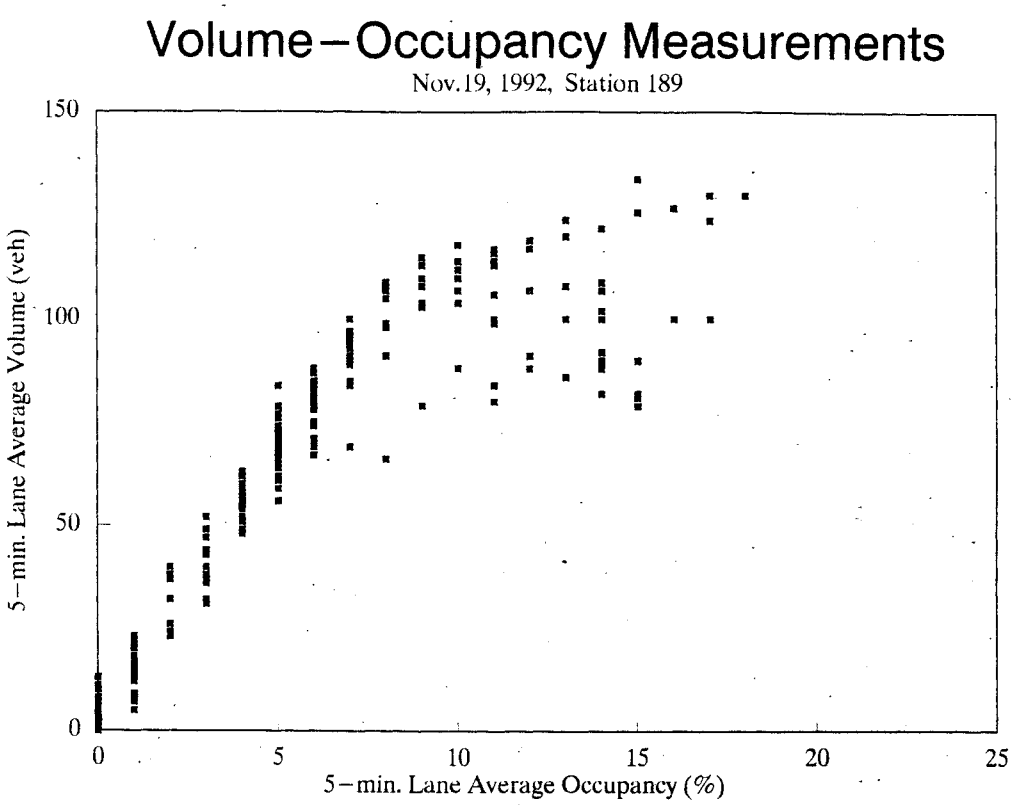

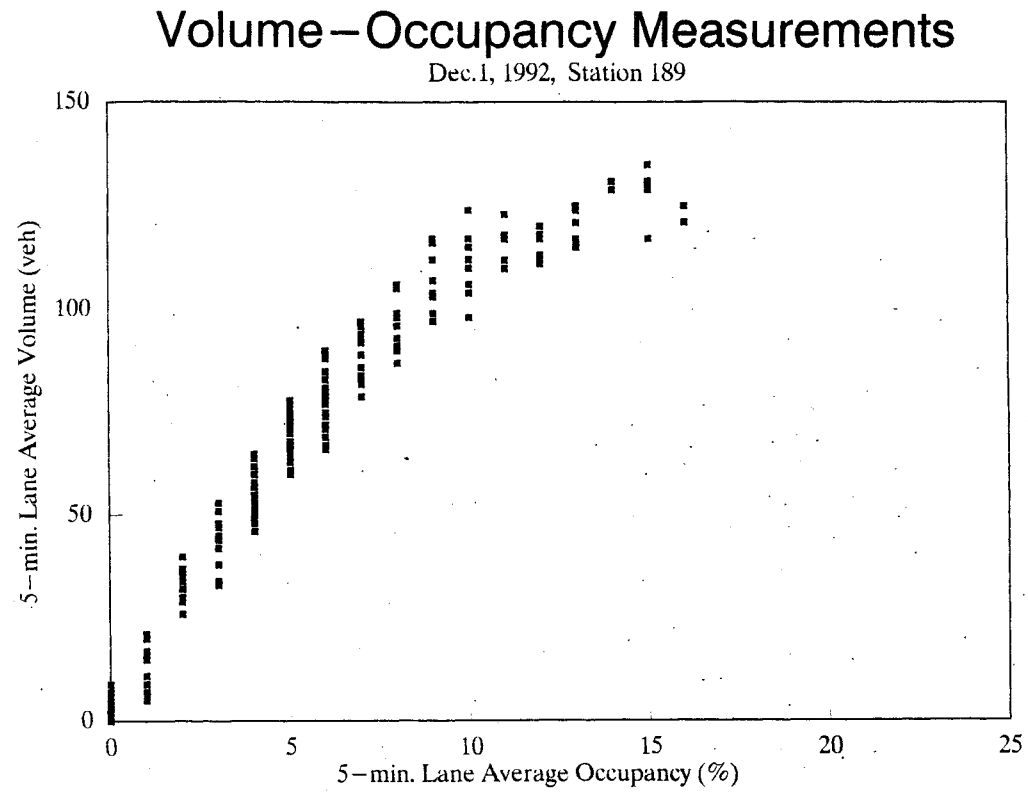

Figure 4.4c Volume-Occupancy measurements at detector station 189 (before new control)

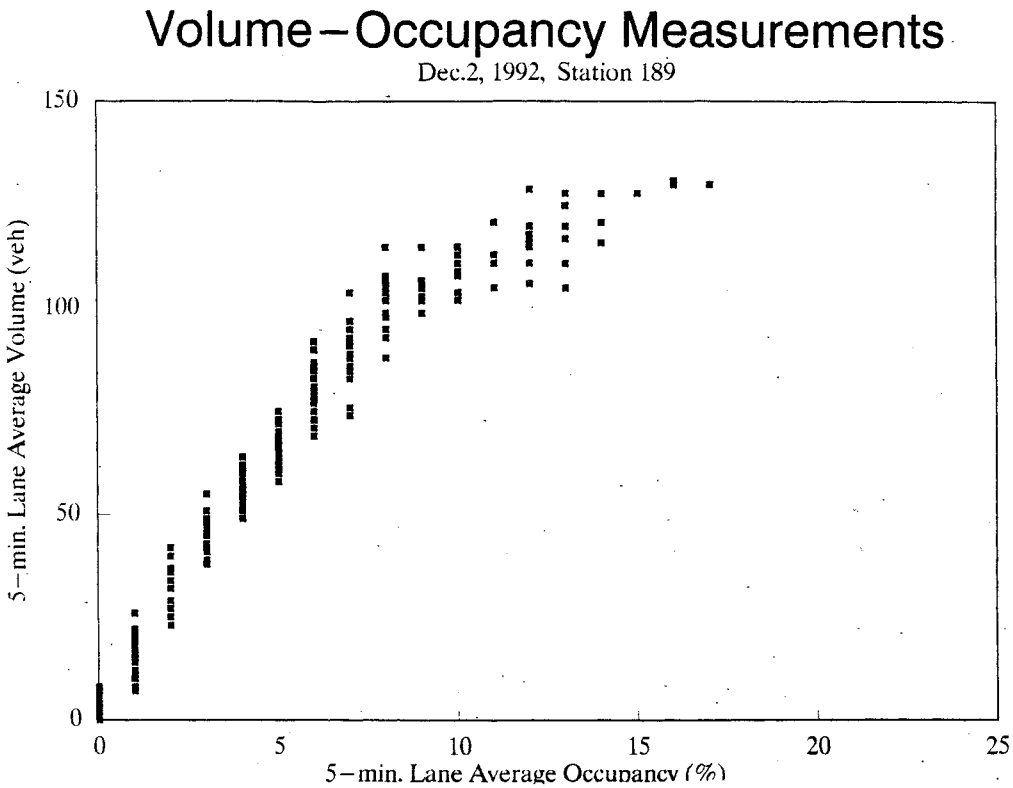

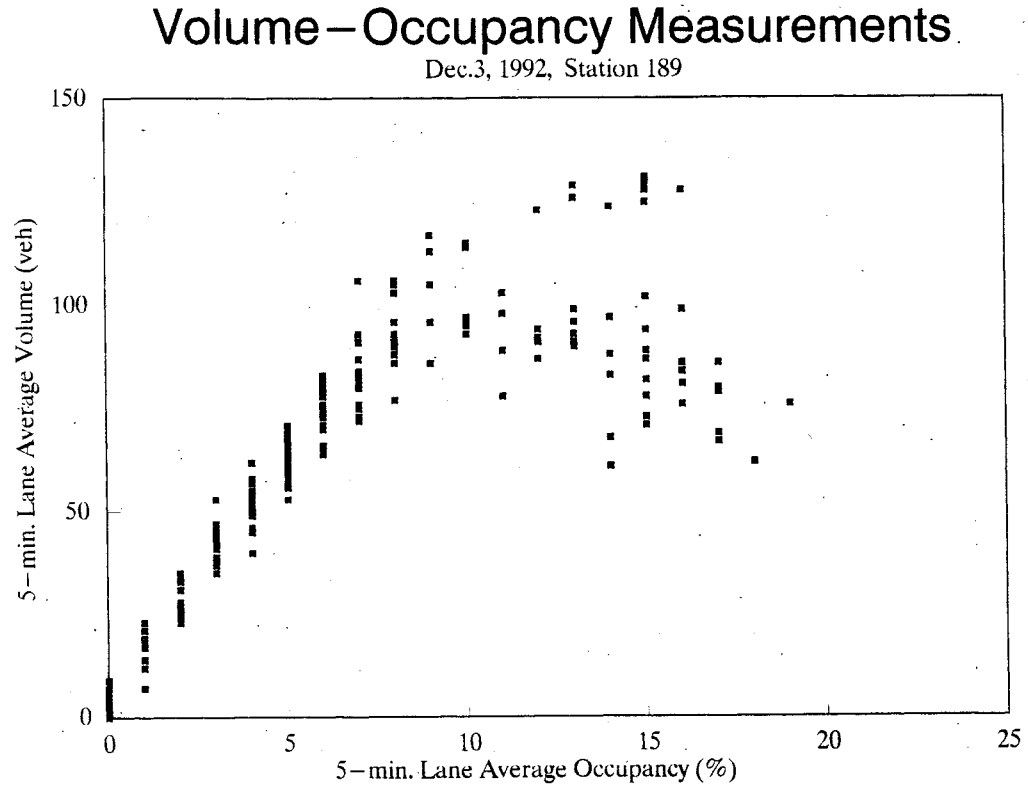

Figure 4.4dVolume-Occupancy measurements at detector station 189 (before new control)

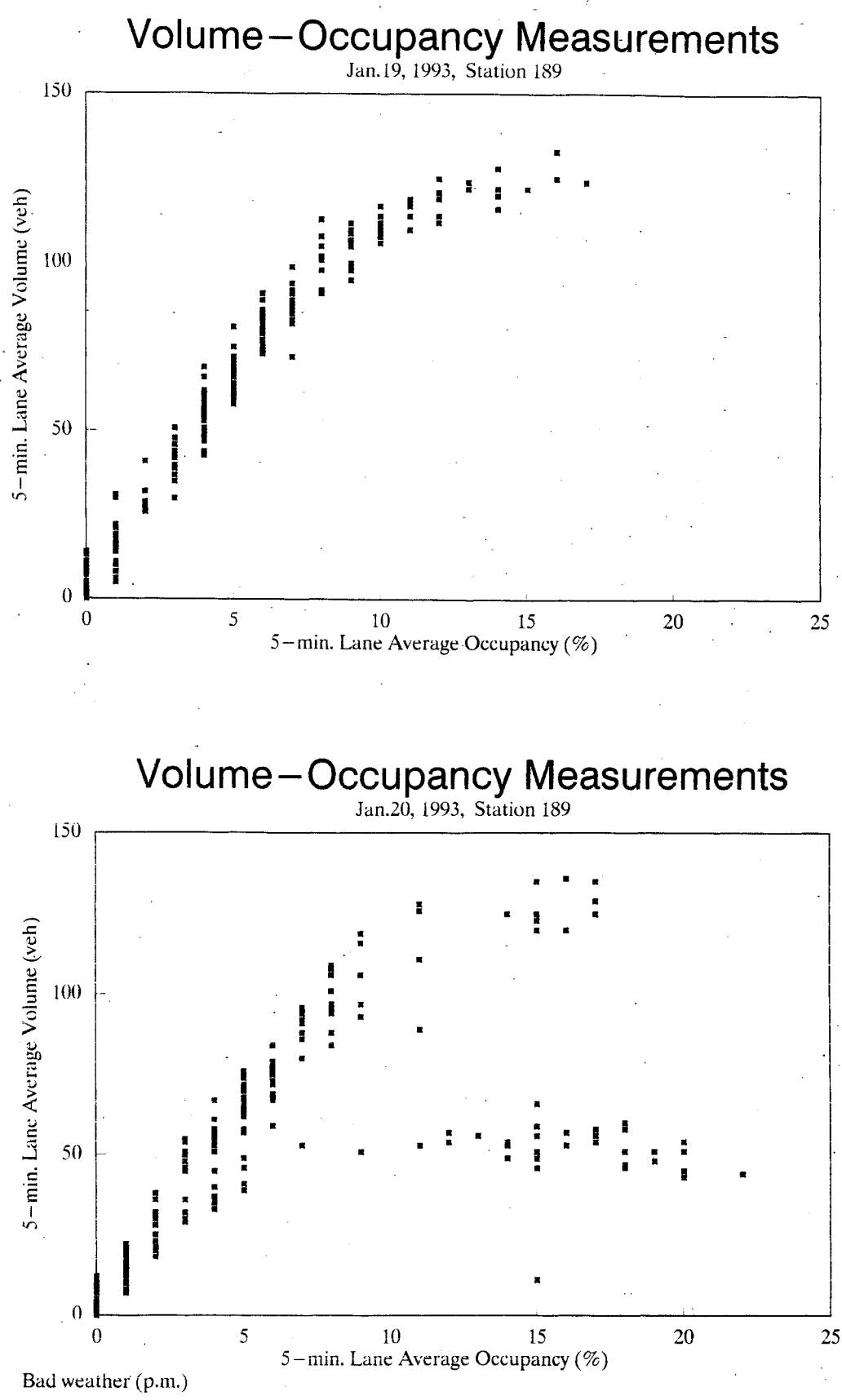

Figure 4.5a Volume-Occupancy measurements at detector station 189 (after new control)

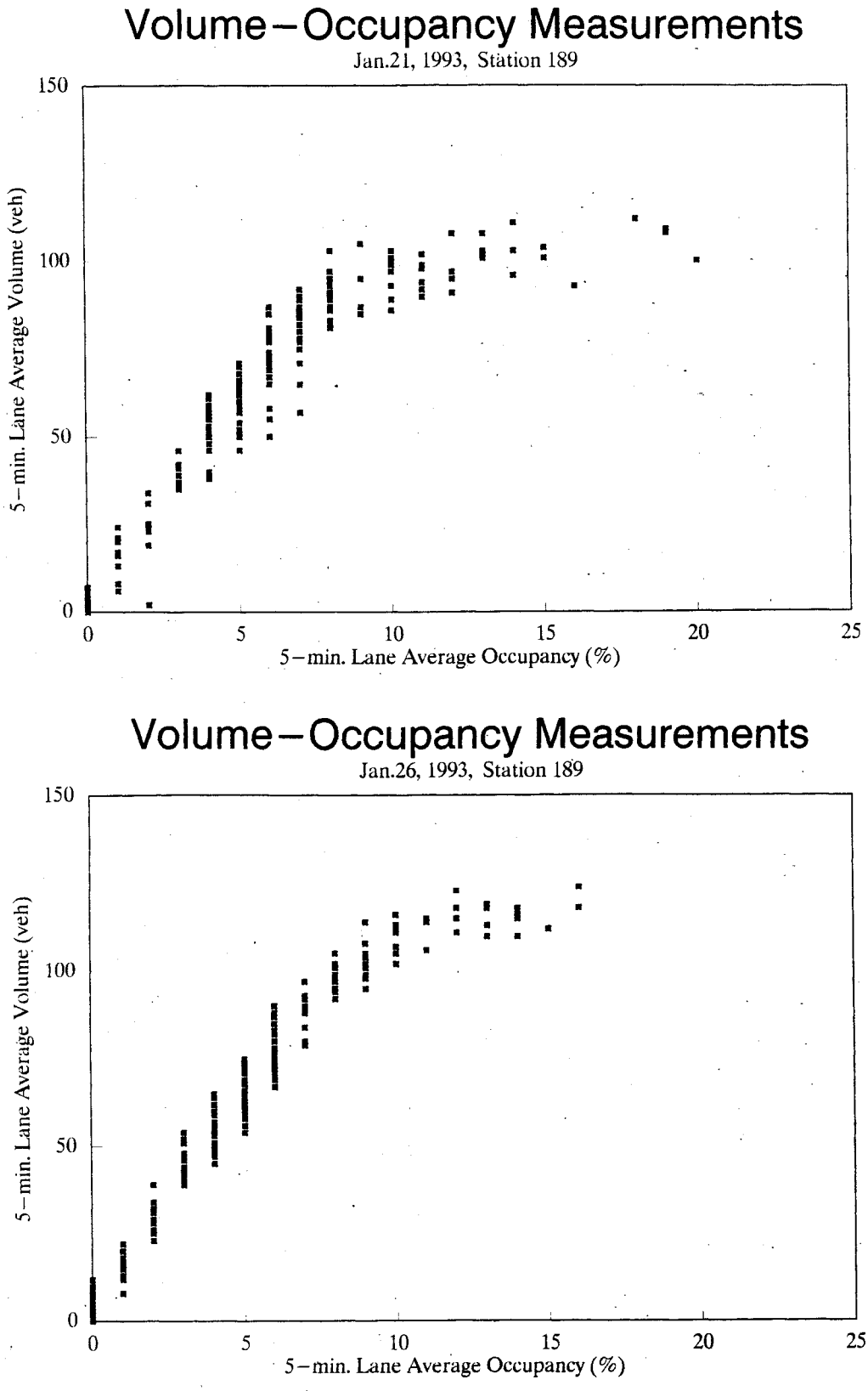

Figure 4.5b Volume-Occupancy measurements at detector station 189 (after new control)

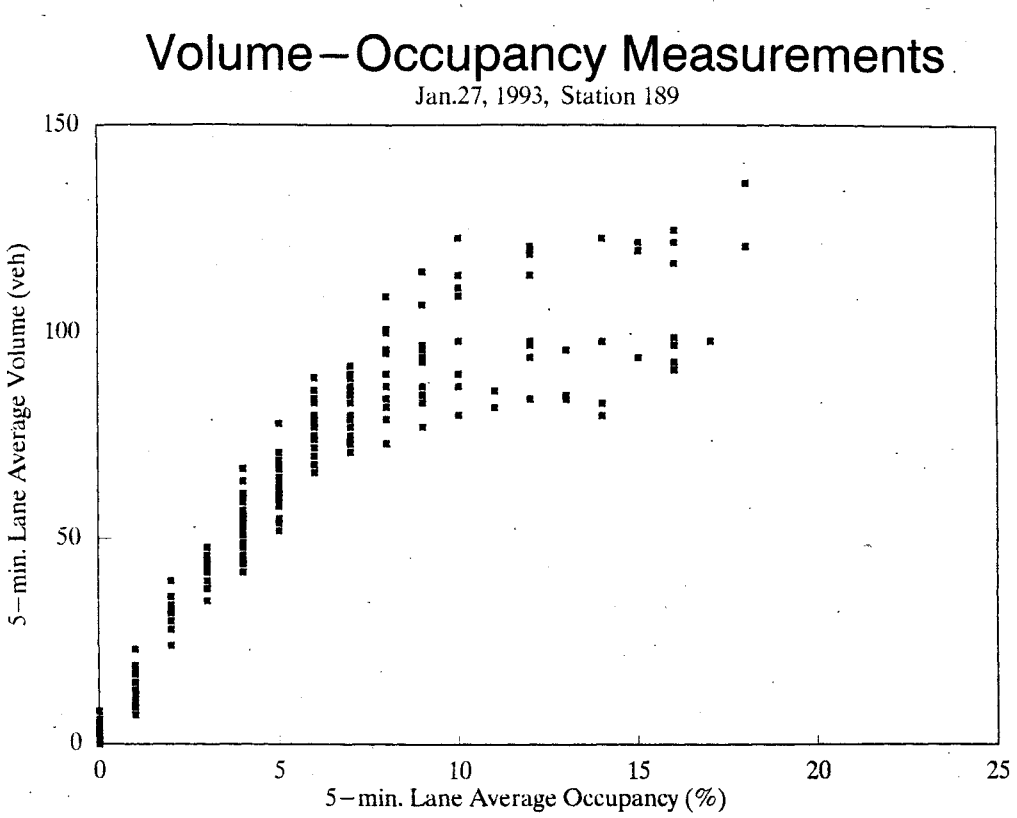

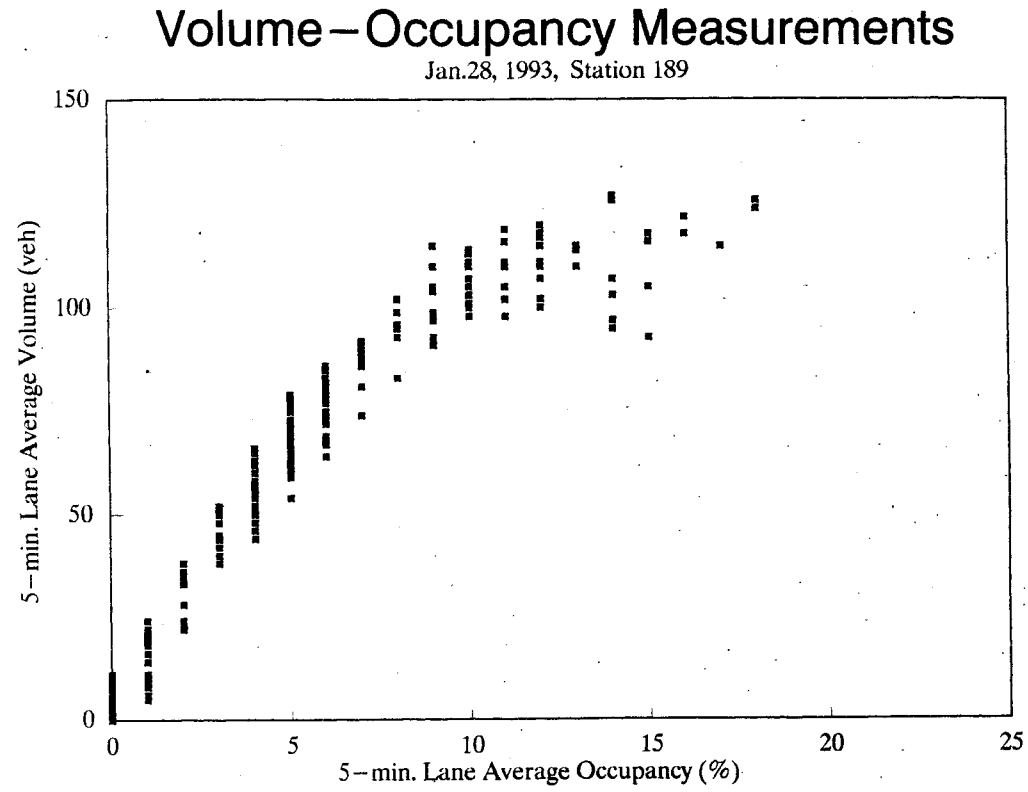

Figure 4.5c Volume-Occupancy measurements at detector station 189 (after new control)

location did not significantly deteriorate except on January 20, when there was ice on the road. The above observation was confirmed by the TMC traffic engineers during the field experimentation. It should be noted that the optimal thresholds developed in this research were based on only the normal weather weekday traffic demand pattern and different sets of thresholds need to be developed for various weather and traffic conditions.

A simulation analysis was also performed to evaluate the relative performance improvement in the traffic system under the new control as compared to the previous control. Table 4.6 includes simulated traffic performance in the test section with both new optimized thresholds and old TMC thresholds. In both cases, the real traffic volume data collected from the test section after the new control was implemented were used in simulation. As indicated in this table, new optimized thresholds allow more vehicles to enter the freeway, while other performance indicators have approximately same values in both cases. It also needs to be noted that with bad weather conditions, the TMC thresholds performed slightly better than the optimized thresholds, which were designed to deal with a normal weather traffic pattern.

IV.6 Summary

In this chapter, the new methods developed in the previous chapter were applied to the I-494 freeway section to determine the optimal thresholds minimizing total travel time for the test section under normal weather conditions. First, a set of thresholds was determined using local traffic conditions for each ramp. These thresholds were used as the initial thresholds in the optimization module. The final optimized thresholds were implemented in the test section and traffic data were collected to evaluate the traffic performance before and after the new control. The field evaluation results indicated that the new control allowed more cars onto the freeway without creating significant congestion under normal weather conditions. However, when there was a serious weather problem, the new thresholds were not restrictive enough to prevent congestion in the main freeway. This problem is due to the fact that the optimal thresholds determined in this research were based on the normal weekday traffic demand pattern in the test section. Future research should address the development of various sets of optimal thresholds depending on weather and traffic situations.

Simulated Traffic Performance of I-494 Freeway Test Section

A.M. (5:00--8:00)	1 /19 /93		1 /20**		1 /21		1 /26		1 /27		1 /28	
	TMC	OPT	TMC	OPT	TMC	OPT	TMC	OPT	TMC	OPT	TMC	OPT
Ramp Entering Volume (veh) (Freeway + Ramps)	12480	13038	12167	12738	9945	10010	12737	12989	12358	13030	12463	12712
Average Speed (miles/hour) (Freeway + Ramps)	54.2	54.5	54.8	55.1	53.3	53.4	55.6	55.6	53.4	53.7	55.6	55.6
Total Travel Time (veh-hrs) *	776	789	756	770	575	577	766	773	838	853	742	750
P.M. (4:00--7:00)												
	TMC	OPT	TMC	OPT	TMC	OPT	TMC	OPT	TMC	OPT	TMC	OPT
Ramp Entering Volume (veh) (Freeway + Ramps)	17527	20898	6491	5645	18405	19842	18016	20699	16433	18166	17203	20846
Average Speed (miles/hour) (Freeway + Ramps)	50.8	51.5	21.9	18.8	52.2	53	51.6	52.3	52.3	51.4	50.3	51
Total Travel Time (veh-hrs) *	1152	1248	1352	1490	1137	1170	1074	1144	1071	1157	1190	1299

TMC: Using previous TMC thresholds
OPT: Using optimized thresholds
* Does not include waiting time on ramps
** Ice on freeway during p.m. period

Table 4.6 Simulated traffic performance of I-494 freeway test section

V. PRELIMINARY STUDY FOR DEVELOPING ON-LINE PREDICTOR FOR FREEWAY EXIT DEMAND

V.1 Introduction

The most advanced concept for optimal freeway management includes a hierarchical traffic control structure, where overall freeway control is decomposed into several components, such as demand prediction, network optimization and local control (see Fig. 5-1), so as to achieve computational feasibility and robustness of control solutions. While this concept is promising, the state of the art in freeway ramp metering has not reached the point where a comprehensive, network-wide control solution is automatically generated and implemented through on-line optimization. A major difficulty lies in the lack of accurate on-line predictors, that can predict traffic demand in freeway networks. To be sure, most ramp metering systems currently in operation use previously collected data, generally 1-minute old, for determining metering rates, thereby reacting to freeway conditions rather than preventing congestion. Further, no demand predictor developed to date is specifically designed to predict freeway exit demand in real time. Developing reliable freeway demand predictors and, thus, developing metering control strategies that can determine metering rates based on predicted traffic demand for a given freeway section is an essential element for optimal management of freeway networks.

In this research, a new method to predict traffic volume exiting from a freeway is developed and tested with real data collected from the I-35W freeway in Minneapolis. The new method uses historical data and current day measurements and employs the Extended Kalman Filter algorithm to update the parameters in the prediction models. The rest of this chapter briefly reviews existing demand prediction algorithms and summarizes the new method along with the test results.

V.2 Review of Existing Demand Prediction Algorithms

The demand prediction algorithm in the 2^{nd} generation Urban Traffic Control System(UTCS-2) represents the first systematic approach for traffic responsive control in urban street networks (FHWA, 1973). The UTCS-2 predicts the traffic volume of the next control interval at each detector location in real time. The main concept of UTCS-2 prediction is the use of current traffic measurements to correct for the traffic deviations from the average historical pattern. The algorithm makes use of both historical data and current day measurements. A large database is required for historical data, and the parameters in the algorithm are calibrated off-line using the representative data obtained from the location in question.

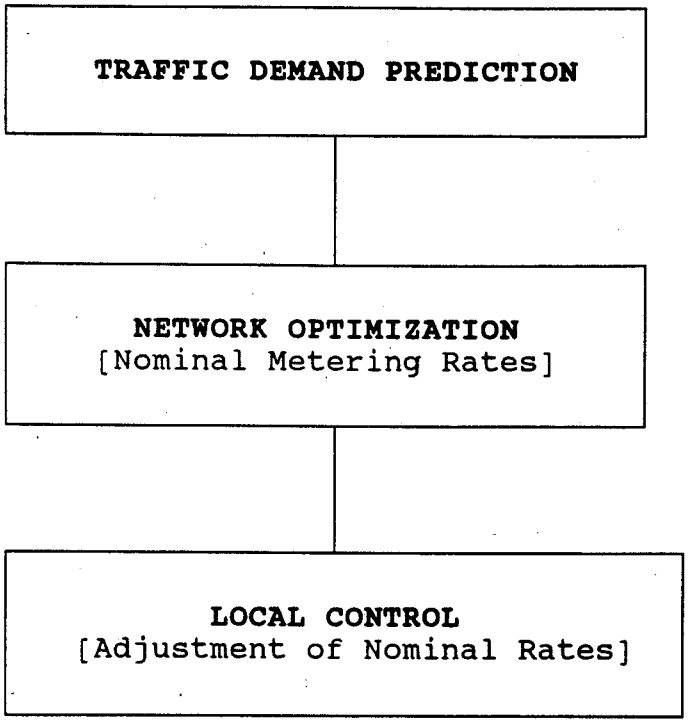

Figure 5.1 Hierarchical control structure

While UTCS-2 relies heavily on the historical demand pattern, the 3rd generation UTCS, UTCS-3, uses only current-day measurements for the prediction (Lieberman, et al., 1974). The predicted value is an interpolation between the most recent smoothed and unsmoothed measurements. The smoothing parameters are calibrated off-line using a representative data set. By employing only the current measurement, UTCS-3 tries to be responsive to the current variations of traffic conditions. Since the prediction is based on the current day measurements only, there is an inherent time lag in the UTCS-3 prediction. Both UTCS-2 and UTCS-3 predictions are based on single-location volume measurements.

Recent research in on-line demand prediction involves the Box-Jenkins type time-series and filter-type estimation models. The Box-Jenkins type models assume demand prediction is a point process and use purely statistical techniques to identify the stochastic nature in the observed data. Recent applications of these types of model, mostly ARIMA type models, include freeway mainline volume and occupancy prediction (Ahmed, 1979, 1983; Moorthy, et al, 1988). However, these models treat demand prediction as an open loop process and, thus, are not adaptive to the dynamically changing traffic environment.

The application of a filtering algorithm is a relatively recent concept in on-line demand prediction. While several filter-predictors have been developed for use in traffic responsive control, these models either predict queue size at an intersection or estimate the traffic density in the freeway mainline. One notable approach by Okutani and Stephanedes (1984) applies the Kalman filtering algorithm to 15-min. volume prediction. This approach predicts the downstream link volume as a linear combination of historical averages and current day measurements including upstream link volumes. The Kalman filter algorithm updates the model parameters using the most recent prediction error. However, similarly to most other predictors, this approach does not explicitly consider the effect of control variables on volume prediction.

By contrast, recent research by these authors, explicitly treats the time-variant effects of control on the traffic demand to be predicted (Stephanedes, et al., 1989). This approach combines behavioral modeling and the Extended Kalman Filter, where the filter continuously updates the model parameters with the most recent prediction error. By continuously updating the model parameters in real time, initial prediction errors are not allowed to propagate through time. The method was applied to predict the traffic demand-diversion at the entrance ramp area in freeway corridors.

V.3 Development of an Adaptive Prediction Algorithm for Freeway Exit Demand

The lack of reliable on-line predictors for freeway traffic demand has been one of the major problems in developing comprehensive optimal control strategies that can reflect network-wide freeway traffic conditions. Most existing on-line predictors have been developed

for intersection control. Further, the vast majority of models use constant parameters computed off-line, significantly restricting model adaptability to the ever-changing traffic environment. For effective freeway control, the development of reliable on-line predictors that can capture the causal interaction between traffic demand and control system is of critical importance. The on-line predictor should be adaptive to the continuously changing traffic environment and simple enough to be easily integrated into the complete feedback control system.

Responding to the need for prediction that can be used for the optimal control of freeway mainline traffic, this study develops an on-line adaptive predictor for freeway exit demand. The new predictor adopts the adaptive prediction approach previously developed by the authors (Stephanedes, et al., 1989). The method updates the parameters of the prediction models in real time using the most recent error. Figure 5.2 illustrates the framework of the freeway exit demand predictor developed in this research. The exit demand for ramp i during time interval k, $X_{i,k}$, is assumed to be a function of historical demand, H, and current day measurements, M, and, therefore, an implicit function of the control. In particular,

$$X_{i,k} = f_k(H,M,\Theta) + v_k \qquad (1)$$

where v denotes noise, M is a function of the freeway ramp control, and the unknown parameters, Θ, are identified in real time by the Extended Kalman Filter. This approach considers the model parameters as state variables representing the behavioral state of traffic flow at a given time interval, and the Extended Kalman Filter algorithm identifies the optimal unbiased estimates of the behavioral state in real time using the most recent prediction error.

The state evolution of the model parameters is assumed to follow the non-stationary random walk process, i.e.,

$$\Theta_{k+1} = \Theta_k + w_k \qquad (2)$$

where w denotes noise. The random walk process has been successfully applied to model physical systems that are subject to rapid variation (Young, et al, 1984). Using the prediction models as observation equations, the Extended Kalman Filter continuously updates the model parameters by recursively determining the minimum variance estimates of the prediction parameters. The Extended Kalman Filter is based on the theory developed by Kalman (1960), and was originally intended for the state identification of a non-linear dynamic system. It relinearizes the system dynamics about each new state as it becomes available. As a consequence of relinearization, large initial estimation errors are not allowed to propagate through time, and therefore, the linearity assumptions are less likely to be violated. The procedure for updating the model parameters via the Extended Kalman Filter is summarized below and in Figure 5.2:

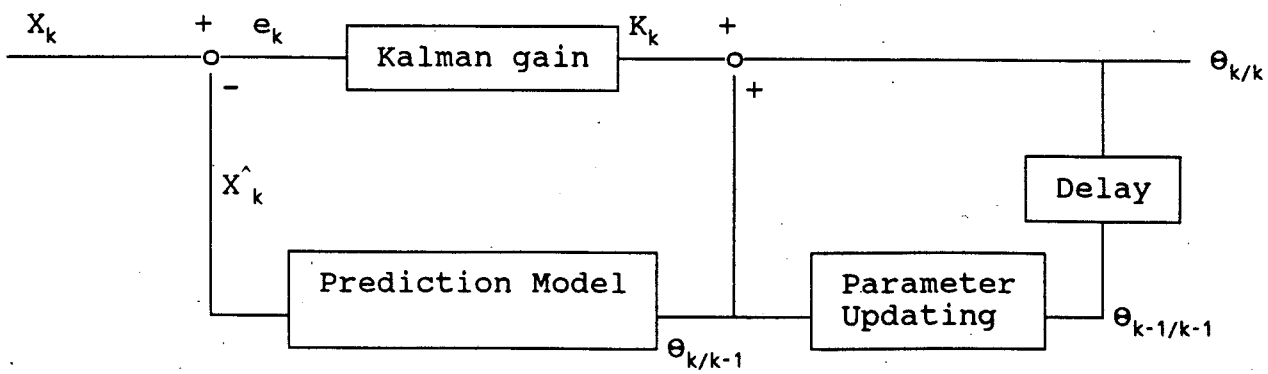

$\hat{X}_k$ = predicted exit volume for k^{th} time interval
X_k = measured exit volume for k^{th} time interval
K_k = Kalman gain
Θ = parameter

Figure 5.2 Parameter update process

1) Initialize algorithm (k=0) with any prior knowledge of model parameters, i.e., for each ramp, determine the initial values Θ_0, Σ_0, s_0, and q_0. Then,

$\hat{\Theta}_{k/k}=\Theta_0$, $\Sigma_{k/k}=\Sigma_0$

where $\Sigma_{k/k} = E[(\Theta_k-\Theta_{k/k})(\Theta_k-\Theta_{k/k})^T]$,

2) Set the model parameters $\hat{\Theta}_{k+1/k} = \hat{\Theta}_{k/k}$

3) Predict the exit ramp demand X_k using the prediction model (1) with the parameters $\hat{\Theta}_{k+1/k}$

4) Measure actual exit ramp volume X_k and obtain prediction error e_k, which is defined as

e_k=[measured value]$_k$ - [predicted value]$_k$

5) Update model parameters $\hat{\Theta}_{k+1/k}$ using gain and error,

$$\hat{\Theta}_{k+1/k+1} = \hat{\Theta}_{k+1/k} + K_{k+1}\, e_k \qquad (3)$$

where $K_{k+1} = \Sigma_{k+1/k}\, S_{k+1}T\, [S_{k+1}\, \Sigma_{k+1/k}\, S_{k+1}T + s_k]^{-1}$ is the gain vector,

$\Sigma_{k+1/k} = \Sigma_k + q_k$, the covariance matrix,

$S_{k+1} = [\partial f/\partial\Theta]^T$, the sensitivity vector,

$^3\Theta=\hat{\Theta}_{k+1/k}$

$\Sigma_{k+1/k+1} = (I-K_{k+1}S_{k+1})\, \Sigma_{k+1/k}$, the updated covariance matrix,

$E[w_k w_j T] = q_k \delta_{kj}$

$E[v_k v_j T] = s_k \delta_{kj}$

and w, v are zero-mean Gaussian white noise sequences for the state equation (2) and the prediction model (1) respectively.

6) Let k = k + 1 and return to step 2.

V.4 Model Formulation and Testing

Model formulation

Commuters' choice of exit ramp is primarily a function of destination unless unexpected congestion occurs on the upstream freeway or at the exit ramp initially selected. The model formulated in this research assumes that the volume exiting the freeway at a given ramp is a function of the historical information regarding the exit volume at that ramp and the current day measurements at the upstream freeway and at the exit ramp, i.e.,

$$\hat{V}_k = \alpha_k U_{k-1} + \beta_k [V^H_{k-1} + V^H_k + V_{k-1}] \qquad (4)$$

where, $\hat{V}_k$ = predicted exit volume during time interval k,

U_k = upstream mainline volume during time interval k,

V^H_k = historical information regarding V_k,

V_k = current day exit volume during time interval k,

α_k, β_k = parameters to be identified in real time.

The historical data regarding exit volume reflect the drivers' origin-destination information. Further, the current-day measurements from freeway mainline and exit ramps indicate current traffic conditions that are closely related to drivers' diversion decisions. The first term of the above model explicitly treats the effects of current upstream mainline volume on the exit volume for the ramp under study, and the second term reflects the effects of O/D by considering historical exit demand. The consideration of historical demand with equal weights for variables V^H_{k-1}, V^H_k, and V_{k-1} is based on extensive survey findings from Minneapolis indicating that, for every 10-15 min. peak interval, an overwhelming portion of traffic consists of the same commuters following the same route every weekday(8). To be sure, this assumption may not be valid for other trips during off-peak periods. The model parameters are updated in real time using the Extended Kalman Filter algorithm presented in the previous section.

Model testing

The on-line prediction algorithm (3) and the prediction model (4) formulated in the previous section are tested and validated with the real data collected from I-35W freeway. Figure 5.3 shows the test freeway section and the location of the loop detector stations operated by the Traffic Management Center, Minnesota Department of Transportation. As a result of the detection system configuration, only 5-minute exit ramp volume data were available, while the mainline detector stations could provide 1-minute volume. Four exit ramps of the test section were selected and their 5-minute exit volume was predicted and compared with the real data

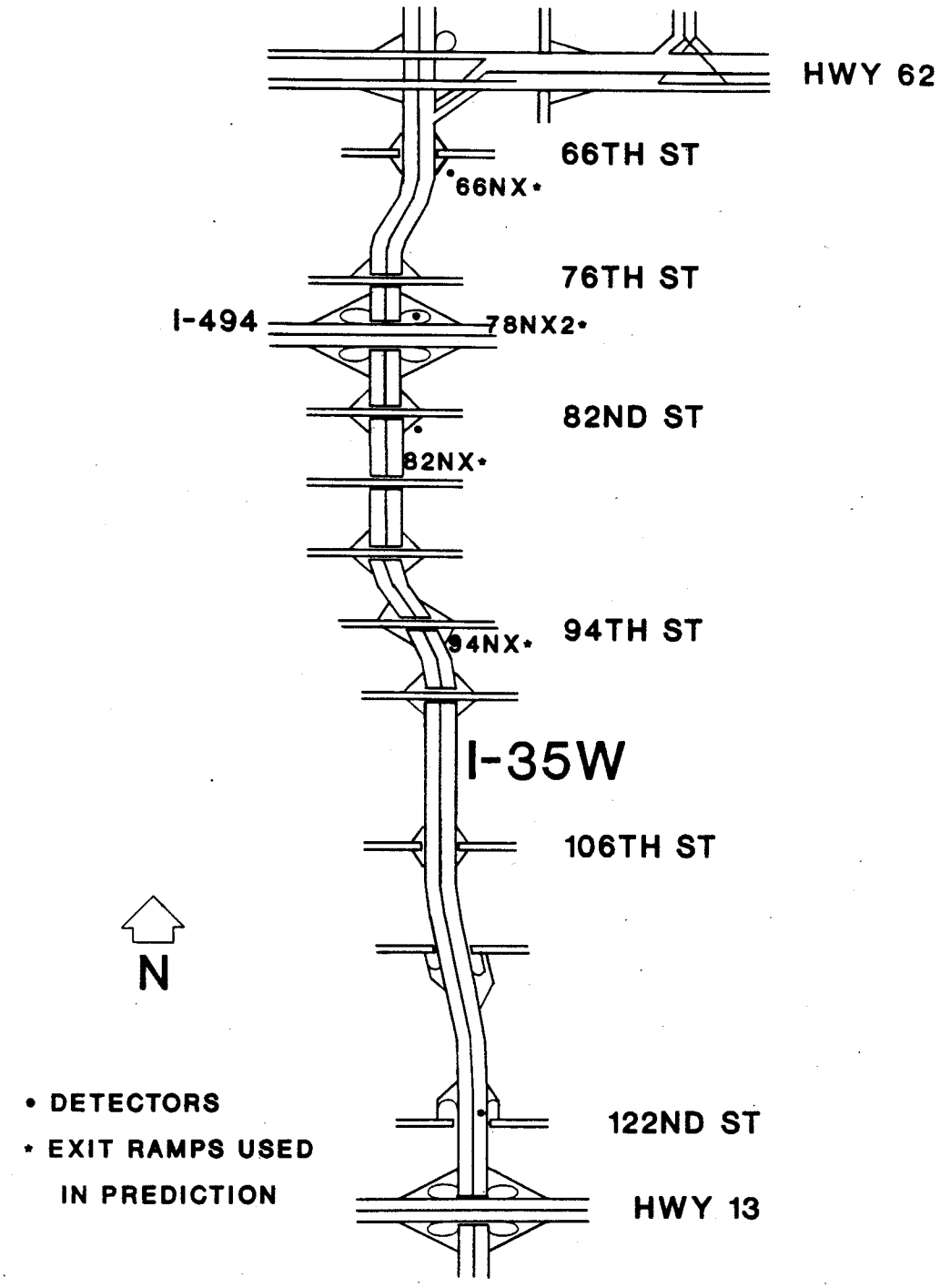

Figure 5.3 Location of test freeway section (I-35W Northbound)

collected in November, 1990. Figure 5.3 also indicates the ramps selected for testing. In particular, 94NX and 66NX ramps are typical low-volume ramps in the test section, and the distance between the 66NX ramp and the adjacent upstream exit ramp is the longest. The notation 94NX and 66NX represents the northbound exit ramps exit to the 94^{th} and 66^{th} streets respectively. The demand at the 82NX ramp is high relative to other ramps, and the 78NX2 ramp is the busiest, serving as the exit to the westbound I-494 freeway. Further, the location of the 122^{nd} detector station is considered as the upstream boundary for this test section, and the arrival volume at this boundary is also predicted and compared with the real data. To evaluate the performance of the predictor, the Mean Absolute Error (MAE) is calculated for each prediction. The MAE is defined as

$$MAE = 1/N * \Sigma_k \, | (Measured)_k - (Predicted)_k |$$

where N denotes the number of predictions. The rest of this section summarizes the test results from four exits, i.e., ramps 94NX, 66NX, 82NX, and 78NX2, and the upstream boundary at 122^{nd} street.

94NX Exit ramp

This ramp represents a typical low-volume exit ramp in the test section with a maximum 5-minute exit volume of 35 vehicles during the morning rush hour in November, 1990. Figures 5-4 a,b,c show the prediction results for 3 days in November, 1990, with the following initial parameter values,

$$\hat{V}_k = \alpha_k U_{k-1} + \beta_k [V^H_{k-1} + V^H_k + V_{k-1}]$$

$$\alpha_0 = 0.025, \quad \beta_0 = 0.165$$

where α_0 is the historical exit turning proportion and β_0 is calculated from statistical analysis of the volume historical data. The volume measurements from the 122^{th} mainline detector station were used as the upstream information. For historical information, V^H_{k-1} and V^H_k, the measurements from the same time interval, same day of the previous week were employed. Alternatively, monthly or weekly average data could be used. The results from the 5-minute exit volume prediction indicate that MAE ranges from 5.1 to 6.3 vehicles/5-minutes. Figure 5-5 shows the error propagation through time for the November 21, 1990, prediction. From the figure, large prediction errors are not propagated through time and this indicates the adaptability of the predictor developed in this research.

66NX Exit ramp

This ramp is characterized by low exit demand, with maximum 5-minute exit volume approximately 30 vehicles/5-min. during morning rush hours, similar to ramp 94NX. However,

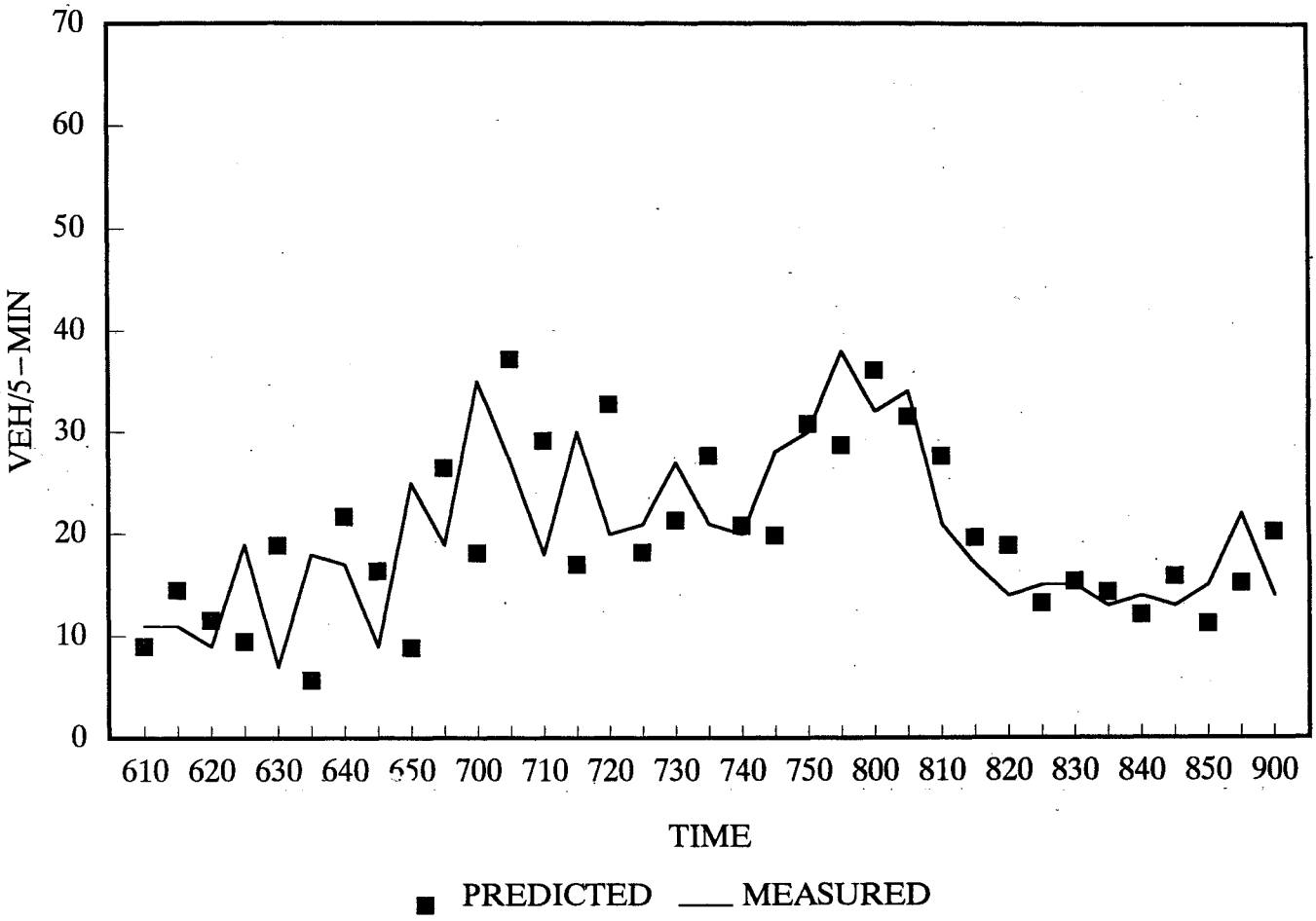

Figure 5.4a Prediction results for 94NX ramp
[Nov. 19, 1990, 6:00-9:00 a.m., MAE=6.31 veh/5-min.]

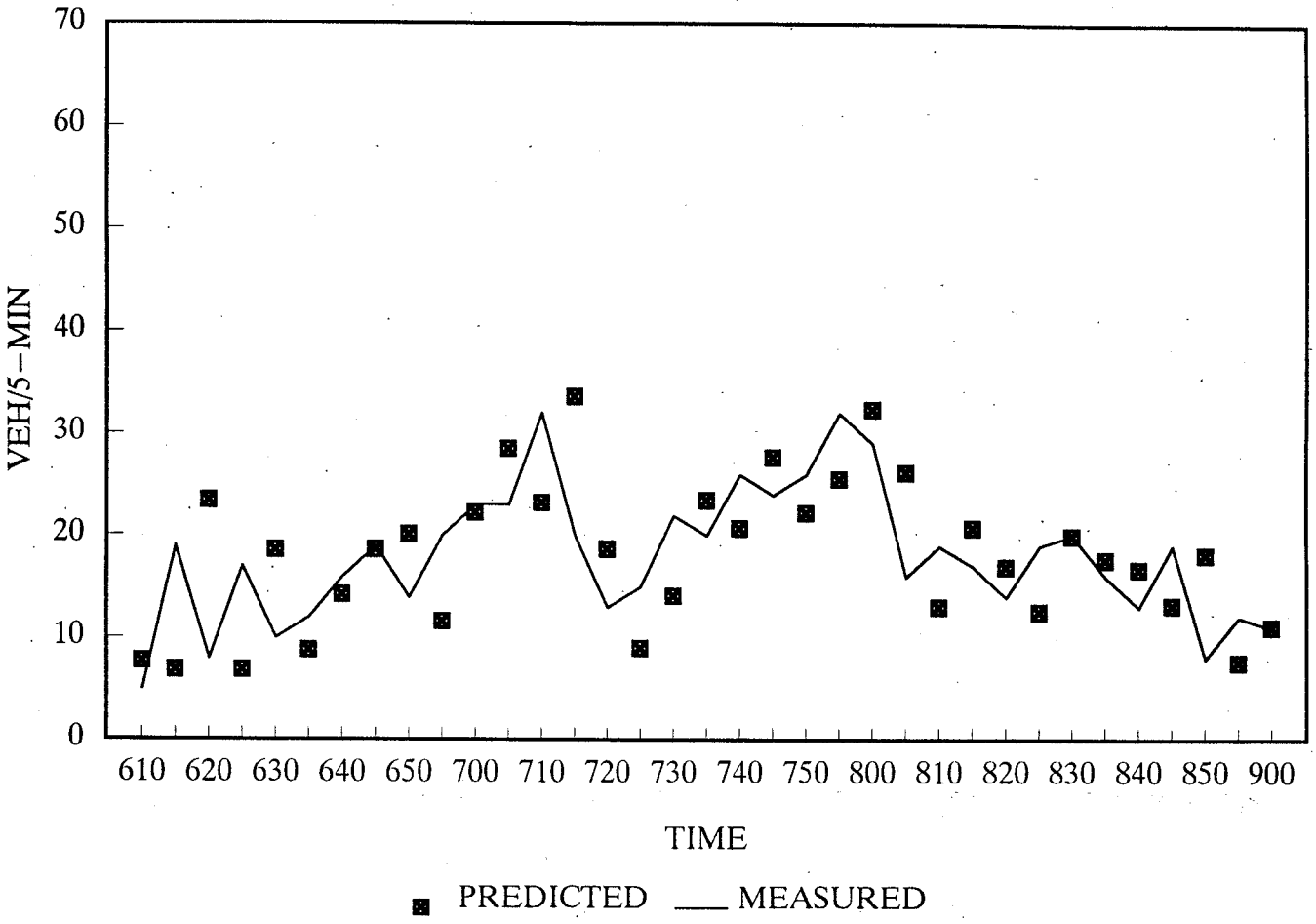

Figure 5.4b Prediction results for 94NX ramp
[Nov. 20, 1990, 6:00-9:00 a.m., MAE=5.66 veh/5-min.]

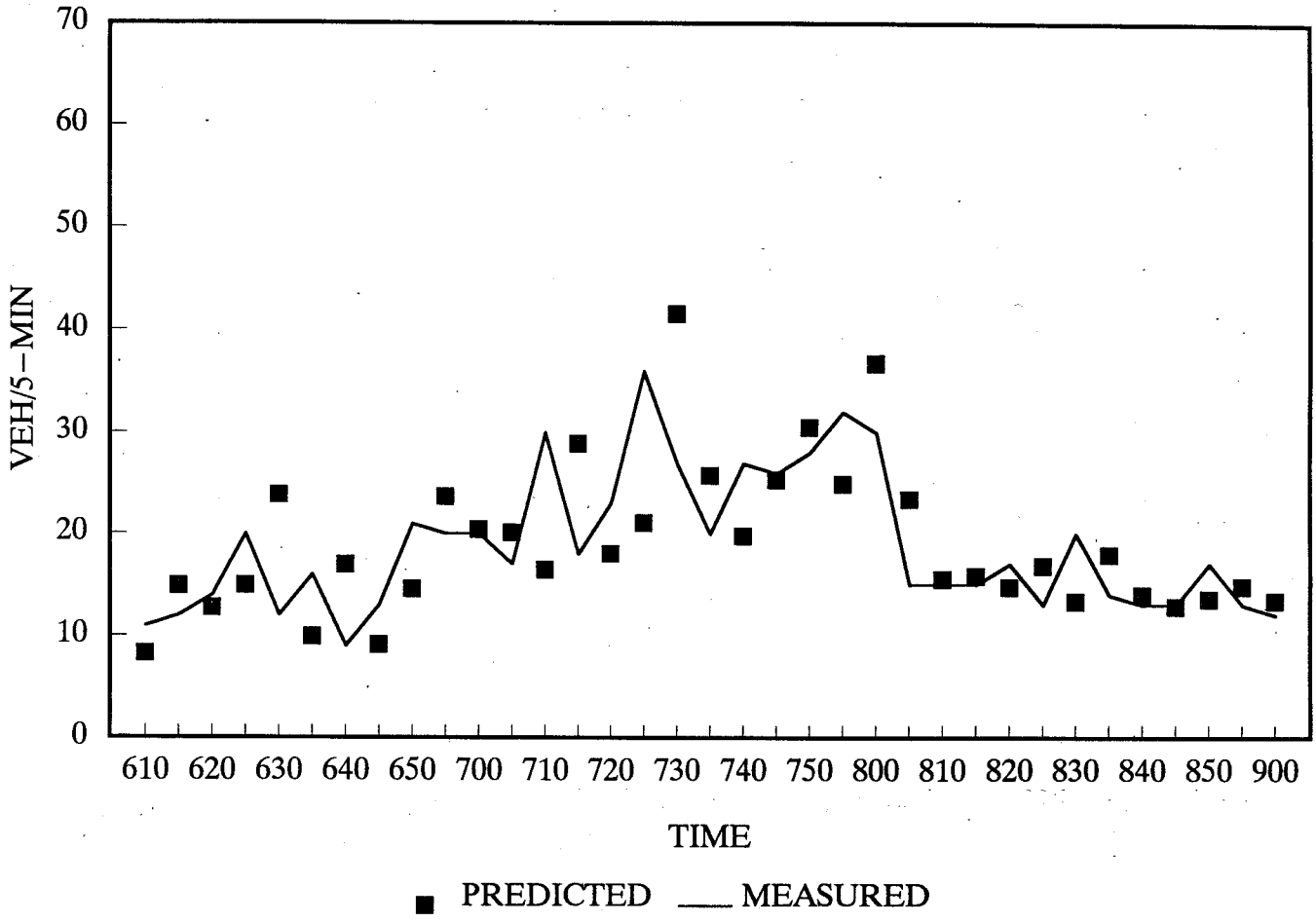

Figure 5.4c Prediction results for 94NX ramp
[Nov. 21, 1990, 6:00-9:00 a.m., MAE=5.08 veh/5-min.]

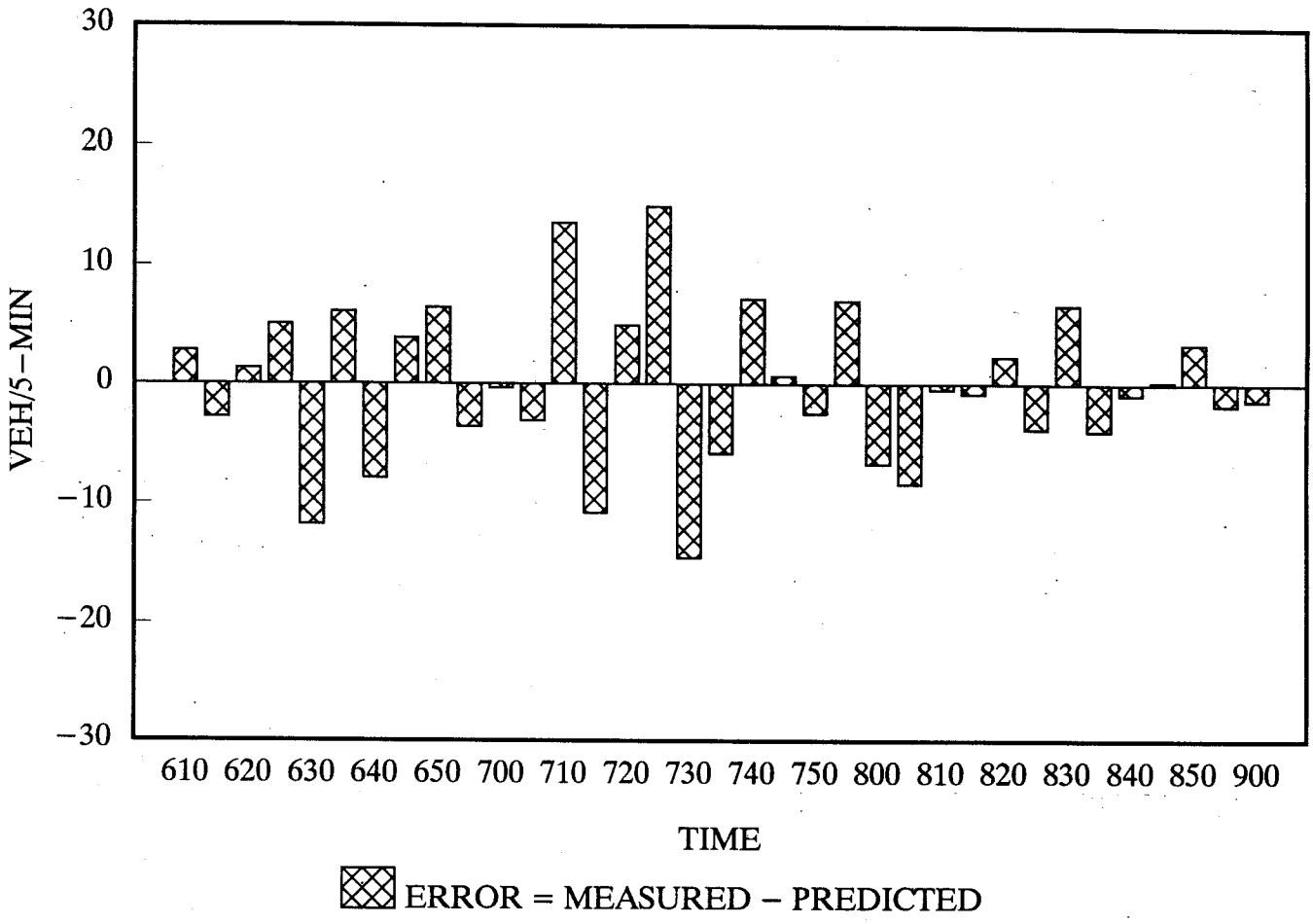

Figure 5.5 Error propagation through time for 94NX exit volume prediction [Nov. 21, 1990]

the distance from the adjacent upstream exit ramp, 78NX2, is much longer than at any other ramp in the test section, and this might lead to differences in traffic diversion behavior. Figures 5-6 a,b,c illustrate the test results for the same 3 days as in ramp 94NX, using the same model with the following initial parameter values;

$\alpha_0 = 0.025$, $ß_0 = 0.165$.

For historical information, the volume measurements from the same time, same day of the previous week were used. Further, the measurements from the 122^{th} mainline detector station were used as the upstream data. The MAE from the 3-day prediction ranges from 4.2 to 4.9 vehicles/5-minutes.

82NX Exit ramp

This ramp records relatively high exit demand, approximately 60 vehicles/5-min. during morning rush hours. Figures 5-7 a,b,c show the prediction results for 3 days in November, 1990, with the following initial parameter values;

$\alpha_0 = 0.01$, $ß_0 = 0.165$.

For historical information, the volume measurements from the same time, same day of the previous week were used. Further, the measurements from the 122^{nd} mainline detector station were used as the upstream data in the prediction. The test results indicate MAE ranging from 5.4 to 7.8 vehicles/5-minutes.

78NX2 Exit ramp

This ramp serves as the exit to the westbound I-494 freeway and has the largest exit demand in the test section, reaching a maximum 120 veh/5-min. during morning rush hours. The following initial parameter values were used for the prediction as in all other ramps.

$\alpha_0 = 0.075$, $ß_0 = 0.165$.

Further, the exit volume measurements during the same time, same day of the previous week were used as historical data and the 122^{nd} mainline detector data were used as the upstream measurements. Figure 5-8 a,b,c show the prediction results with MAE ranging from 10.8 to 15.1 vehicles/5-minutes.

Upstream boundary volume prediction (122^{nd}detector station)

To predict the volume entering the upstream mainline boundary, the original prediction model was modified as follows;

$\hat{V}_k = ß_k [V^H_{k-1}+V^H_k+V_{k-1}]$

$ß_k = 0.333$

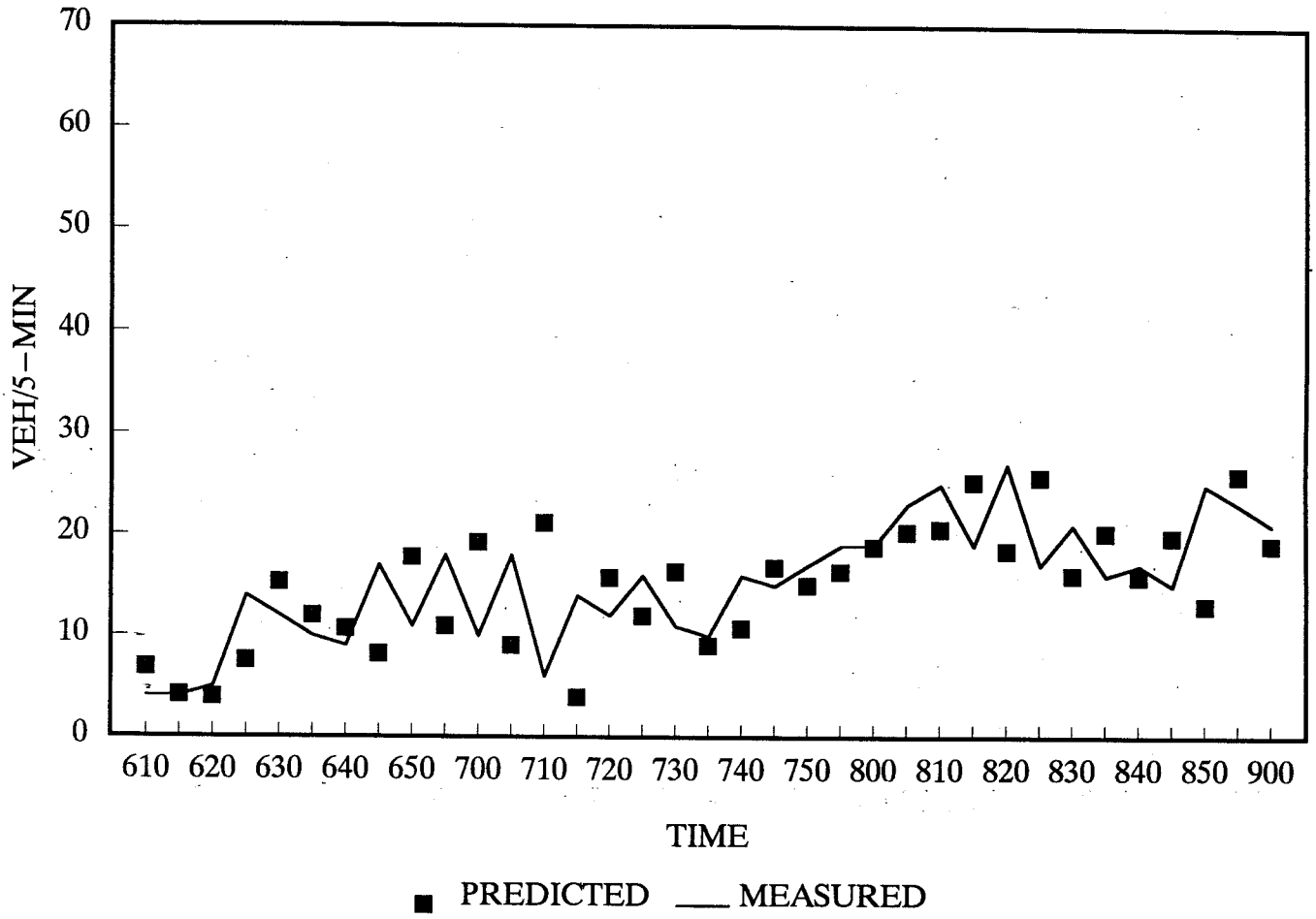

Figure 5.6a Prediction results for 66NX ramp
[Nov. 19, 1990, 6:00-9:00 a.m., MAE=5.92 veh/5-min.]

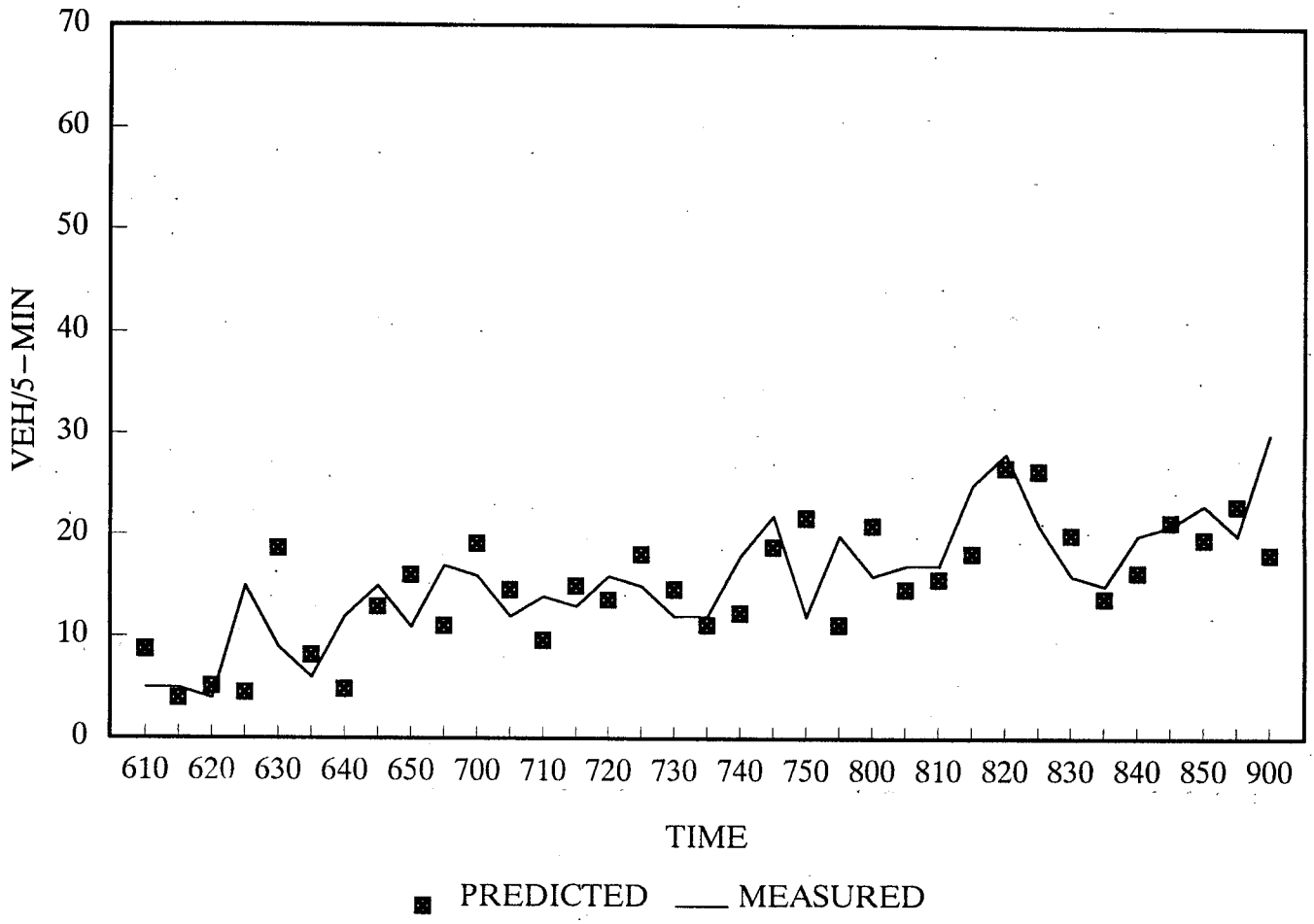

Figure 5.6b Prediction results for 66NX ramp
[Nov. 20, 1990, 6:00-9:00 a.m., MAE=5.19 veh/5-min.]

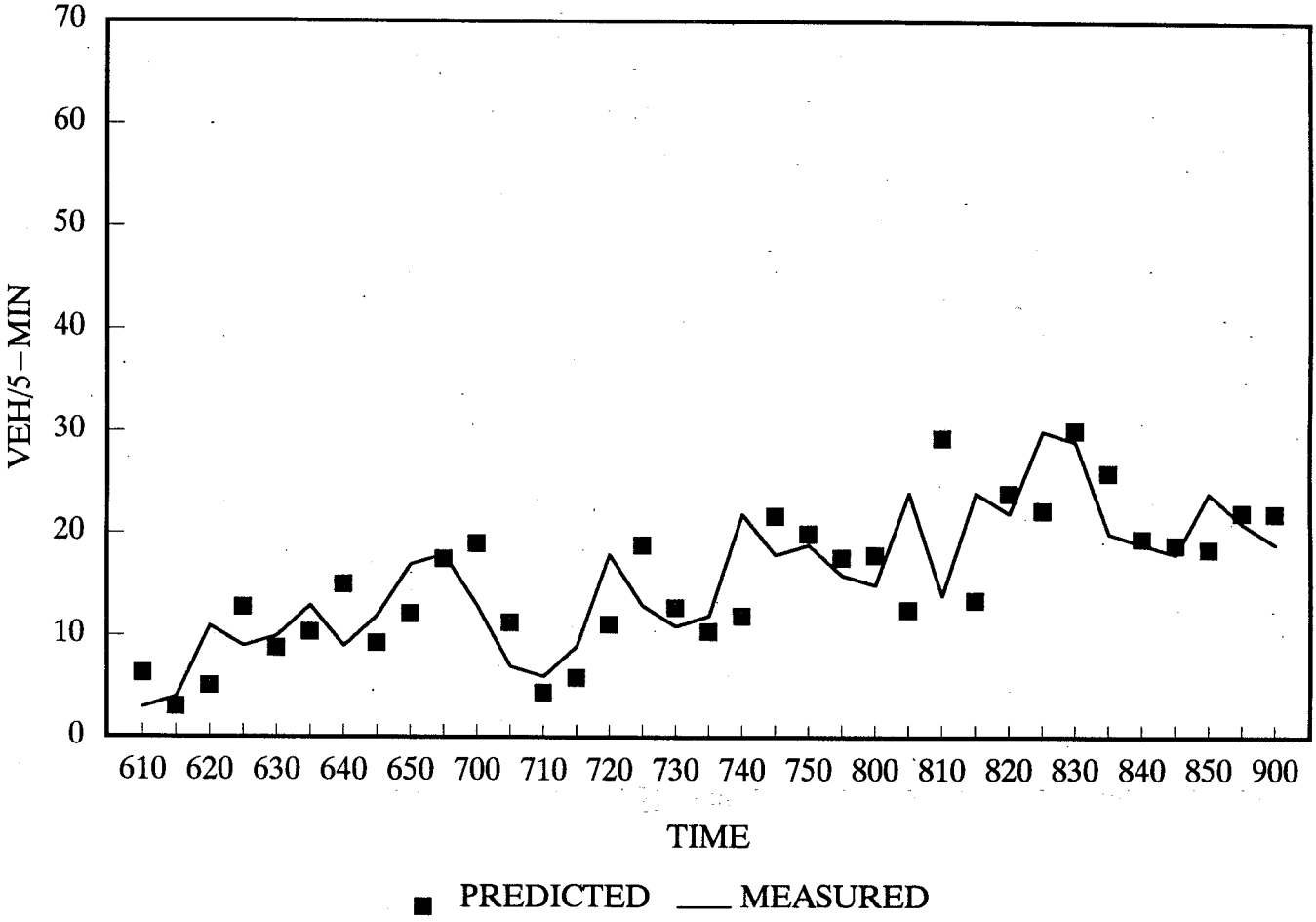

Figure 5.6c Prediction results for 66NX ramp
[Nov. 21, 1990, 6:00-9:00 a.m., MAE=5.21 veh/5-min.]

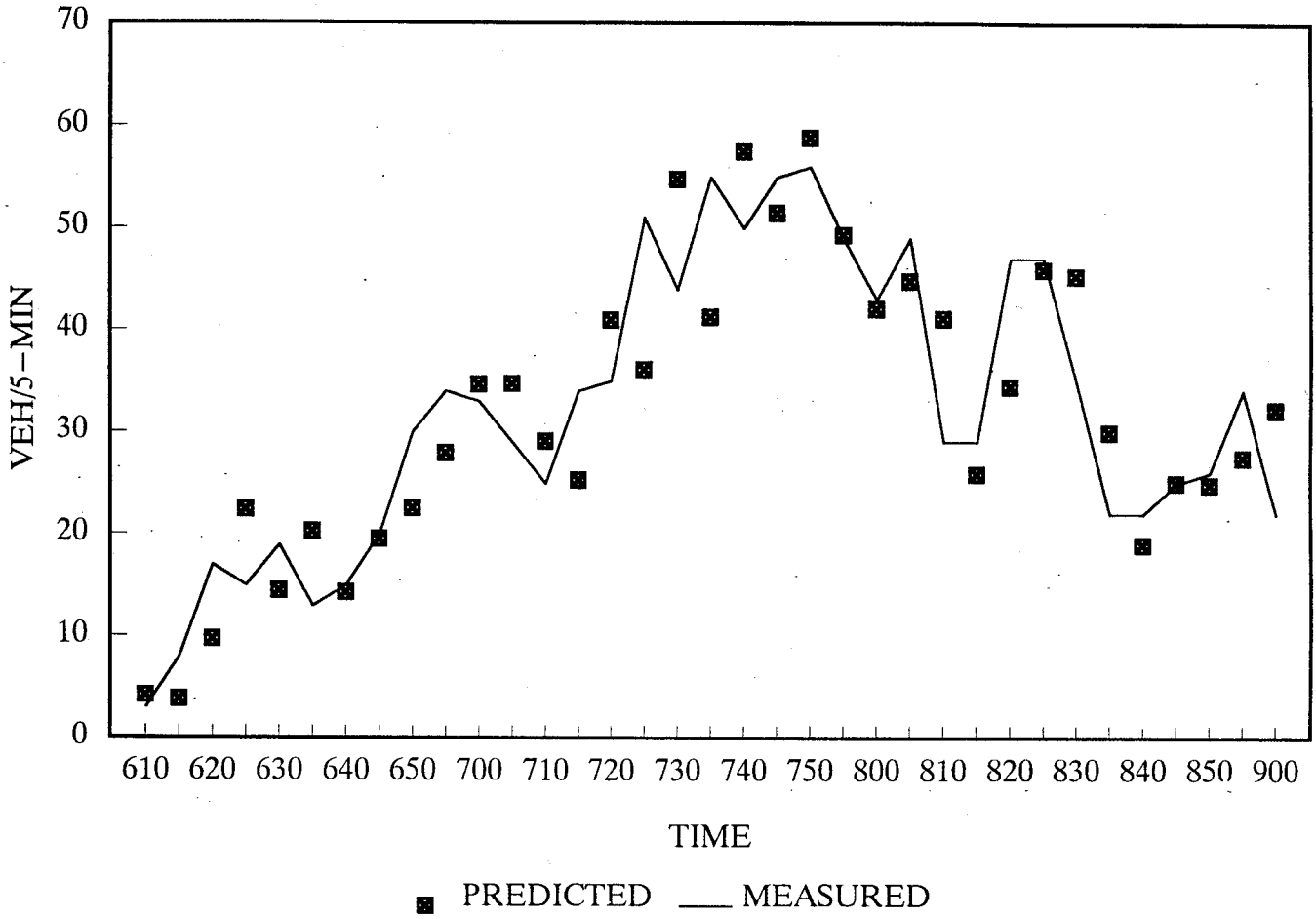

Figure 5.7a Prediction results for 82NX ramp
[Nov. 19, 1990, 6:00-9:00 a.m., MAE=5.70 veh/5-min.]

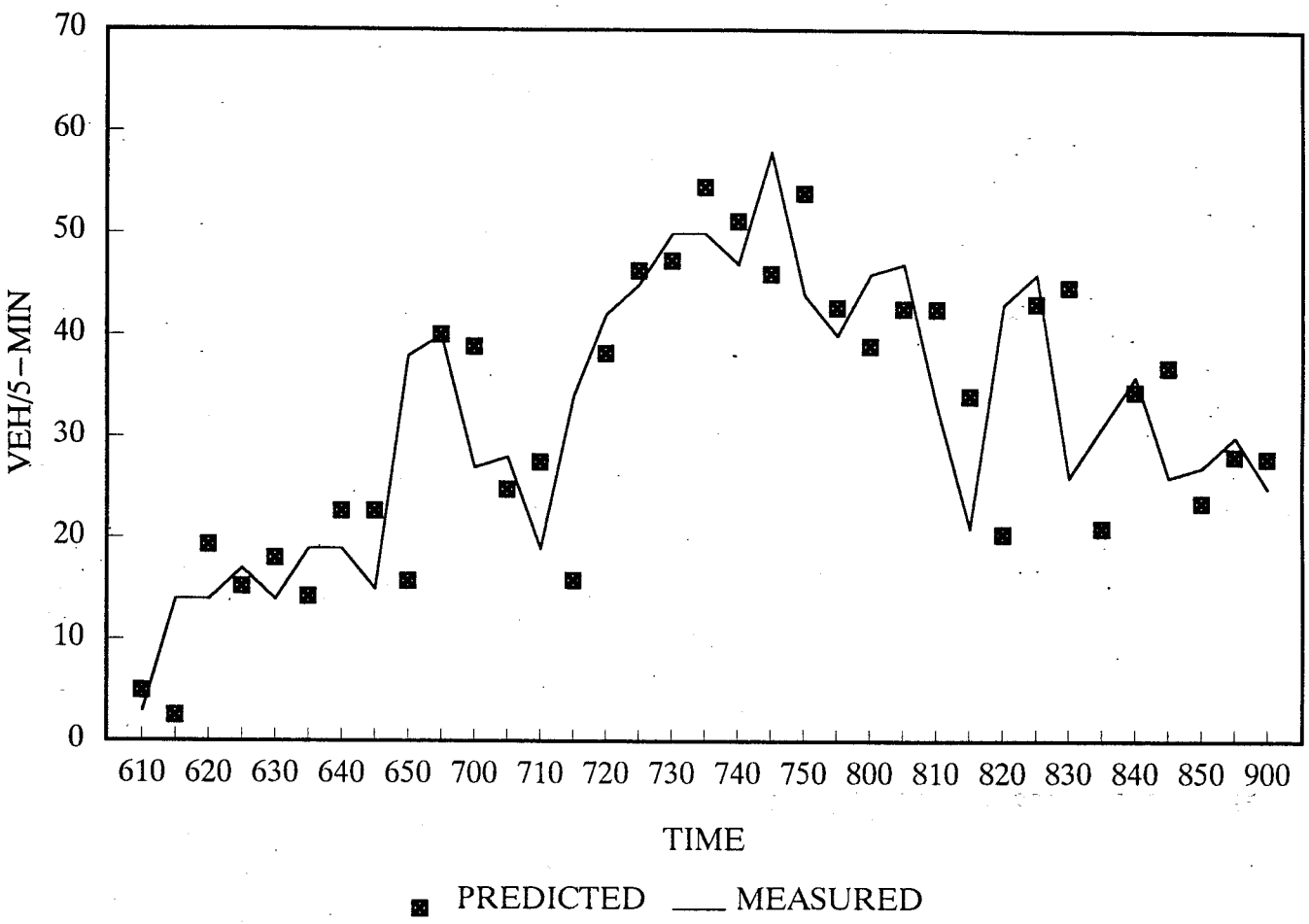

Figure 5.7b Prediction results for 82NX ramp
[Nov.20, 1990, 6:00-9:00 a.m., MAE=7.28 veh/5-min.]

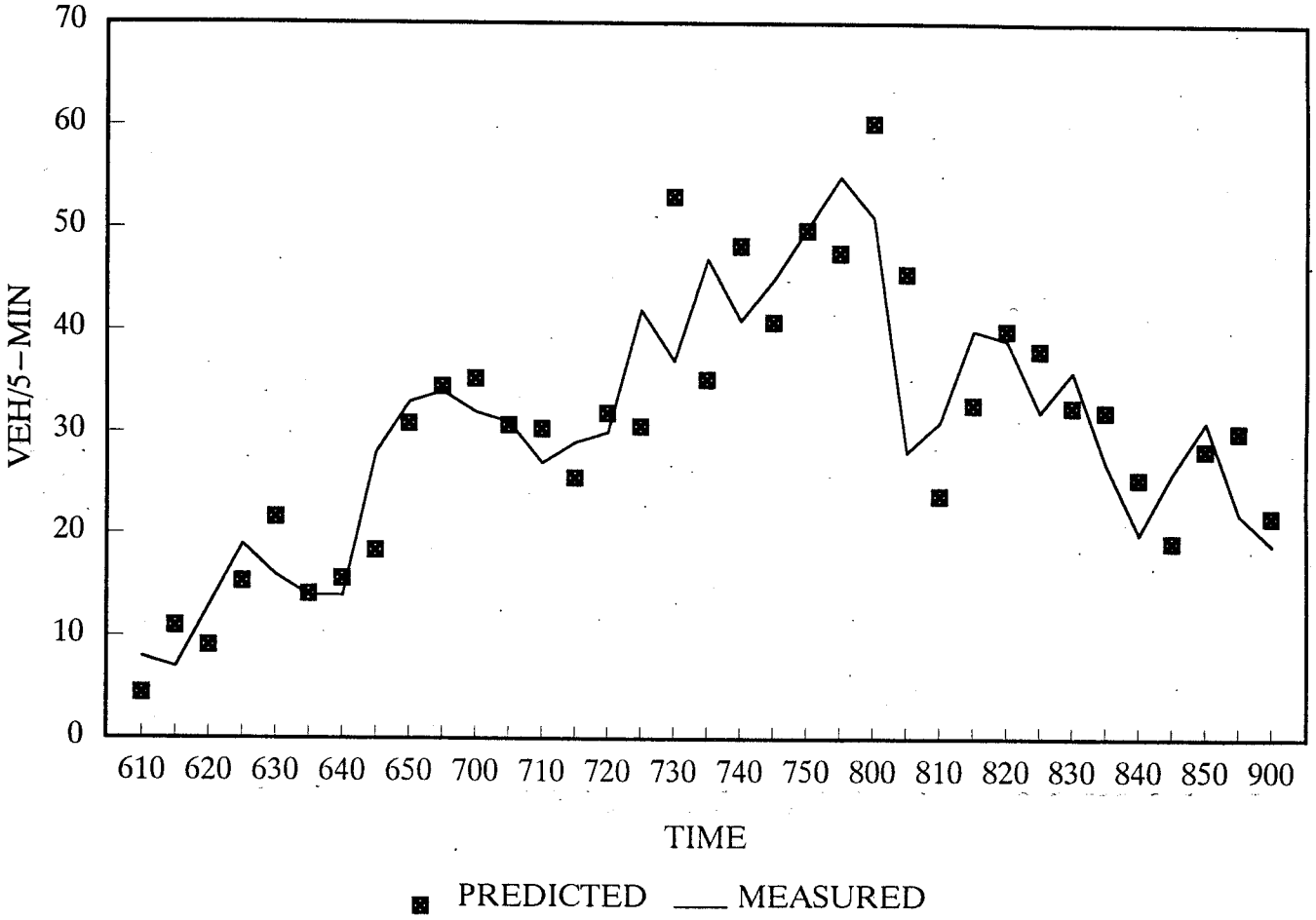

Figure 5.7c Prediction results for 82NX ramp
[Nov. 21, 1990, 6:00-9:00 a.m., MAE=5.37 veh/5-min.]

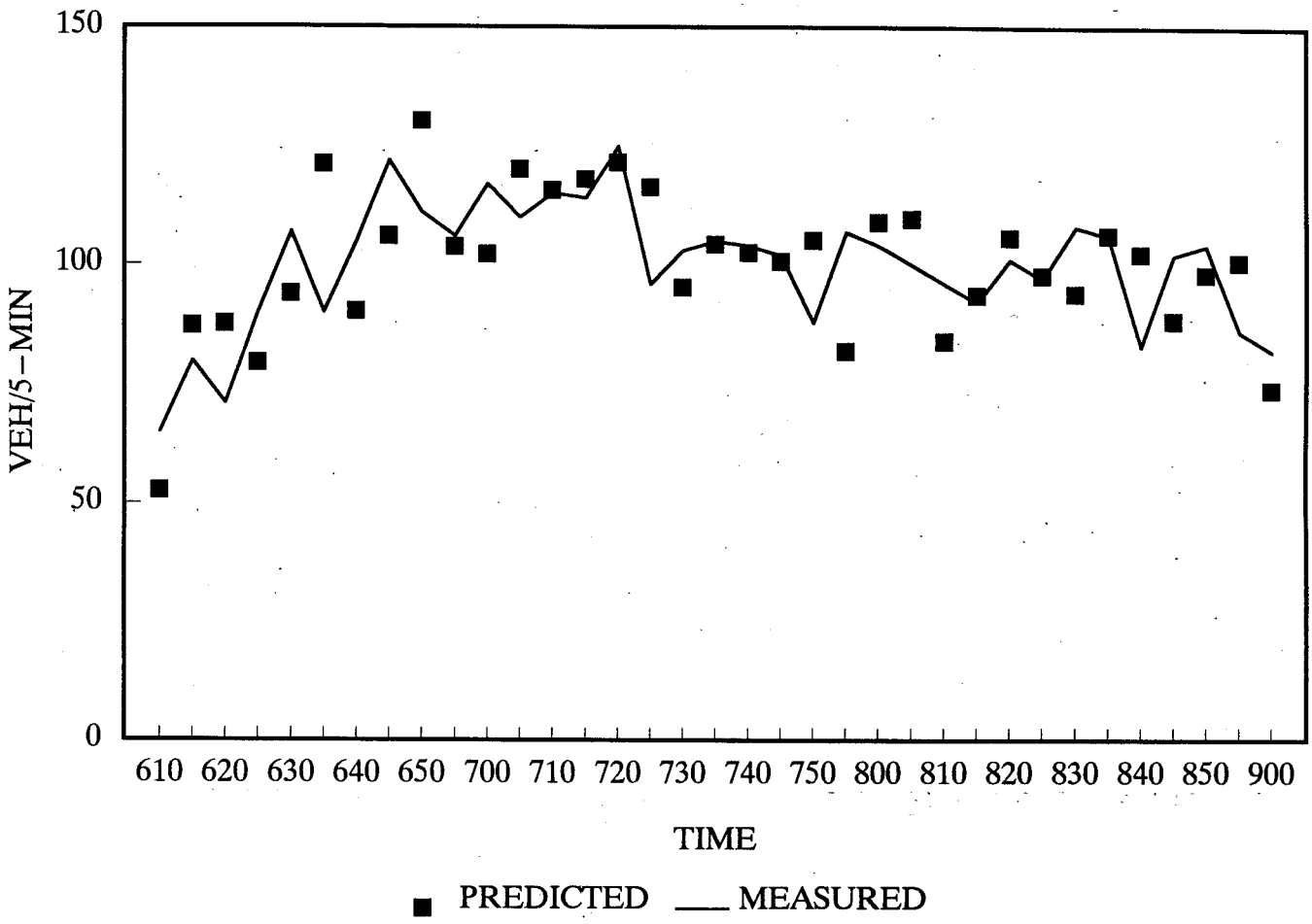

Figure 5.8a Prediction results for 78nx2 ramp
[Nov. 19, 1990, 6:00-9:00 a.m., MAE=10.77 veh/5-min.]

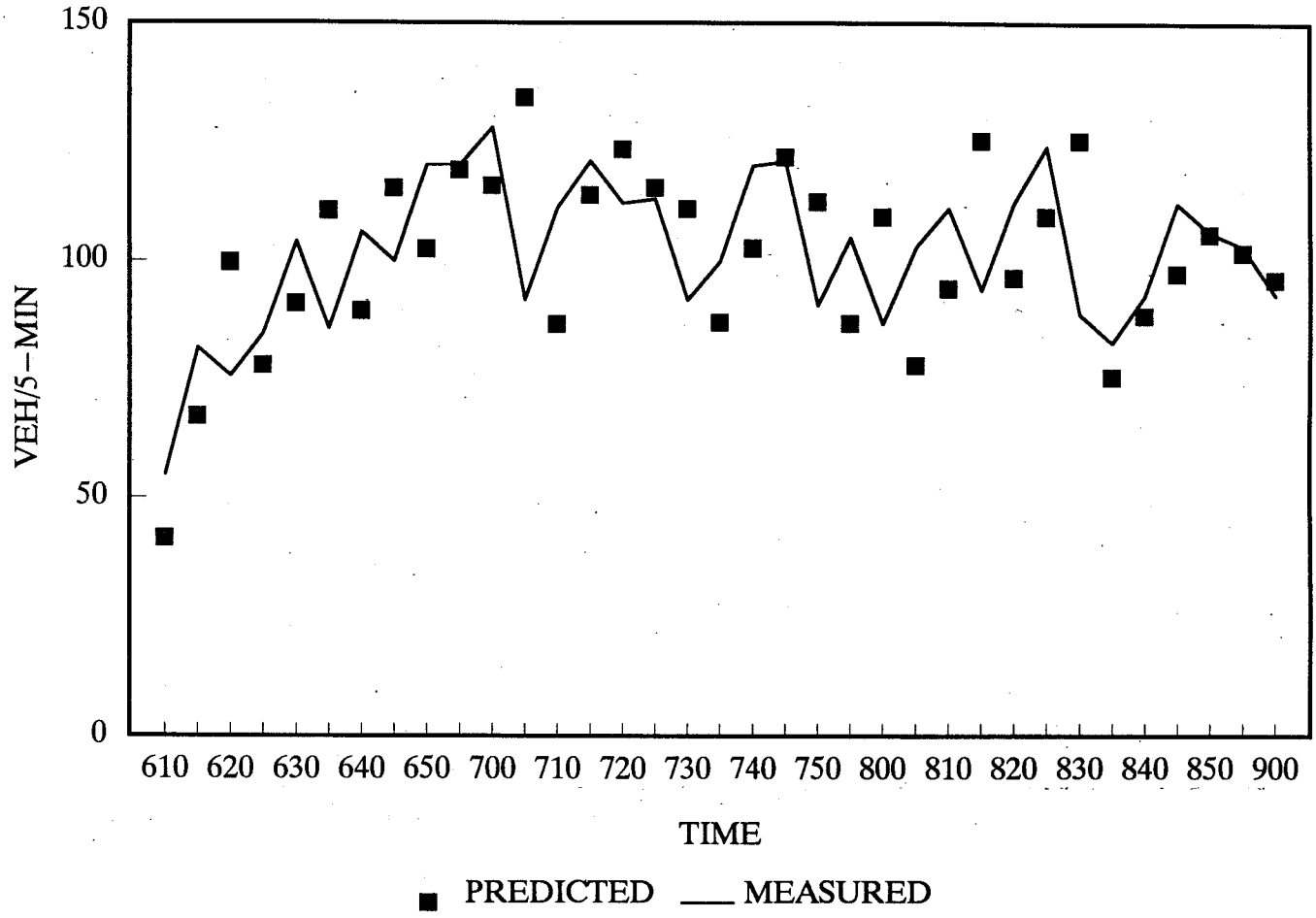

Figure 5.8b Prediction results for 78nx2 ramp
[Nov.20, 1990, 6:00-9:00 a.m., MAE=15.08 veh/5-min.]

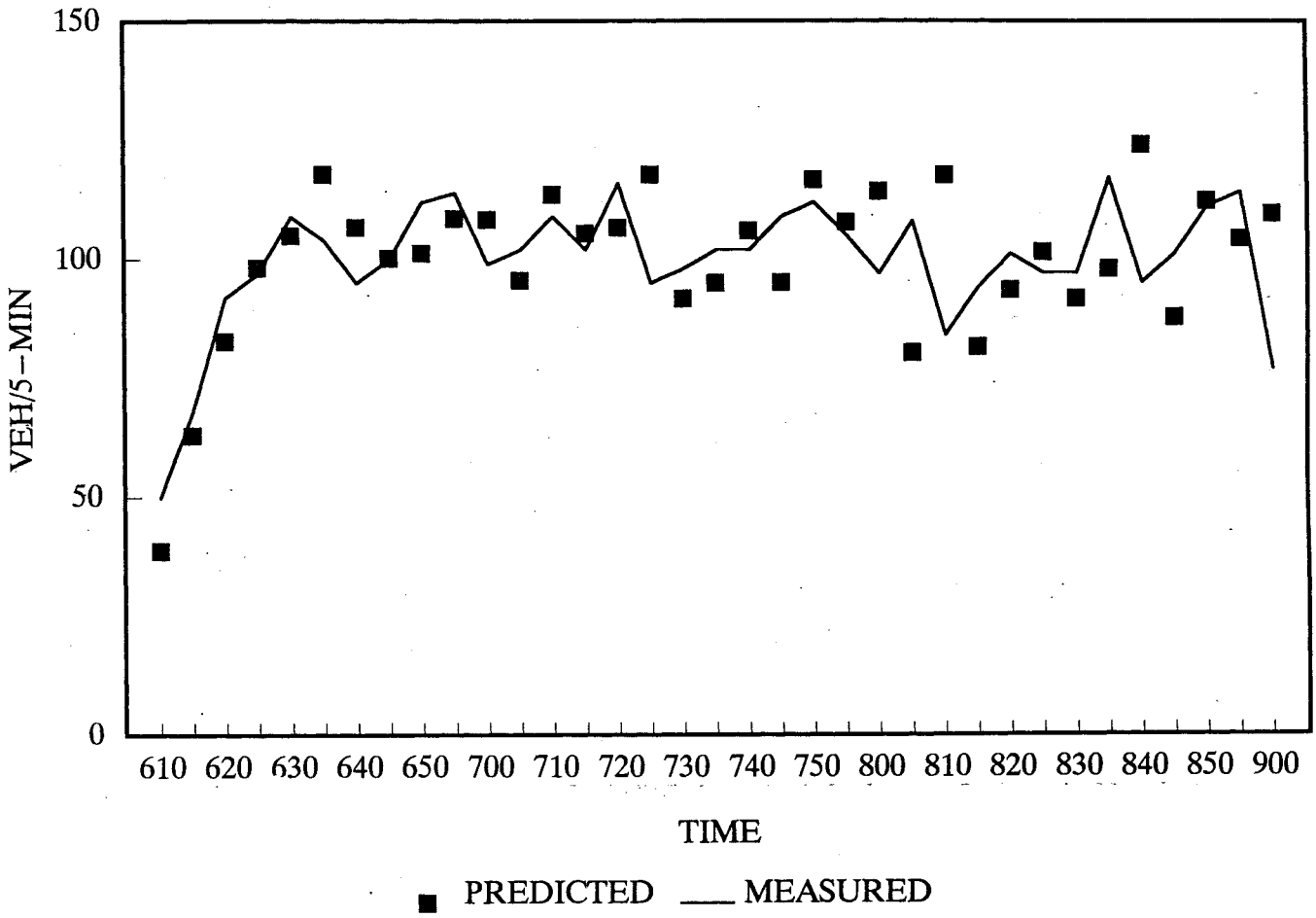

Figure 5.8c Prediction results for78nx2 ramp
[Nov. 21, 1990, 6:00-9:00 a.m., MAE=10.86 veh/5-min.]

where, for each k^{th} time interval,

$\hat{V}_k$ = predicted volume entering upstream mainline boundary,

V^H_k = historical measurements at the same location,

ß = parameter to be updated in real time.

Using the above model with the same prediction procedure as for exit volume prediction, the volume passing the 122^{nd} mainline detector location in the test section was predicted for every 5-minute interval and compared with the real data (Figures 5-9 a,b,c). The prediction results for 3 days in November, 1990, indicate the MAE ranges from 17.6 to 28.2 vehicles/5-minutes.

V.4 Summary

In this research, an adaptive predictor for freeway exit demand was developed and tested with the real data collected from the I-35W freeway in Minneapolis. The new predictor continuously updates the parameters of the prediction models in real time using the most recent prediction error, so that the control system realistically reflects current traffic conditions. The prediction model formulated in this research assumes that the freeway exit demand at an exit ramp is a function of historical exit demand at that ramp, and current day volume measurements at the upstream mainline and at that ramp. The test results are promising and large prediction errors do not propagate through time indicating adaptability of the prediction algorithm. However, in certain cases the predicted values time-lag the actual measurements. To improve prediction accuracy, an alternative model has been formulated by considering the behavioral characteristics of flow diversion. The model predicts the total volume, T_k, on the mainline freeway near the exit ramp under study, and the proportion of exit volume over total volume, P_k, i.e.,

$$\hat{V}_k = \hat{T}_k * \hat{P}_k$$

and,

$$\hat{T}_k = \alpha_k [T^H_{k-1} + T^H_k + T_{k-1}]$$

$$\hat{P}_k = P_{o,k}/[1 + \exp(\beta_k + \Gamma_k O_{k-1})]$$

where, $\hat{V}_k$ = predicted volume exiting main freeway during time interval k,

T^H_k = historical mainline demand during time interval k,

T_k = current day total mainline volume during time interval k,

$P_{o,k}$ = historical information regarding P_k,

O_k = downstream occupancy during time interval k.

α_k, β_k, Γ_k = parameters to be identified in real time.

The above model assumes that the total mainline volume near the exit ramp is a function of historical demand and current day measurement at the same location. Further, the diversion resulting from the downstream traffic condition is assumed to be reflected in the proportion of exit volume over total mainline volume. A logit utility model is formulated to estimate the

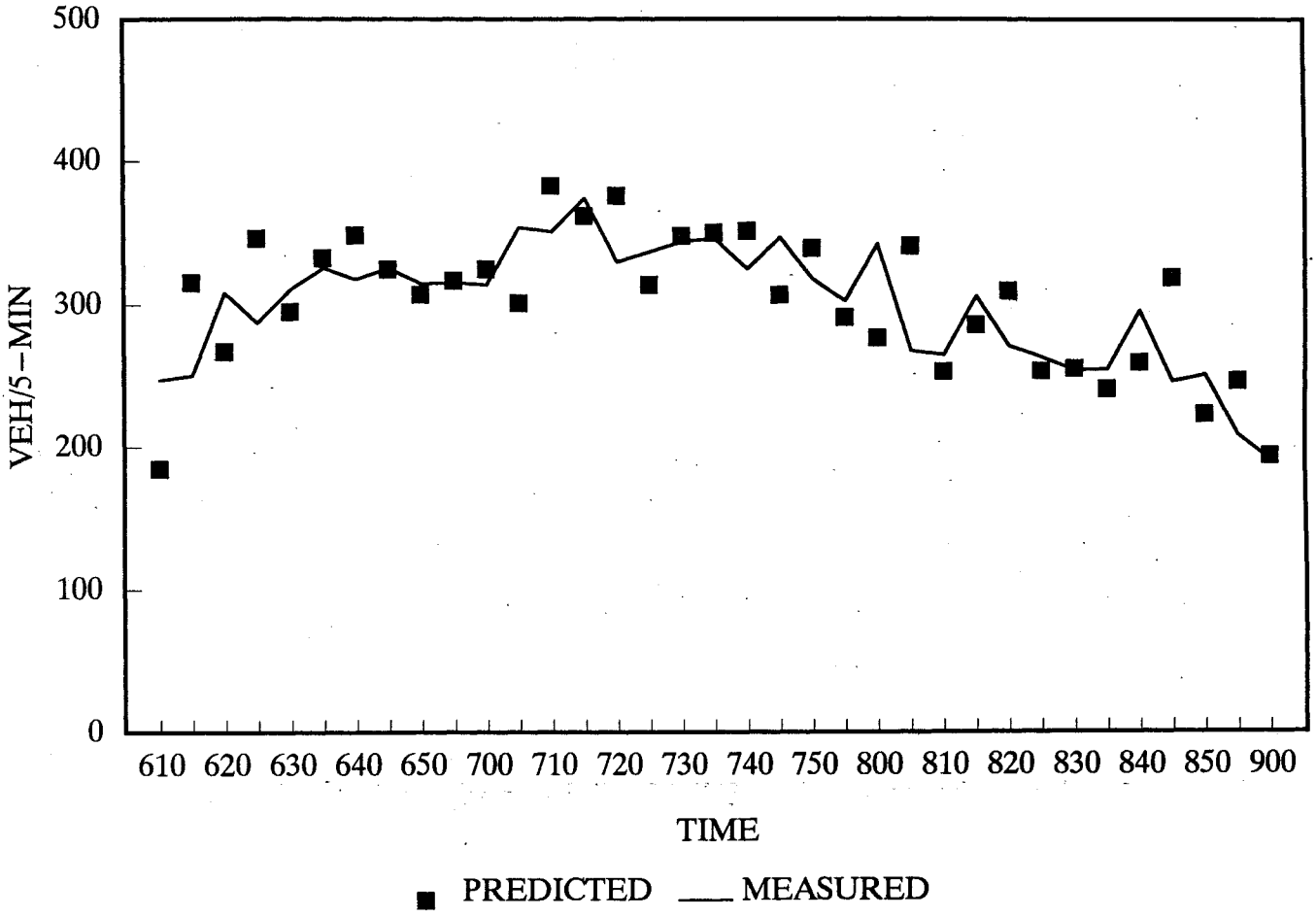

Figure 5.9a Prediction results for 122nd St.
[Nov. 19, 1990, 6:00-9:00 a.m., MAE=28.09 veh/5-min.]

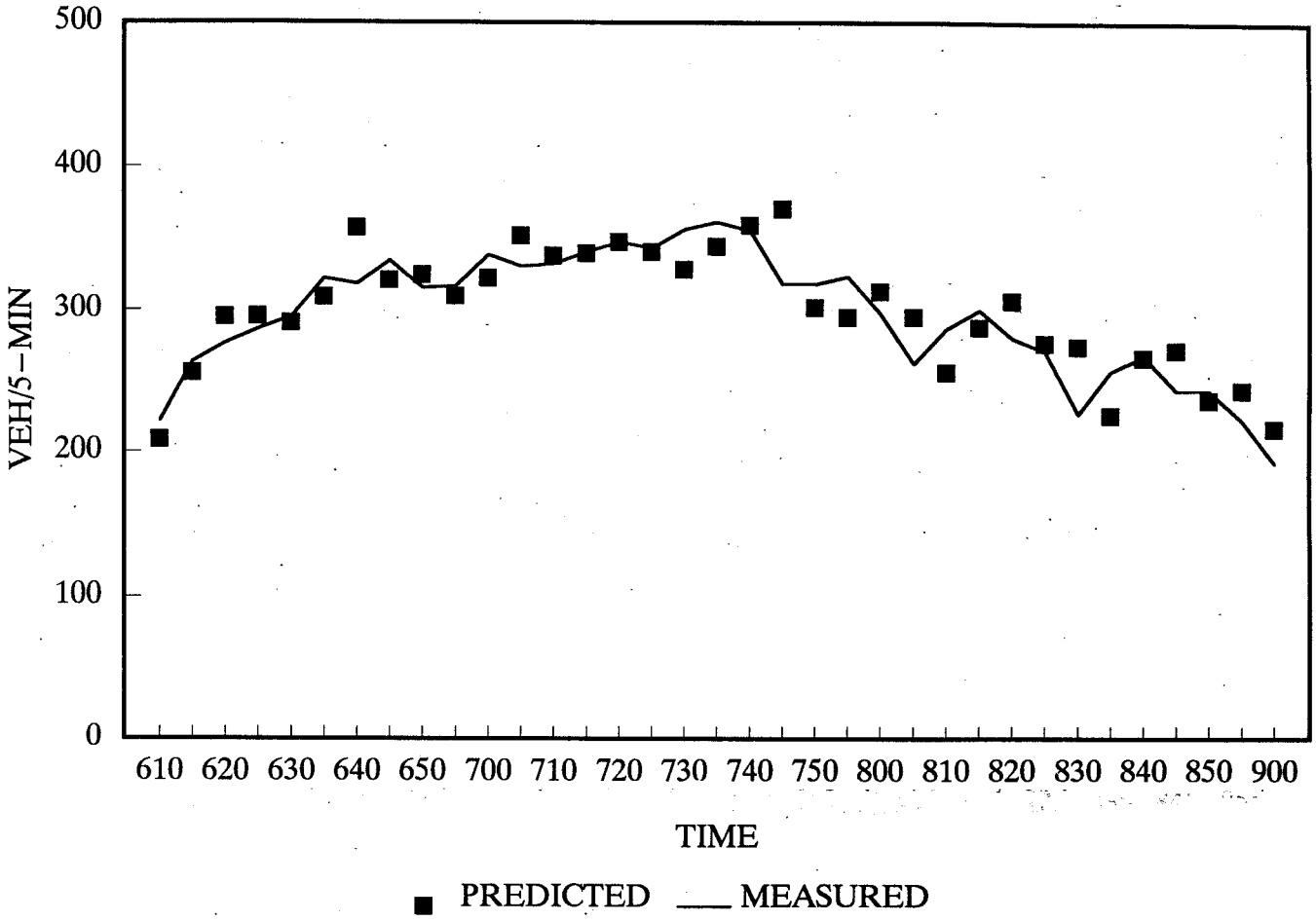

Figure 5.9b Prediction results for 122nd St.
[Nov.20, 1990, 6:00-9:00 a.m., MAE=17.56 veh/5-min.]

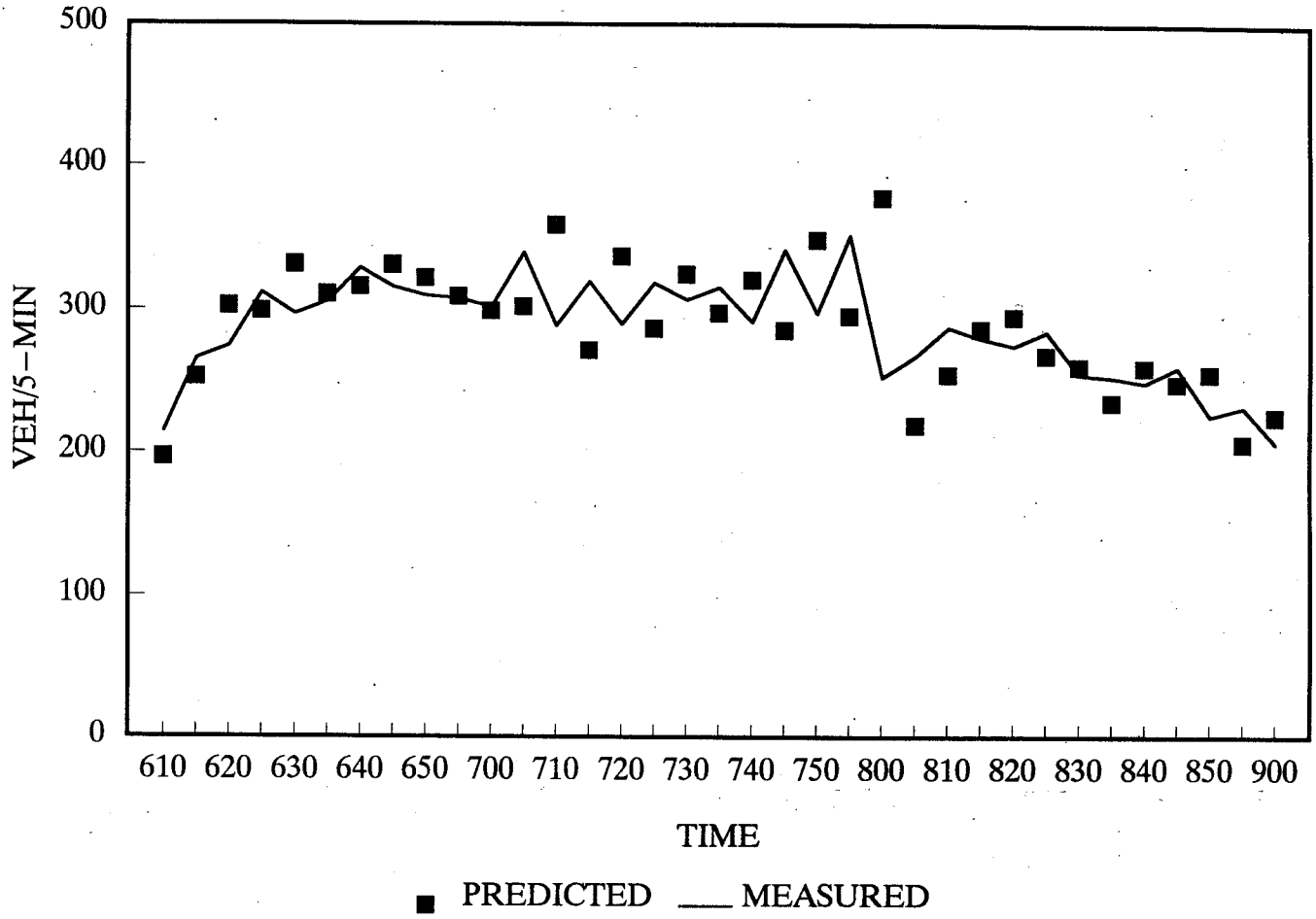

Figure 5.9c Prediction results for 122nd St.
[Nov. 21, 1990, 6:00-9:00 a.m., MAE=28.22 veh/5-min.]

diversion utility as a function of downstream occupancy. While the above model is appealing, it requires frequent e.g., 1-minute, measurements, such as volume and occupancy, that reflect the effects of downstream congestion on the diversion more accurately. The model will be tested by the authors in future phases of this research. Nevertheless, collecting and processing 1-minute traffic data for both mainline and ramps can impose a substantial burden to the data collection system. Further, the potential benefit from 1-min. prediction needs to be assessed relative to the time required to compute an optimal control solution in real time.

A number of additional areas for future research have been identified. First, extensive research is needed for incorporating prediction into automatic rate-selection metering strategies, so that metering control can be preventive rather than reactive. Determining the most suitable historical information for the prediction could improve prediction accuracy substantially. Further, the effect of on-line information and guidance on the exit volume needs to be modeled and incorporated into the exit volume prediction formulation. Finally, future phases of this research will address the need for developing optimal control algorithms that can determine metering rates based on the predicted traffic demand.

VI. CONCLUSION

Optimal freeway management requires an integrated approach involving demand-responsive ramp metering, incident management and driver guidance. While a freeway network acts as a system, i.e., conditions on any part affect other parts in the network, the state of the art in real-time freeway management has not reached the point where comprehensive, network-wide optimal control schemes are automatically generated and implemented through on-line optimization and coordination of various control actions. A major difficulty lies in the lack of efficient computational algorithms implementable for on-line optimization, and the lack of accurate on-line predictors, that can predict traffic demand and diversion in freeway networks.

As a result of the above limitations, most traffic responsive metering systems, such as the Twin Cities freeway control system, employ automatic rate-selection procedures. These procedures select the most appropriate metering rates for a ramp from a predetermined library using the information received from loop detectors on the main freeway, upstream and downstream from the ramp. Although this method provides a degree of self-adjustment to prevailing traffic conditions, the lack of an efficient analysis tool for evaluating and updating the key components of the control, i.e., thresholds and rate-libraries, significantly restricts the effectiveness of the control.

To address the above problems, a computer-based control-emulation method that can evaluate various automatic rate-selection strategies was developed by this research team in the previous phase of this research. Further, software was developed that operationalizes this method for field applications. While a prototype version was completed and tested off-line, the software required substantial enhancements before becoming fully operational for traffic management. Such enhancements include, software field validation with new automatic rate-selection strategies in the real freeway environment, and development of efficient input/output modules.

This report summarizes the final results of the current project, which include enhancement and validation of the control-emulation method in the real freeway environment. First, an efficient input/output module was developed and incorporated into the software. The new input module allows the user to construct a freeway section on the monitor screen by selecting and combining different components of freeway geometrics. All input data can be entered interactively and stored in a file for later analysis. The output module provides detailed evaluation results for every 100-foot segment in terms of volume, density and speed for each time interval specified by the user. Further, volume and occupancy information at particular detector locations is also provided. The graphics option of the output module enables the user to analyze the evaluation results using 2-/3-dimensional plots and contours. The performance indices commonly used in traffic engineering, such as total travel time, are also calculated and presented in a tabular format.

Secondly, a method was developed to determine the best metering thresholds for a given section of a freeway, under normal weather conditions, using the control-emulation method and the downhill simplex optimization procedure. The method finds the optimal thresholds for each ramp in a given section of the freeway by considering the system-wide traffic conditions. Further, an independent procedure to determine the initial thresholds that can be used to initialize the optimization process was also developed. The method was applied to a section of the westbound I-494 freeway, from Portland Ave. to East Bush Lake Rd., and a set of thresholds was determined for each ramp using normal weekday traffic demand pattern collected from the test section. The new optimized thresholds were implemented in the test section and the performance of the traffic system under these thresholds were compared with that under the previous TMC thresholds using the traffic demand pattern recorded at the test section in a three-week period. The test results indicate that the new control allowed more cars onto the freeway without creating serious congestion under normal weather conditions. However, with ice on the road, the new optimized thresholds were not restrictive enough to prevent congestion in the main freeway. This problem can be resolved by developing different sets of thresholds for various weather and traffic situations.

Finally, a preliminary study for developing an on-line predictor for freeway exit demand was performed and an adaptive prediction procedure was developed. The prediction model formulated in this research uses historical demand and current day measurements. Further, the parameters in the prediction model are updated in real time using the Extended Kalman Filter, so that the propagation of prediction error can be minimized. The new method was tested with real data collected from 4 exit ramps in the I-35W freeway. The initial test results look promising and prediction errors do not propagate through time.

For future phases of this research, the following research directions were identified:

1) Extension of the control-emulation method to a large freeway network.

2) Automation of the procedure for determining the best set of thresholds for a given freeway section through control-emulation.

3) Development of an optimal metering control algorithm based on predicted freeway demand.

4) Development of an efficient algorithm for determining the optimal control solution, that is computationally feasible and leads to robust control, for real time management of the freeway.

5) Extension of the zone-based threshold optimization method considering exit ramp data and estimated length of queue at enterance ramps.

BIBLIOGRAPHY

Ahmed, M.S. and Cook, A.R. (1979) Analysis of freeway traffic time series data by using Box-Jenkins techniques. Transpn Res. Rec. No. 722, 1-9.

Ahmed, S.A. (1983) Stochastic processes in freeway traffic. Traffic Engng and Contrl, Vol. 24, 306-310

FHWA (1973). Urban traffic control system and bus priority system traffic adaptive network signal timing program: Software description. Federal Highway Administration, U.S. Dept. of Transp., Washington, D.C., August.

Gartner, N.H. and Reiss, R.A. (1987) Congestion control in freeway corridors: The IMIS system. In Flow Control of Congested Networks. Edited by A.R. Odoni et al. NATO ASI Series F: Computer and Systems Science, Vol. 38, Springer-Verlag, Germany, ISBN 3-540-18398-1, 113-132.

Hall, R.W. (1983) Traveler route choice: Travel time implications of improved information and adaptive decisions. Transpn Res. Vol. 17A, 201-214.

Jazwinski, A.H. (1970) Stochastic process and filtering theory. Academic Press, New York.

Kalman, R.E. (1960) A new approach to linear filtering and prediction problems. J. Basic Engng Vol. 82-D, No. 1, 35-45.

Keen, K.G., Scofield, M.J. and Hay, G.C. (1989) Ramp metering access control on M6 motorway. Proc. 2nd International Conference on Road Traffic Control, IEE, April, 39-42.

Kyte, M., Marek, J. and Frith, D. (1989) Using multivariate time series analysis to model freeway traffic flow. Pres. at Ann. Transpn Res. Board Mtg., January.

Lieberman, E.B. et al. (1974) Variable cycle signal timing program: Volume 4 -Prediction algorithms, software and hardware requirements, and logical flow diagrams. FHWA, U.S. Dept. of Transpn, NTIS: PB 241720, Wash. D.C., May.

Moorthy, C.K. and Ratcliffe, B.G. (1988) Short-term traffic forecasting using time series methods. Transpn Plann. Tech., Vol. 12, 45-56.

Montgomery, D., (1992) Design of Experiments. McGraw Hill.

Okutani, I. and Stephanedes, Y.J. (1984) Dynamic prediction of traffic volume through Kalman Filtering theory. Transpn Res. Vol. 18B, 1-11.

Rutherford, G.S., Schroder, M., Jacobson, L. and Hallenbeck, M.E. (1990) Arterial control and integration. WA-RD 188.2, Washington State Transportation Center, March.

Stephanedes, Y.J., Kwon, E. and Michalopoulos, P.G. (1989) Demand diversion for vehicle guidance, simulation and control in freeway corridors. Transpn Res. Rec. No. 1220, 12-20.

Stephanedes, Y.J. and Kwon, E. (1992a) Adaptive demand-diversion prediction for integrated control of freeway corridors. Transpn Res. Vol. 26B, No. 6.

Stephanedes, Y.J., Kwon, E., Chang, K., and Yao, P. (1992b) Development and application of demand-responsive ramp metering control to improve traffic management in freeway corridors. Phase I, Final report. Dept. of Civil and Mineral Engineering., University of Minnesota, Minneapolis, Minnesota. January.

Wardrop, J.G. (1952) Some theoretical aspects of road traffic research. Proc. Inst. of Civil Engineers. Road Paper N36, 325-378.

Young, P.C. and Jakeman, A.J. (1984) Recursive filtering and smoothing procedures for the inversion of ill-posed causal problems. Utilitas Mathematica, Vol. 25, 351-376.